Eur. Phys. J. C (2023) 83:740
https://doi.org/10.1140/epjc/s10052-023-11847-7

THE EUROPEAN PHYSICAL JOURNAL C

Regular Article

Spectroscopic behavior of fully heavy tetraquarks

Hong-Tao An[1,2,3,4,a], **Si-Qiang Luo**[1,2,3,4,b], **Zhan-Wei Liu**[1,2,3,4,5,c], **Xiang Liu**[1,2,3,4,5,d]

[1] School of Physical Science and Technology, Lanzhou University, Lanzhou 730000, China
[2] Research Center for Hadron and CSR Physics, Lanzhou University and Institute of Modern Physics of CAS, Lanzhou 730000, China
[3] Key Laboratory of Quantum Theory and Applications of MoE, Lanzhou University, Lanzhou 730000, China
[4] MoE Frontiers Science Center for Rare Isotopes, Lanzhou University, Lanzhou 730000, China
[5] Lanzhou Center for Theoretical Physics, Lanzhou University, Lanzhou 730000, Gansu, China

Received: 18 February 2023 / Accepted: 17 July 2023 / Published online: 22 August 2023

Abstract Stimulated by the observation of the $X(6900)$ from LHCb in 2020 and the recent results from CMS and ATLAS in the di-J/ψ invariant mass spectrum, in this work we systematically study all possible configurations for the ground states of fully heavy tetraquark in the constituent quark model. By our calculation, we present their spectroscopic behaviors including binding energy, lowest meson–meson thresholds, specific wave function, magnetic moment, transition magnetic moment, radiative decay width, rearrangement strong width ratio, internal mass contributions, relative lengths between (anti)quarks, and the spatial distribution of four valence (anti)quarks. We cannot find a stable S-wave state for the fully heavy tetraquark system. We hope that our results will be valuable to further experimental exploration of fully heavy tetraquark states.

1 Introduction

With the birth of the quark model [1–3], exotic states beyond conventional hadrons were proposed. The search for exotic hadronic states is full of challenges and opportunities. Since the $X(3872)$ was first reported by the Belle Collaboration in 2003 [4–6], a series of charmonium-like or bottomonium-like exotic states [7–21] and P_c states [22–24] have been observed experimentally, which stimulates extensive discussions of their properties by introducing the assignments of conventional hadron, compact multiquark states, molecular state, hybrid, glueball, and kinematic effects [7–21].

In 2003, the BaBar Collaboration observed a narrow heavy–light state $D_{s0}^*(2317)$ in the $D_s^+\pi^0$ invariant mass spectrum [25]. However, since the mass of the observed $D_{s0}^*(2317)$ is about 100 MeV below the quark model predictions in Ref. [26], it is difficult to understand the $D_{s0}^*(2317)$ in a conventional quark model directly, which is referred to as the "low-mass puzzle" of $D_{s0}^*(2317)$. In order to solve the low-mass puzzle, the tetraquark explanation with the $Qq\bar{q}\bar{q}$ configuration was proposed in Refs. [27–29]. Later, the CLEO Collaboration [30] confirmed the $D_{s0}^*(2317)$ and announced another narrow resonance $D_{s1}(2460)$ in the $D_s^{*+}\pi^0$ final states. The low-mass puzzle also happens to the $D_{s1}(2460)$ [26]. A discussion of the $D_{s1}(2460)$ as a tetraquark state can be found in Refs. [31–38]. In particular, the LHCb Collaboration reported the discovery of two new exotic structures $X_0(2900)$ and $X_1(2900)$ [39,40], which inspired the study of exotic charmed tetraquarks [41–50]. In addition, theorists began to study the doubly charmed tetraquark states in the earlier works [51–55]. In 2017, the LHCb Collaboration observed a doubly charmed baryon $\Xi_{cc}^{++}(3620)$ in the $\Lambda_c^+K^-\pi^+\pi^+$ decay mode [56]. Using the $\Xi_{cc}^{++}(3620)$ as the scaling point, the theorists further explored the possible stable doubly charmed tetraquark states with the $QQ\bar{q}\bar{q}$ configuration [57–66]. Surprisingly, as a candidate of the doubly charmed tetraquark, the T_{cc}^+ was detected by LHCb in the $D^0D^0\pi^+$ invariant mass spectrum, which has a minimal quark configuration of $cc\bar{u}\bar{d}$ [67]. In addition to these singly and doubly charmed tetraquarks, there should be a triply charmed tetraquark. To our knowledge, the triply charmed tetraquark states with the $QQ\bar{Q}\bar{q}$ configuration have also been studied by various approaches [68–72].

Briefly reviewing the status of heavy flavor tetraquark states, we must mention the fully heavy tetraquark with the $QQ\bar{Q}\bar{Q}$ configuration, which has attracted the attention of both theorists and experimentalists. Chao et al. suggested

[a] e-mail: anht14@lzu.edu.cn
[b] e-mail: luosq15@lzu.edu.cn
[c] e-mail: liuzhanwei@lzu.edu.cn
[d] e-mail: xiangliu@lzu.edu.cn (corresponding author)

that the peculiar resonance-like structures of $R(e^+e^- \to \text{hadrons})$ for $\sqrt{s} = 6{-}7$ GeV may be due to the production of the predicted P-wave (cc)–$(\bar{c}\bar{c})$ states in the energy range of 6.4–6.8 GeV, which could dominantly decay into charmed mesons [73]. The calculation of the fully heavy tetraquark was then carried out using the potential model [74,75] and the MIT bag model with the Born–Oppenheimer approximation [76]. This system has also been studied in a nonrelativistic potential model, where no $QQ\bar{Q}\bar{Q}$ bound state can be found [77]. However, Lloyd et al. adopted a parameterized nonrelativistic Hamiltonian to study such system [78], where they found several closely lying bound states with a large oscillator basis. Later, Karliner et al. estimated the masses of the fully heavy tetraquark states by a simple quark model, and obtained $\mathrm{M}(X_{cc\bar{c}\bar{c}}) = 6192 \pm 25$ MeV and $\mathrm{M}(X_{bb\bar{b}\bar{b}}) = 18826 \pm 25$ MeV for the fully charmed and fully bottom tetraquarks with the $J^{PC} = 0^{++}$ quantum number, respectively [79]. Anwar et al. calculated the ground-state energy of the $bb\bar{b}\bar{b}$ bound state in a nonrelativistic effective field theory with one-gluon-exchange (OGE) color Coulomb interaction, and the ground-state $bb\bar{b}\bar{b}$ tetraquark mass was predicted to be (18.72 ± 0.02) GeV [80]. In Ref. [81], Bai et al. presented a calculation of the $bb\bar{b}\bar{b}$ tetraquark ground-state energy using a diffusion Monte Carlo method to solve the nonrelativistic many-body system. Debastiani et al. extended the updated Cornell model to study the fully charmed tetraquark in a diquark–antidiquark configuration [82]. Chen et al. used a moment quantum chromodynamics (QCD) sum rule method to give the existence of the exotic states $cc\bar{c}\bar{c}$ and $bb\bar{b}\bar{b}$ in the compact diquark–antidiquark configuration, where they suggested searching for them in the $J/\psi J/\psi$ and $\eta_c(1S)\eta_{1S}$ channels [83].

With the accumulation of experimental data, many collaborations have tried to search for it. The CMS Collaboration reported the first observation of the $\Upsilon(1S)$ pair production in pp collisions, where there is evidence that a structure around 18.4 GeV with a global significance of 3.6 σ exists in the four-lepton channel, which is probably a fully bottom tetraquark state [84]. However, this structure was not confirmed by the later CMS analysis [85]. Subsequently, the LHCb Collaboration studied the $\Upsilon(1S)_{\mu^+\mu^-}$ invariant mass distribution to search for a possible $bb\bar{b}\bar{b}$ exotic meson, but they did not see any significant excess in the range 17.5–20.0 GeV [86]. By 2020, the LHCb Collaboration declared a narrow resonance $X(6900)$ in the di-J/ψ mass spectrum with a significance of more than 5σ [87]. In addition, a broad structure ranging from 6.2 to 6.8 GeV and an underlying peak near 7.3 GeV were reported at the same time [87]. The ATLAS and CMS collaborations recently published their measurements on the di-J/ψ invariant mass spectrum. Here, they not only confirmed the existence of the $X(6900)$, but also found some new peaks [88–90]. There have been extensive discussions about the observed $X(6900)$ from different approaches and with different assignments [91–108].

The problem of the stability of the fully heavy tetraquark state has long been debated. Debastiani et al. found that the lowest S-wave $cc\bar{c}\bar{c}$ tetraquarks may be below the di-charmonium thresholds in their updated Cornell model [109]. The 1^+ $bb\bar{b}\bar{c}$ state is thought to be a narrow state in the extended chromomagnetic model [110]. However, many other studies have suggested that the ground state of fully heavy tetraquarks is above the di-meson threshold. Wang et al. also calculated the fully heavy tetraquark state in two nonrelativistic quark models with different OGE Coulomb, linear confinement, and hyperfine potentials [111]. Based on the numerical calculations, they suggested that the ground states should be located about 300–450 MeV above the lowest scattering states, indicating that there is no bound tetraquark state. The lattice nonrelativistic QCD method was applied to study the lowest energy eigenstate of the $bb\bar{b}\bar{b}$ system, and no state was found below the lowest bottomonium-pair threshold [112]. In another work, Richard et al. claimed that the fully heavy configuration $QQ\bar{Q}\bar{Q}$ is not stable if one adopts a standard quark model and treats the four-body problem appropriately [113]. Jin et al. studied full-charm and full-bottom tetraquarks using the quark delocalization color screening model and the chiral quark model, respectively, and the results within the quantum numbers $J^P = 0^+, 1^+$, and 2^+ show that the bound state exists in both models [114]. Frankly, theorists have not come to an agreement on the stability of the fully heavy tetraquark state.

Facing the present status of the fully heavy tetraquark, in this work we adopt the variational method to systematically study the fully heavy tetraquark states, where the mass spectrum of the fully heavy tetraquark is given in the framework of the nonrelativistic quark model associated with a potential containing Coulomb, linear, and hyperfine terms. The constructed total wave functions involved in these systems satisfy the requirement of the Pauli principle. We should emphasize that we can also reproduce the masses of these conventional hadrons with the same parameters, which is a test of our adopted framework. With this preparation, we calculate the binding energies, the lowest meson–meson thresholds, and the rearrangement strong width ratio, and study the stability of the fully heavy tetraquark states against the decay into two meson states. Furthermore, we discuss whether these tetraquarks have a compact configuration based on the eigenvalue of the hyperfine potential matrix. According to specific wave functions, we obtain the magnetic moments, transition magnetic moments, and radiative decay widths, which may reflect their electromagnetic properties and internal structures. We also give the size of the tetraquarks, the relative distances between (anti)quarks, and the spatial distribution of the four valence (anti)quarks for each state. Through the present systematic work, we can test whether compact bound fully heavy tetraquarks exist within the given Hamiltonian.

This paper is organized as follows. After the introduction, we present the Hamiltonian of the constituent quark model and list the corresponding parameters in Sect. 2. Then, in Sect. 3, we give the spatial function with a simple Gaussian form and construct the flavor, color, and spin wave functions of the fully heavy tetraquark states. In Sect. 4, we show the numerical results obtained by the variational method and further calculate their magnetic moment, transition magnetic moment, radiative decay width, rearrangement strong width ratio, internal mass contributions, and relative lengths between (anti) quarks. In addition, we compare our results with those of other theoretical groups in Sect. 5. Finally, we end the paper with a short summary in Sect. 6.

2 Hamiltonian

We choose a nonrelativistic Hamiltonian for the fully heavy tetraquark system, which is written as

$$H=\sum_{i=1}^{4}\left(m_i+\frac{\mathbf{p}_i^2}{2m_i}\right)-\frac{3}{4}\sum_{i<j}^{4}\frac{\lambda_i^c}{2}.\frac{\lambda_j^c}{2}(V_{ij}^{\text{Con}}+V_{ij}^{SS}). \quad (1)$$

Here, m_i is the (anti)quark mass, λ_i^c is the $SU(3)$ color operator for the i-th quark, and for the antiquark, λ_i^c is replaced by $-\lambda_i^{c*}$. The internal quark potentials V_{ij}^{Con} and V_{ij}^{SS} have the following forms:

$$V_{ij}^{\text{Con}}=-\frac{\kappa}{r_{ij}}+\frac{r_{ij}}{a_0^2}-D,$$
$$V_{ij}^{SS}=\frac{\kappa'}{m_i m_j}\frac{1}{r_{0ij}r_{ij}}e^{-r_{ij}^2/r_{0ij}^2}\vec{\sigma}_i\cdot\vec{\sigma}_j, \quad (2)$$

where $r_{ij}=|\mathbf{r}_i-\mathbf{r}_j|$ is the distance between the i-th (anti)quark and the j-th (anti)quark, and σ_i is the $SU(2)$ spin operator for the i-th quark. As for the r_{0ij} and κ', we have

$$r_{0ij}=1/\left(\alpha+\beta\frac{m_i m_j}{m_i+m_j}\right),$$
$$\kappa'=\kappa_0\left(1+\gamma\frac{m_i m_j}{m_i+m_j}\right). \quad (3)$$

The corresponding parameters appearing in Eqs. (2–3) are shown in Table 1. Here, κ and κ' are the couplings of the Coulomb and hyperfine potentials, respectively, and they are proportional to the running coupling constant $\alpha_s(r)$ of QCD. The Coulomb and hyperfine interactions can be deduced from the one-gluon-exchange model. $1/a_0^2$ represents the strength of the linear potential. r_{0ij} is the Gaussian-smearing parameter. Furthermore, we introduce κ_0 and γ in κ' to better describe the interaction between different quark pairs [115].

Table 1 Parameters of the Hamiltonian

Parameter	κ	a_0	D
Value	120.0 MeV fm	0.0318119 (MeV^{-1}fm)$^{1/2}$	983 MeV
Parameter	α	β	m_c
Value	1.0499 fm^{-1}	0.0008314 (MeV fm)$^{-1}$	1918 MeV
Parameter	κ_0	γ	m_b
Value	194.144 MeV	0.00088 MeV^{-1}	5343 MeV

Table 2 All possible flavor combinations for the fully heavy tetraquark system

System	Flavor combinations		
$QQ\bar{Q}\bar{Q}$	$cc\bar{c}\bar{c}$	$bb\bar{b}\bar{b}$	$cb\bar{c}\bar{b}$
	$cc\bar{b}\bar{b}$ ($bb\bar{c}\bar{c}$)	$cc\bar{c}\bar{b}$ ($bc\bar{c}\bar{c}$)	$bb\bar{b}\bar{c}$ ($cb\bar{b}\bar{b}$)

3 Wave functions

Here, we focus on the ground states of fully heavy tetraquark. We present the flavor, spatial, and color-spin parts of the total wave function for fully heavy tetraquark system. In order to consider the constraint by the Pauli principle, we use a diquark–antidiquark picture to analyze this tetraquark system.

3.1 Flavor part

First we discuss the flavor part. Here, we list all the possible flavor combinations for the fully heavy tetraquark system in Table 2.

In Table 2, the three flavor combinations in the first row are purely neutral particles, and the C-parity is a "good" quantum number. For the other six states in the second row, each state has a charge conjugation anti-partner, and their masses, internal mass contributions, and relative distances between (anti)quarks are absolutely identical, so we only need to discuss one of the pair.

Furthermore, the $cc\bar{c}\bar{c}$, $bb\bar{b}\bar{b}$, and $cc\bar{b}\bar{b}$ states have the two pairs of (anti)quarks which are identical, but only the first two quarks in the $cc\bar{c}\bar{b}$ and $bb\bar{b}\bar{c}$ states are identical.

3.2 Spatial part

In this part, we construct the wave function for the spatial part in a simple Gaussian form. We denote the fully heavy tetraquark state as the $Q(1)Q(2)\bar{Q}(3)\bar{Q}(4)$ configuration, and choose the Jacobian coordinate system as follows:

$$\mathbf{x}_1 = \sqrt{1/2}(\mathbf{r}_1 - \mathbf{r}_2),$$
$$\mathbf{x}_2 = \sqrt{1/2}(\mathbf{r}_3 - \mathbf{r}_4),$$
$$\mathbf{x}_3 = \left[\left(\frac{m_1\mathbf{r}_1 + m_2\mathbf{r}_2}{m_1 + m_2}\right) - \left(\frac{m_3\mathbf{r}_3 + m_4\mathbf{r}_4}{m_3 + m_4}\right)\right]. \quad (4)$$

Here, we set the Jacobi coordinates with the following conditions:

$$\begin{aligned}
&m_1 = m_2 = m_3 = m_4 = m_c, \quad \text{for } cc\bar{c}\bar{c},\\
&m_1 = m_2 = m_3 = m_4 = m_b, \quad \text{for } bb\bar{b}\bar{b},\\
&m_1 = m_2 = m_c, m_3 = m_4 = m_b, \quad \text{for } cc\bar{b}\bar{b},\\
&m_1 = m_2 = m_3 = m_c, m_4 = m_b, \quad \text{for } cc\bar{c}\bar{b},\\
&m_1 = m_2 = m_3 = m_b, m_4 = m_c, \quad \text{for } bb\bar{b}\bar{c},\\
&m_1 = m_c, m_2 = m_b, m_3 = m_c, m_4 = m_b, \quad \text{for } cb\bar{c}\bar{b}.
\end{aligned}$$

Based on this, we construct the spatial wave functions of the $QQ\bar{Q}\bar{Q}$ states in a single Gaussian form. The spatial wave function can satisfy the required symmetry property:

$$R^s = \exp[-C_{11}\mathbf{x}_1^2 - C_{22}\mathbf{x}_2^2 - C_{33}\mathbf{x}_3^2], \quad (5)$$

where C_{11}, C_{22}, and C_{33} are the variational parameters.

It is also useful to introduce the center of mass frame so that the kinetic term in the Hamiltonian of Eq. (1) can be appropriately reduced for our calculations. The kinetic term, denoted by T_c, is as follows:

$$T_c = \sum_{i=1}^{4} \frac{\mathbf{p}_i^2}{2m_i} - \frac{\mathbf{p}_{rC}^2}{2M} = \frac{\mathbf{p}_{x_1}^2}{2m_1'} + \frac{\mathbf{p}_{x_2}^2}{2m_2'} + \frac{\mathbf{p}_{x_3}^2}{2m_3'}, \quad (6)$$

where different states have different reduced masses m_i', which are listed in Table 3.

3.3 Color-spin part

In the color space, the color wave functions can be analyzed using the SU(3) group theory, where the direct product of the diquark and antidiquark components reads

$$(3_c \otimes 3_c) \otimes (\bar{3}_c \otimes \bar{3}_c) = (6_c \oplus \bar{3}_c) \otimes (\bar{6}_c \oplus 3_c). \quad (7)$$

Based on this, we get two types of color-singlet states:

$$\phi_1 = |(Q_1Q_2)^{\bar{3}}(\bar{Q}_3\bar{Q}_4)^3\rangle, \phi_2 = |(Q_1Q_2)^6(\bar{Q}_3\bar{Q}_4)^{\bar{6}}\rangle. \quad (8)$$

In the spin space, the allowed wave functions are in the diquark–antidiquark picture:

$$\begin{aligned}
&\chi_1 = |(Q_1Q_2)_1(\bar{Q}_3\bar{Q}_4)_1\rangle_2,\ \chi_2 = |(Q_1Q_2)_1(\bar{Q}_3\bar{Q}_4)_1\rangle_1,\\
&\chi_3 = |(Q_1Q_2)_1(\bar{Q}_3\bar{Q}_4)_0\rangle_1,\ \chi_4 = |(Q_1Q_2)_0(\bar{Q}_3\bar{Q}_4)_1\rangle_1,\\
&\chi_5 = |(Q_1Q_2)_1(\bar{Q}_3\bar{Q}_4)_1\rangle_0,\ \chi_6 = |(Q_1Q_2)_0(\bar{Q}_3\bar{Q}_4)_0\rangle_0.
\end{aligned} \quad (9)$$

In the notation $|(Q_1Q_2)_{\text{spin1}}(\bar{Q}_3\bar{Q}_4)_{\text{spin2}}\rangle_{\text{spin3}}$, the spin1, spin2, and spin3 represent the spin of the diquark, the spin of the antidiquark, and the total spin of the tetraquark state, respectively.

Since the flavor part and spatial parts are chosen to be fully symmetric for the (anti)diquark, the color-spin part of the total wave function should be fully antisymmetric. Combining the flavor part, we show all possible color-spin parts satisfying the Pauli principle with J^{PC} in Table 4.

In addition, it is convenient to consider the strong decay properties, and we again use the meson–meson configuration to represent color-singlet and spin wave functions. The color wave functions in the meson–meson configuration can be derived from the following direct product:

$$(3_c \otimes \bar{3}_c) \otimes (3_c \otimes \bar{3}_c) = (1_c \oplus 8_c) \otimes (1_c \oplus 8_c). \quad (10)$$

Based on Eq. (10), they can be expressed as

$$\psi_1 = |(Q_1\bar{Q}_3)^1(Q_2\bar{Q}_4)^1\rangle, \psi_2 = |(Q_1\bar{Q}_3)^8(Q_2\bar{Q}_4)^8\rangle. \quad (11)$$

Similarly, the spin wave functions in the meson–meson configuration read as

$$\begin{aligned}
&\zeta_1 = |(Q_1\bar{Q}_3)_1(Q_2\bar{Q}_4)_1\rangle_2, \zeta_2 = |(Q_1\bar{Q}_3)_0(Q_2\bar{Q}_4)_1\rangle_1,\\
&\zeta_3 = |(Q_1\bar{Q}_3)_1(Q_2\bar{Q}_4)_0\rangle_1, \zeta_4 = |(Q_1\bar{Q}_3)_1(Q_2\bar{Q}_4)_1\rangle_1,\\
&\zeta_5 = |(Q_1\bar{Q}_3)_1(Q_2\bar{Q}_4)_1\rangle_0, \zeta_6 = |(Q_1\bar{Q}_3)_0(Q_2\bar{Q}_4)_0\rangle_0.
\end{aligned} \quad (12)$$

4 Numerical analysis

4.1 Mass spectrum, internal contribution, and spatial size

In this subsection, we check the consistency between the experimental masses and the masses of traditional hadrons obtained using the variational method based on the Hamiltonian of Eq. (1) and the parameters in Table 1. We show the results in Table 5 and note that our values are relatively reliable since the deviations for most states are less than 20 MeV.

In addition, in the previous section we systematically constructed the total wave function satisfied by the Pauli principle. The corresponding total wave function can be expanded as follows:

$$|\Psi_\alpha\rangle = \sum_{ij} C_{ij}^\alpha |F\rangle |R^s\rangle |[\phi_i \chi_j]\rangle. \quad (13)$$

To study the mass of the fully heavy tetraquarks with the variational method, we calculate the Schrödinger equation $H|\Psi_\alpha\rangle = E_\alpha|\Psi_\alpha\rangle$, diagonalize the corresponding matrix, and then determine the ground state masses for the fully heavy tetraquarks. According to the corresponding variational parameters, we also give the internal mass contributions, including the quark mass part, the kinetic energy part, the confinement potential part, and the hyperfine potential

Table 3 The reduced mass m'_i in different states

States	m'_1	m'_2	m'_3	States	m'_1	m'_2	m'_3
$cc\bar{c}\bar{c}$	m_c	m_c	m_c	$cc\bar{c}\bar{b}$	m_c	$\frac{2m_cm_b}{m_c+m_b}$	$\frac{(m_c+m_b)m_c}{2(3m_c+m_b)}$
$bb\bar{b}\bar{b}$	m_b	m_b	m_b	$bb\bar{b}\bar{c}$	m_b	$\frac{2m_cm_b}{m_c+m_b}$	$\frac{(m_c+m_b)m_b}{2(3m_b+m_c)}$
$cc\bar{b}\bar{b}$	m_c	m_b	$\frac{2m_cm_b}{m_c+m_b}$	$cb\bar{c}\bar{b}$	$\frac{2m_cm_b}{m_c+m_b}$	$\frac{2m_cm_b}{m_c+m_b}$	$\frac{m_c+m_b}{2}$

Table 4 The allowed color-spin parts for each flavor configuration

Type	$J^{P(C)}$	Color-spin part			
$cc\bar{c}\bar{c}$ $bb\bar{b}\bar{b}$ $cc\bar{b}\bar{b}$	$2^{+(+)}$	$\phi_1\chi_1$			
	$1^{+(-)}$	$\phi_1\chi_2$			
	$0^{+(+)}$	$\phi_1\chi_5$	$\phi_2\chi_6$		
$cc\bar{c}\bar{b}$ $bb\bar{b}\bar{c}$	2^+	$\phi_1\chi_1$			
	1^+	$\phi_1\chi_2$	$\phi_1\chi_3$	$\phi_2\chi_4$	
	0^+	$\phi_1\chi_5$	$\phi_2\chi_6$		
$cb\bar{c}\bar{b}$	2^{++}	$\phi_1\chi_1$	$\phi_2\chi_1$		
	1^{+-}	$\phi_1\chi_2$	$\phi_2\chi_2$	$\frac{1}{\sqrt{2}}(\phi_1\chi_3+\phi_1\chi_4)$	
		$\frac{1}{\sqrt{2}}(\phi_2\chi_3+\phi_2\chi_4)$			
	1^{++}	$\frac{1}{\sqrt{2}}(\phi_1\chi_3-\phi_1\chi_4)$		$\frac{1}{\sqrt{2}}(\phi_2\chi_3-\phi_2\chi_4)$	
	0^{++}	$\phi_1\chi_5$	$\phi_2\chi_5$	$\phi_1\chi_6$	$\phi_2\chi_6$

part. For comparison, we also show the lowest meson–meson thresholds for the tetraquarks with different quantum numbers and their internal contributions. This is how we define the binding energy:

$$B_T = M_{\text{tetraquark}} - M_{\text{meson1}} - M_{\text{meson2}}, \tag{14}$$

where $M_{\text{tetraquark}}$, M_{meson1}, and M_{meson2} are the masses of the tetraquark and the two mesons at the lowest threshold allowed in the rearrangement decay of the tetraquark, respectively. To facilitate the discussion in the next subsection, we also define the V^C, which is the sum of the Coulomb potential and the linear potential.

Here, it is also useful to investigate the spatial size of the tetraquarks, which is strongly related to the magnitude of the various kinetic energies and the potential energies between the quarks. It is also important to understand the relative lengths between the quarks in the tetraquarks and their lowest thresholds, and the relative distance between the heavier quarks is generally shorter than that between the lighter quarks [61]. This tendency is also maintained in each tetraquark state according to the corresponding tables.

4.1.1 Magnetic moments, transition magnetic moments, and radiative decay widths

The magnetic moment of hadrons is a physical quantity that reflects their internal structures [121]. The total magnetic moment $\vec{\mu}_{\text{total}}$ of a compound system contains the spin magnetic moment $\vec{\mu}_{\text{spin}}$ and the orbital magnetic moment $\vec{\mu}_{\text{orbital}}$ from all of its constituent quarks. For ground hadron states, their contribution of the orbital magnetic moment $\vec{\mu}_{\text{orbital}}$ is zero, and so we only concentrate on the spin magnetic moment $\vec{\mu}_{\text{spin}}$. The explicit expression for the spin magnetic moment $\vec{\mu}_{\text{spin}}$ is written as

$$\vec{\mu}_{\text{spin}} = \sum_i \mu_i \vec{\sigma}_i = \sum_i \frac{Q_i^{\text{eff}}}{2M_i^{\text{eff}}}\vec{\sigma}_i, \tag{15}$$

where Q_i^{eff} and M_i^{eff} are the effective charge and effective mass of the i-th constituent quark, respectively. The $\vec{\sigma}_i$ denotes the Pauli spin matrix of the i-th constituent quark. According to Ref. [122], the effective charge of the quark is affected by other quarks in the inner hadron. We now assume that the effective charge is linearly dependent on the charge of the shielding quarks. Therefore, the effective charge Q_i^{eff} is defined as

$$Q_i^{\text{eff}} = Q_i + \sum_{i\neq j}\alpha_{ij}Q_j, \tag{16}$$

where Q_i is the bare charge of the i-th constituent quark, and α_{ij} is a corrected parameter that reflects the extent to which the charge of other quarks affects the charge of the i-th quark. To simplify the calculation, we also set α_{ij} always equal to 0.033 according to Ref. [122]. The effective quark masses M_i^{eff} contain the contributions from both the bare quark mass terms and the interaction terms in the chromomagnetic model, and their values are taken from Ref. [123].

To obtain the magnetic moment of the discussed hadron, we calculate the z-component of the magnetic moment operator $\hat{\mu}^z$ sandwiched by the corresponding total wave function Ψ_α (Eq. (9)). Now, only the spin part of the total wave function is involved. The total spin wave functions of the discussed hadrons are written as

$$|\chi_{\text{total}}\rangle = C_1\chi_1 + C_2\chi_2 + \cdots \quad (17)$$

Based on this, we can quantitatively obtain the magnetic moment of the discussed hadron

$$\begin{aligned}\mu &= \langle\Psi_\alpha|\hat{\mu}^z|\Psi_\alpha\rangle = \langle\chi_\alpha|\hat{\mu}^z|\chi_\alpha\rangle \\ &= C_1^2\mu(\chi_1) + C_2^2\mu(\chi_2) + \cdots + 2C_1C_2\mu^{\text{tr}}(\chi_1,\chi_2) + \cdots\end{aligned} \quad (18)$$

where μ^{tr} is the cross-term representing the transition moment, and C_1, C_2 are the eigenvectors of the given mixing state [124]. Similarly, the transition magnetic moments between the hadrons can be obtained as $\mu_{H'\to H\gamma} = \langle\Psi_{H_f}|\hat{\mu}^z|\Psi_{H_i}\rangle$.

According to Eq. (18), the numerical values for the magnetic moments of the traditional hadrons have been listed in Table 5. Here, $\mu_N = e/2m_N$ is the nuclear magnetic moment with $m_N = 938$ MeV as the nuclear mass, which is the unit of the magnetic moment. For comparison, we also show the experimental values and other theoretical results from Refs. [121,122,124–127]. Because of the $\mu_Q = -\mu_{\bar{Q}}$, the magnetic moment of all the $J^P = 0^+$ ground mesons and tetraquarks and the ground states with certain C-parity is 0.

The decay property is another important aspect to investigate the nature of the exotic hadron. According to the transition magnetic moments in the above subsection, we can further obtain the radiative decay widths around fully heavy tetraquarks [128–137].

$$\Gamma = \frac{|\mathbf{k}|^2}{\pi}\frac{2}{2J_i+1}\frac{M_f}{M_i}\sum_{M_{J_f},M_{J_i}}|\mathcal{M}_{M_{J_f},M_{J_i}}|^2, \quad (19)$$

where J_i and J_f are the total angular momentum of the initial and final hadrons, respectively. The M_i and M_f in Eq. (19) represent initial and final hadron masses, respectively.

4.1.2 Relative decay widths of tetraquarks

In addition to radiative decay, we also consider the rearrangement strong decay properties for fully heavy tetraquarks. Based on Eqs. (10–12), the color wave function also falls into two categories: the color-singlet $\psi_1 = |(Q_1\bar{Q}_3)^1(Q_2\bar{Q}_4)^1\rangle$, which can easily decay into two S-wave mesons, and the color-octet $\psi_2 = |(Q_1\bar{Q}_3)^8(Q_2\bar{Q}_4)^8\rangle$, which can only fall apart by gluon exchange. Thus we transform the total wave functions Ψ_α into the new configuration,

$$|\Psi_\alpha\rangle = \sum_{ij} C'^{\alpha}_{ij}|F\rangle|R^s\rangle|[\psi_i\zeta_j]\rangle. \quad (20)$$

Among the decay behaviors of the tetraquarks, one decay mode is that the quarks simply fall apart into the final decay channels without quark pair creation or annihilation, which is denoted as "Okubo–Zweig–Iizuka (OZI)-superallowed" decays. In this part, we will only focus on this type of decay channel. For two-body decay by L-wave, the partial decay width is expressed as [72,110,138–140]:

$$\Gamma_i = \gamma_i\alpha\frac{k^{2L+1}}{m^{2L}}|c_i|^2, \quad (21)$$

where α is an effective coupling constant, c_i is the overlap corresponding exactly to C'^{α}_{ij} of Eq. (20), m is the mass of the initial state, and k is the momentum of the final state in the rest frame of the initial state. For the decays of the S-wave tetraquarks, $(k/m)^{-2}$ is of order $\mathcal{O}(10^{-2})$ or even smaller, so all higher-wave decays are suppressed, and thus we only need to consider the S-wave decays. As for γ_i, it is determined by the spatial wave functions of the initial and final states, which are different for each decay process. In the quark model in the heavy quark limit, the spatial wave functions of the ground S-wave pseudoscalar and the vector meson are the same. The relations of γ_i for fully heavy tetraquarks are given in Table 6. Based on this, the branching fraction is proportional to the square of the coefficient of the corresponding component in the eigenvectors, and the strong decay phase space, i.e., $k\cdot|c_i|^2$, for each decay mode. From the value of $k\cdot|c_i|^2$, one can roughly estimate the ratios of the relative decay widths between different decay processes of different initial tetraquarks.

In the following subsections, we concretely discuss all possible configurations for fully heavy tetraquarks.

4.2 $cc\bar{c}\bar{c}$ and $bb\bar{b}\bar{b}$ states

First we investigate the $cc\bar{c}\bar{c}$ and $bb\bar{b}\bar{b}$ systems. There are two $J^{PC} = 0^{++}$ states, one $J^{PC} = 1^{+-}$ state, and one $J^{PC} = 2^{++}$ state according to Table 4. We show the masses of the ground states, the variational parameters, the internal mass contributions, the relative lengths between the quarks, their lowest meson–meson thresholds, the specific wave function, the magnetic moments, the transition magnetic moments, the radiative decay widths, and the rearrangement strong width ratios in Tables 7, 8, and 9, respectively.

Here, we take the $J^{PC} = 0^{++}$ $bb\bar{b}\bar{b}$ ground state as an example, and the others have similar discussions, according to Tables 7, 8, and 9. We now analyze the numerical results obtained from the variational method. For the $J^{PC} = 0^{++}$ $bb\bar{b}\bar{b}$ ground state, its mass is 19240.0 MeV and the corresponding binding energy B_T is +461.9 MeV. Its variational

Table 5 Masses and magnetic moments of some ground hadrons obtained from the theoretical calculations. M_{result}, μ_{results}, μ_{bag}, $\mu_{\mathrm{the}(1)}$, and $\mu_{the(2)}$ are theoretical masses and magnetic moments for Eq. (1), Eq. (15), and Refs. [121,122,124], respectively. M_{exp} and μ_{exp} are the observed values of masses and magnetic moments. The masses and errors are in units of MeV. The magnetic moment is in units of the nuclear magnetic moment μ_N. The variational parameter is in units of fm^{-2}

Hadron	Σ^+	Σ^0	Σ^-	Ξ^0	Ξ^-	Σ_c^{++}	Σ_c^+	Σ_c^0	Σ_c^{*++}	Σ_c^{*+}	Σ_c^{*0}	Σ_b^+	Σ_b^0	Σ_b^-	Σ_b^{*+}	Σ_b^{*0}	Σ_b^{*-}
M_{result}	1187.7			1295.4		2445.2			2518.3			5832.1			5860.8		
Parameters	2.1			3.3		2.1			2.0			2.1			2.0		
	3.1			2.9		3.7			3.4			4.0			3.4		
M_{exp}	1189.4			1314.9		2454.0			2851.4			5811.3			5832.1		
Error	-1.7			-19.5		-8.8			-0.1			20.8			28.7		
μ_{result}	2.53	0.75	-1.04	-1.31	-0.52	2.34	0.55	-1.24	4.09	1.38	-1.32	2.37	0.58	-1.21	3.48	0.78	-1.92
μ_{bag} [124]	2.72	0.86	-1.01	-1.58	-0.64	2.13	0.41	-1.31	4.07	1.39	-1.29	2.23	0.58	-1.07	3.29	0.76	-1.77
$\mu_{the(1)}$[121]	2.74	0.84	-1.06	-1.47	-0.52	2.36	0.50	-1.37	4.09	1.30	-1.49						
$\mu_{the(2)}$ [122]	2.46	0.47	-1.10	-1.61	-0.65	3.57	1.96	0.04									
μ_{exp}	2.46		-1.16	-1.25	-0.65								6.14	2.70			-2.02
Hadron	D^{*0}	D^{*+}	D_s^{*+}	B^{*0}	B^{*+}	B_s^{*0}	J/ψ	η_c	Υ	η_b	B_c	B_c^*	Δ^{++}	Δ^+	Δ^0	Δ^0	Ω^-
M_{result}	1996.9		2093.3	5363.6		5434.7	3092.2	2998.5	9468.9	9389.0	6287.9	6350.5	1245.6				1675.8
Parameters	3.8		6.2	4.2		7.5	12.5	15.0	49.7	57.4	22.9	20.2	1.8				3.3
M_{exp}	2010.3		2112.2	5324.7		5415.4	3096.9	2983.9	9460.3	9399.0	6274.9	(6332)	1232.0				1672.5
Error	-13.4		-18.9	38.8		19.3	-4.7	14.6	8.6	10.0	13.0	(17.5)	13.6				3.1
μ_{result}	-1.37	1.24	1.00	-0.78	1.83	0.51	0	-	0	-	-	0.44	5.57	-2.78	0	-2.78	-1.86
μ_{bag} [124]	-0.98	1.21	1.08	-0.53	1.21	1.01	0	-	0	-	-	0.52	5.70	2.85	0	-2.85	-2.20
$\mu_{the(1)}$ [121]	-1.49	1.30	1.07				0	-					5.58	2.79	0	-2.79	-1.88

Table 6 The approximate relation for γ_i for the $QQ\bar{Q}\bar{Q}$ system

States	γ_i
$cc\bar{c}\bar{c}$	$\gamma_{J/\psi J/\psi} = \gamma_{\eta_c J/\psi} = \gamma_{\eta_c\eta_c}$
$bb\bar{b}\bar{b}$	$\gamma_{\Upsilon\Upsilon} = \gamma_{\eta_b\Upsilon} = \gamma_{\eta_b\eta_b}$
$cc\bar{b}\bar{b}$	$\gamma_{B_c^* B_c^*} = \gamma_{B_c B_c^*} = \gamma_{B_c B_c}$
$cc\bar{c}\bar{b}$	$\gamma_{J/\psi B_c^*} = \gamma_{J/\psi B_c} = \gamma_{\eta_c B_c^*} = \gamma_{\eta_c B_c}$
$bb\bar{b}\bar{c}$	$\gamma_{\Upsilon \bar{B}_c^*} = \gamma_{\Upsilon \bar{B}_c} = \gamma_{\eta_b \bar{B}_c^*} = \gamma_{\eta_b \bar{B}_c}$
$cb\bar{c}\bar{b}$	$\gamma_{J/\psi\Upsilon} = \gamma_{J/\psi\eta_b} = \gamma_{\eta_c\Upsilon} = \gamma_{\eta_c\eta_b}$
	$\gamma_{B_c^*\bar{B}_c^*} = \gamma_{B_c^*\bar{B}_c} = \gamma_{B_c\bar{B}_c^*} = \gamma_{B_c\bar{B}_c}$

parameters are given as $C_{11} = 7.7$ fm^{-2}, $C_{22} = 7.7$ fm^{-2}, and $C_{33} = 11.4$ fm^{-2}, giving roughly the inverse ratios of the size for the diquark, the antidiquark, and between the center of the diquark and the antidiquark, respectively. We naturally find that C_{11} is equal to C_{22}, so the distance of $(b-b)$ would be equal to that of $(\bar{b}-\bar{b})$, and the reason is that the $bb\bar{b}\bar{b}$ system is a neutral system.

The total wave function in the diquark–antidiquark configuration is given by

$$|\Psi_{\mathrm{tot}}\rangle = -0.936|F\rangle|R^s\rangle|[\phi_2\chi_6]\rangle + 0.352|F\rangle|R^s\rangle|[\phi_1\chi_5]\rangle. \quad (22)$$

The meson–meson configuration is connected to the diquark–antidiquark configuration by a linear transformation. We then obtain the total wave function in the meson–meson configuration:

$$|\Psi_{\mathrm{tot}}\rangle = 0.558|F\rangle|R^s\rangle|[\psi_1\zeta_5]\rangle + 0.560|F\rangle|R^s\rangle|[\psi_1\zeta_6]\rangle + 0.021|F\rangle|R^s\rangle|[\psi_2\zeta_5]\rangle + 0.612|F\rangle|R^s\rangle|[\psi_2\zeta_6]\rangle. \quad (23)$$

According to Eq. (23), we are sure that the overlaps c_i of $\eta_b\eta_b$ and $\Upsilon\Upsilon$ are 0.560 and 0.558, respectively. Then, based on Eq. (21), the rearrangement strong width ratios are

$$\frac{\Gamma_{T_{b^2\bar{b}^2}(19240.0,0^{++})\to\Upsilon\Upsilon}}{\Gamma_{T_{b^2\bar{b}^2}(19240.0,0^{++})\to\eta_b\eta_b}} = 1{:}1.2, \quad (24)$$

i.e., both the $\Upsilon\Upsilon$ and $\eta_b\eta_b$ are dominant decay channels for the $T_{b^2\bar{b}^2}(19240.0, \Upsilon\Upsilon)$ state.

As for the magnetic moments of the $cc\bar{c}\bar{c}$ and $bb\bar{b}\bar{b}$ ground states, their values are all 0, because the same quark and antiquark have exactly opposite magnetic moments, which cancel each other out. We also discuss the transition magnetic moment of the $T_{b^2\bar{b}^2}(19303.9, 1^{+-}) \to T_{b^2\bar{b}^2}(19240.0, 0^{++})\gamma$ process. We construct their flavor ⊗ spin wave functions as

$$|\Psi\rangle^{S=1;S_s=0}_{T_{b^2\bar{b}^2}(1^{+-})} = |R^s\rangle|\psi\rangle|bb\bar{b}\bar{b}\rangle|\frac{1}{\sqrt{2}}(\uparrow\uparrow\downarrow\downarrow - \downarrow\downarrow\uparrow\uparrow)\rangle$$
$$|\Psi\rangle^{S=0;S_s=0}_{T_{b^2\bar{b}^2}(0^{++})} = |R^s\rangle|\psi\rangle|bb\bar{b}\bar{b}\rangle$$
$$|0.352\frac{1}{\sqrt{3}}(\uparrow\uparrow\downarrow\downarrow + \downarrow\downarrow\uparrow\uparrow) + \cdots\rangle. \quad (25)$$

And then the transition magnetic momentum of the $T_{b^2\bar{b}^2}(19303.9, 1^{+-}) \to T_{b^2\bar{b}^2}(19240.0, 0^{++})\gamma$ process can be given by the z-component of the magnetic moment operator $\hat{\mu^z}$ sandwiched by the flavor-spin wave functions of the $T_{b^2\bar{b}^2}(19303.9, 1^{+-})$ and $T_{b^2\bar{b}^2}(19240.0, 0^{++})$. Therefore, the corresponding transition magnetic momentum is

$$\mu_{T_{b^2\bar{b}^2}(1^{+-})\to T_{b^2\bar{b}^2}(0^{++})} = \langle\Psi^{1^{+-}}_{\text{tot}}|\hat{\mu^z}|\Psi^{0^{++}}_{\text{tot}}\rangle$$
$$= 0.352 \times \frac{1}{\sqrt{6}}(4\mu_b - 4\mu_{\bar{b}}) = -0.072\ \mu_N. \quad (26)$$

As for the transition magnetic moment of the $T_{b^2\bar{b}^2}(19327.9, 2^{++}) \to T_{b^2\bar{b}^2}(19240.0, 0^{++})\gamma$ process, its value is 0 due to the C-parity conservation restriction.

Furthermore, according to Eqs. (19) and (26), we also obtain the corresponding radiative decay widths

$$\Gamma_{T_{b^2\bar{b}^2}(19303.9,1^{+-})\to T_{c^2\bar{b}^2}(19240.0,0^{++})\gamma} = 2.8\,\text{keV}, \quad (27)$$
$$\Gamma_{T_{b^2\bar{b}^2}(19327.9,2^{++})\to T_{c^2\bar{b}^2}(19240.0,0^{++})\gamma} = 0\,\text{keV}. \quad (28)$$

4.2.1 Relative distances and symmetry

Here, we concentrate on the relative distances between the (anti)quarks in tetraquarks. Looking at the relative distances in Table 9, we find that the relative distances of (1,2) and (3,4) pairs are the same, and other relative distances are the same in all the $cc\bar{c}\bar{c}$ and $bb\bar{b}\bar{b}$ states. This is due to the permutation symmetry for the ground state wave function in each tetraquark [65]. For the $c_1c_2\bar{c}_3\bar{c}_4$ and $b_1b_2\bar{b}_3\bar{b}_4$ states, they need to satisfy the Pauli principle for identical particles as follows:

$$A_{12}|\Psi_{\text{tot}}\rangle = A_{34}|\Psi_{\text{tot}}\rangle = -|\Psi_{\text{tot}}\rangle, \quad (29)$$

where the operator A_{ij} means exchanging the coordinates of Q_i ($\bar{Q}_i$) and Q_j ($\bar{Q}_j$).

Meanwhile, they are pure neutral particles with definite C-parity, so the permutation symmetries for total wave functions are as follows:

$$A_{12-34}|\Psi_{\text{tot}}\rangle = \pm|\Psi_{\text{tot}}\rangle, \quad (30)$$

where A_{12-34} means that the coordinates of the diquark and the antidiquark are exchanged.

Based on this, the relationship of the relative distances for all the $c_1c_2\bar{c}_3\bar{c}_4$ and $b_1b_2\bar{b}_3\bar{b}_4$ states can be obtained as follows:

$$\begin{aligned}
&\langle\Psi_{\text{tot}}|\mathbf{r}_1 - \mathbf{r}_3|\Psi_{\text{tot}}\rangle \\
&= \langle\Psi_{\text{tot}}|A^{-1}_{12}A_{12}|\mathbf{r}_1 - \mathbf{r}_3|A^{-1}_{12}A_{12}|\Psi_{\text{tot}}\rangle \\
&= \langle\Psi_{\text{tot}}|\mathbf{r}_2 - \mathbf{r}_3|\Psi_{\text{tot}}\rangle \\
&= \langle\Psi_{\text{tot}}|A^{-1}_{34}A_{34}|\mathbf{r}_2 - \mathbf{r}_3|A^{-1}_{34}A_{34}|\Psi_{\text{tot}}\rangle \\
&= \langle\Psi_{\text{tot}}|\mathbf{r}_2 - \mathbf{r}_4|\Psi_{\text{tot}}\rangle \\
&= \langle\Psi_{\text{tot}}|A^{-1}_{12}A_{12}|\mathbf{r}_2 - \mathbf{r}_4|A^{-1}_{12}A_{12}|\Psi_{\text{tot}}\rangle \\
&= \langle\Psi_{\text{tot}}|\mathbf{r}_1 - \mathbf{r}_4|\Psi_{\text{tot}}\rangle, \quad (31)
\end{aligned}$$

and

$$\begin{aligned}
&\langle\Psi_{\text{tot}}|\mathbf{r}_1 - \mathbf{r}_2|\Psi_{\text{tot}}\rangle \\
&= \langle\Psi_{\text{tot}}|A^{-1}_{12-34}A_{12-34}|\mathbf{r}_1 - \mathbf{r}_2||A^{-1}_{12-34}A_{12-34}|\Psi_{\text{tot}}\rangle \\
&= \langle\Psi_{\text{tot}}|\mathbf{r}_3 - \mathbf{r}_4|\Psi_{\text{tot}}\rangle. \quad (32)
\end{aligned}$$

Obviously, our theoretical derivations are in perfect agreement with the calculated results in Table 9.

We can also prove that three Jacobi coordinates, $\mathbf{R}_{1,2} = \mathbf{r}_1 - \mathbf{r}_2$, $\mathbf{R}_{3,4} = \mathbf{r}_3 - \mathbf{r}_4$, and $\mathbf{R}' = 1/2(\mathbf{r}_1 + \mathbf{r}_2 - \mathbf{r}_3 - \mathbf{r}_4)$, are orthogonal to each other for all the $cc\bar{c}\bar{c}$ and $bb\bar{b}\bar{b}$ states:

$$\begin{aligned}
&\langle\Psi_{\text{tot}}|(\mathbf{R}_{1,2}\cdot\mathbf{R}_{3,4})|\Psi_{\text{tot}}\rangle \\
&= \langle\Psi_{\text{tot}}|(34)^{-1}(34)|(\mathbf{R}_{1,2}\cdot\mathbf{R}_{3,4})|(34)^{-1}(34)|\Psi_{\text{tot}}\rangle \\
&= -\langle\Psi_{\text{tot}}|(\mathbf{R}_{1,2}\cdot\mathbf{R}_{3,4})|\Psi_{\text{tot}}\rangle = 0, \quad (33) \\
&\langle\Psi_{\text{tot}}|(\mathbf{R}_{1,2}\cdot\mathbf{R}')|\Psi_{\text{tot}}\rangle \\
&= \langle\Psi_{\text{tot}}|(12)^{-1}(12)|(\mathbf{R}_{1,2}\cdot\mathbf{R}')|(12)^{-1}(12)|\Psi_{\text{tot}}\rangle \\
&= -\langle\Psi_{\text{tot}}|(\mathbf{R}_{1,2}\cdot\mathbf{R}')|\Psi_{\text{tot}}\rangle = 0, \quad (34)
\end{aligned}$$

and

$$\begin{aligned}
&\langle\Psi_{\text{tot}}|(\mathbf{R}_{3,4}\cdot\mathbf{R}')|\Psi_{\text{tot}}\rangle \\
&= \langle\Psi_{\text{tot}}|(34)^{-1}(34)|(\mathbf{R}_{1,2}\cdot\mathbf{R}')|(34)^{-1}(34)|\Psi_{\text{tot}}\rangle \\
&= -\langle\Psi_{\text{tot}}|(\mathbf{R}_{3,4}\cdot\mathbf{R}')|\Psi_{\text{tot}}\rangle = 0. \quad (35)
\end{aligned}$$

According to the relative distances in Table 9 and the relationship of Eqs. (29–35), the relative positions of the four valence quarks can be well described for all the $cc\bar{c}\bar{c}$ and $bb\bar{b}\bar{b}$ states. Meanwhile, using the relative distances between (anti)quarks and the orthogonal relation, we can also determine the relative distance of (12)–(34), which is consistent with our results in Table 9. We can also give the relative position of R_c and the spherical radius of the tetraquarks. Here, we define R_c as the geometric center of the four quarks (the center of the sphere). Based on these results, we show the spatial distribution of the four valence quarks for the $J^{PC} = 0^{++}$ $bb\bar{b}\bar{b}$ ground state in Fig. 1.

In the quark model, a compact tetraquark state has no color-singlet substructure, while a hadronic molecule is a loosely bound state which contains several color-singlet

Table 7 The masses, binding energies, variational parameters, the internal contribution, total wave functions, magnetic moments, transition magnetic moments, radiative decay widths, rearrangement strong width ratios, and the relative lengths between the quarks for the $J^{PC}=0^{++}$, 1^{+-} $cc\bar{c}\bar{c}$ states and their lowest meson–meson thresholds. Here, (i,j) denotes the contribution of the i-th and j-th quarks. The number is given as $i=1$ and 2 for the quarks, and 3 and 4 for the antiquark. The masses and corresponding contributions are given in units of MeV, and the relative lengths (variational parameters) are in units of fm (fm^{-2}). Meanwhile, we present a comparison with the other two CMI models [110,123] to further secure the effective quark mass

$cc\bar{c}\bar{c}$		The contribution from each term			Relative Lengths (fm)		
$J^{PC}=0^{++}$		Value	$\eta_c\eta_c$	Difference	(i,j)	Value	$\eta_c\eta_c$
Mass/B_T		6384.4	5997.0	387.4	(1,2)	0.406	
Variational Parameters (fm^{-2})	C_{11}	7.7	15.0		(1,3)	0.371	$0.290(\eta_c)$
	C_{22}	7.7	15.9				
	C_{33}	11.4	-		(2,3)	0.371	
Quark Mass		7672.0	7672.0	0.0	(1,4)	0.371	
Confinement Potential		-2083.8	-2440.4	356.6	(2,4)	0.371	$0.290(\eta_c)$
Kinetic Energy		814.0	915.1	-101.1	(3,4)	0.406	
CS Interaction		22.7	-150.0	172.7	(1,2)-(3,4):		0.235 fm
V^C	(1,2)	-6.8			Radius:		0.235 fm
	(2,3)	-26.1					
	(1,4)	-26.1			(1,3)	-26.1	$-237.2(\eta_c)$
	Subtotal	-117.8	-474.4	356.6	(3,4)	-6.8	
Total Contribution		718.9	291.0	427.9	(2,4)	-26.1	$-237.2(\eta_c)$

Total Wave function:

$$\Psi_{tot}=0.535|F\rangle|R^s\rangle|[\phi_1\chi_5]\rangle-0.845|F\rangle|R^s\rangle|[\phi_2\chi_6]\rangle=0.612|F\rangle|R^s\rangle|[\psi_1\zeta_5]\rangle$$
$$+0.443|F\rangle|R^s\rangle|[\psi_1\zeta_6]\rangle=0.612|F\rangle|R^s\rangle|[\psi_1\zeta_5]\rangle+0.443|F\rangle|R^s\rangle|[\psi_1\zeta_6]\rangle$$

The rearrangement strong width ratios:

$\Gamma_{T_{c^2\bar{c}^2}(6384.3,0^{++})\to J/\psi J/\psi}:\Gamma_{T_{c^2\bar{c}^2}(6384.3,0^{++})\to\eta_c\eta_c}=1:2.8$

The radiative decay widths: $\Gamma_{T_{c^2\bar{c}^2}(6482.7,2^{++})\to T_{c^2\bar{c}^2}(6384.3,0^{++})\Upsilon}=0$ keV

$\Gamma_{T_{c^2\bar{c}^2}(6451.5,1^{+-})\to T_{c^2\bar{c}^2}(6384.3,0^{++})\Upsilon}=238.1$ keV

The magnetic moments: $\mu_{T_{c^2\bar{c}^2}(6384.3,0^{++})}=\langle\Psi_{tot}^{0^{++}}|\hat{\mu^z}|\Psi_{tot}^{0^{++}}\rangle=0$

The transition magnetic moments:

$\mu_{T_{c^2\bar{c}^2}(6451.5,1^{+-})\to T_{c^2\bar{c}^2}(6384.3,0^{++})\gamma}=\langle\Psi_{tot}^{1^{+-}}|\hat{\mu^z}|\Psi_{tot}^{0^{++}}\rangle=0.671\ \mu_N$

$\mu_{T_{c^2\bar{c}^2}(6482.7,2^{++})\to T_{c^2\bar{c}^2}(6384.3,0^{++})\gamma}=\langle\Psi_{tot}^{2^{++}}|\hat{\mu^z}|\Psi_{tot}^{0^{++}}\rangle=0$

Overall	Present Work Contribution	Value	CMI Model Ref. [110]	CMI Model Ref. [123]
c-quark: m_c^{eff}	$2m_c$	3836.0		
	$\frac{\mathbf{p}_{x_1}^2}{2m_1'}$	233.9		
	$\frac{m_{\bar{c}}}{m_c+m_{\bar{c}}}\frac{\mathbf{p}_{x_3}^2}{2m_3'}$	123.1		
	$V^C(12)$	-6.8	$-\frac{1}{4}m_{cc}$	
	$\frac{1}{2}[V^C(13)+V^C(14)$ $+V^C(23)+V^C(24)]$	-52.1	-792.9 $\frac{5}{4}m_{c\bar{c}}$	$2m_c$
	$-D$	-983.0	3835.6	3449.6
	Subtotal	3151.1	3042.7	3449.6
$\bar{c}$-quark: $m_{\bar{c}}^{eff}$	$2m_c$	3836.0		
	$\frac{\mathbf{p}_{x_2}^2}{2m_2'}$	233.9		
	$\frac{m_{\bar{c}}}{m_c+m_{\bar{c}}}\frac{\mathbf{p}_{x_3}^2}{2m_3'}$	123.1		
	$V^C(34)$	-6.8	$-\frac{1}{4}m_{cc}$	
	$\frac{1}{2}[V^C(13)+V^C(14)$ $+V^C(23)+V^C(24)]$	-52.1	-792.4 $\frac{5}{4}m_{c\bar{c}}$	$2m_c$
	$-D$	-983.0	3835.6	3449.6
	Subtotal	3151.1	3042.7	3449.6
CS Interaction	$\frac{3}{4}V^{SS}(12)$	11.4	$4v_{cc}$ 14.2	$4C_{cc}$ 21.2
	$\frac{3}{4}V^{SS}(12)$	11.4	$4v_{\bar{c}\bar{c}}$ 14.2	$4C_{\bar{c}\bar{c}}$ 21.2
	Subtotal	22.7	28.4	42.4
Matrix nondiagonal element		-40.5	-60.9	159.2
Total contribution		6384.4	6044.9	7016.0

$J^{PC}=1^{+-}$		Value	$J/\psi\eta_c$	Difference	Relative Lengths (fm)		
Mass/B_T		6451.5	6090.7	360.8	(i,j)	Value	$J/\psi\eta_c$
Variational Parameters (fm^{-2})	C_{11}	9.1	15.0		(1.2)	0.373	
	C_{22}	9.1	12.5		(1,3)	0.395	$0.290(\eta_c)$
	C_{33}	7.3	-				
Quark Mass		7672.0	7672.0	0.0	(2,3)	0.395	
Confinement Potential		-1998.8	-2367.4	368.6	(1,4)	0.395	
Kinetic Energy		767.2	839.0	-71.8	(2,4)	0.395	$0.318(J/\psi)$
CS Interaction		1.5	-53.9	54.4	(3,4)	0.373	
V^C	(1,2)	-19.4			(1,2)-(3,4):		0.294 fm
	(2,3)	1.5			Radius:		0.235 fm
	(1,4)	1.5			(1,3)	1.5	$-237.2(\eta_c)$
	Subtotal	-32.8	-401.4	368.6	(3,4)	-19.4	
Total Contribution		718.9	291.0	427.9	(2,4)	-1.5	$-164.2(J/\psi)$

Total Wave function: $\Psi_{tot}=|F\rangle|R^s\rangle|[\phi_1\chi_2]\rangle=-0.408|F\rangle|R^s\rangle|[\psi_1\zeta_2]\rangle$

$$-0.408|F\rangle|R^s\rangle|[\psi_1\zeta_3]\rangle+0.577|F\rangle|R^s\rangle|[\psi_2\zeta_5]\rangle+0.577|F\rangle|R^s\rangle|[\psi_2\zeta_6]\rangle$$

The rearrangement strong decay channel: $J/\psi\eta_c$

The radiative decay widths:

$\Gamma_{T_{c^2\bar{c}^2}(6482.7,2^{++})\to T_{c^2\bar{c}^2}(6451.5,1^{+-})\Upsilon}=70.4$ keV

$\Gamma_{T_{c^2\bar{c}^2}(6451.5,1^{+-})\to T_{c^2\bar{c}^2}(6384.3,0^{++})\Upsilon}=238.1$ keV

The magnetic moments: $\mu_{T_{c^2\bar{c}^2}(6451.5,1^{+-})}=\langle\Psi_{tot}^{1^{+-}}|\hat{\mu^z}|\Psi_{tot}^{1^{+-}}\rangle=0$

The transition magnetic moments:

$\mu_{T_{c^2\bar{c}^2}(6482.7,2^{++})\to T_{c^2\bar{c}^2}(6451.4,1^{+-})\gamma}=\langle\Psi_{tot}^{2^{++}}|\hat{\mu^z}|\Psi_{tot}^{1^{+-}}\rangle=0.750\mu_N$

$\mu_{T_{c^2\bar{c}^2}(6451.5,1^{+-})\to T_{c^2\bar{c}^2}(6384.3,0^{++})\gamma}=\langle\Psi_{tot}^{1^{+-}}|\hat{\mu^z}|\Psi_{tot}^{0^{++}}\rangle=0.335\mu_N$

Overall	Contribution	Value	Ref. [110]	Ref. [123]
c-quark: m_c^{eff}	$2m_c$	3836.0		
	$\frac{\mathbf{p}_{x_1}^2}{2m_1'}$	277.2		
	$\frac{m_{\bar{c}}}{m_c+m_{\bar{c}}}\frac{\mathbf{p}_{x_3}^2}{2m_3'}$	111.2	$\frac{1}{2}m_{cc}$	
	$V^C(12)$	-19.4	1585.8	
	$\frac{1}{2}[V^C(13)+V^C(14)$ $+V^C(23)+V^C(24)]$	3.0	$\frac{1}{2}m_{c\bar{c}}$	$2m_c$
	$-D$	-983.0	1534.3	3449.6
	Subtotal	3225.0	3120.0	3449.6
$\bar{c}$-quark: $m_{\bar{c}}^{eff}$	$2m_c$	3836.0		
	$\frac{\mathbf{p}_{x_2}^2}{2m_2'}$	277.2		
	$\frac{m_{\bar{c}}}{m_c+m_{\bar{c}}}\frac{\mathbf{p}_{x_3}^2}{2m_3'}$	111.2	$\frac{1}{2}m_{cc}$	
	$V^C(12)$	-19.4	1585.8	
	$\frac{1}{2}[V^C(13)+V^C(14)$ $+V^C(23)+V^C(24)]$	3.0	$\frac{1}{2}m_{c\bar{c}}$	$2m_c$
$-D$	-983.0	1534.3	3449.6	
	Subtotal	3225.0	3120.0	3449.6
CS Interaction	$\frac{1}{2}V^{SS}(12)$	8.7	$\frac{8}{3}v_{cc}$ 9.5	$\frac{8}{3}C_{cc}$ 14.1
	$\frac{1}{2}V^{SS}(34)$	8.7	$\frac{8}{3}v_{\bar{c}\bar{c}}$ 9.5	$\frac{8}{3}C_{\bar{c}\bar{c}}$ 14.1
	$-\frac{1}{4}(V^{SS}(13)+V^{SS}(14)$ $+V^{SS}(23)+V^{SS}(24)$	-15.8	$-\frac{16}{3}v_{c\bar{c}}$ -28.4	$-\frac{16}{3}C_{c\bar{c}}$ -28.2
	Subtotal	1.5	-9.5	0.0
Total contribution		6451.5	6231.0	6899.0

Table 8 The masses, binding energies, variational parameters, the internal contribution, total wave functions, magnetic moments, transition magnetic moments, radiative decay widths, rearrangement strong width ratios, and the relative lengths between quarks for the $J^{PC}=2^{++}$ $cc\bar{c}\bar{c}$ and $bb\bar{b}\bar{b}$ states and their lowest meson–meson thresholds. The notation is the same as that in Table 7

$cc\bar{c}\bar{c}$		The contribution from each term			Relative Lengths (fm)		
$J^{PC}=2^{++}$		Value	$J/\psi J/\psi$	Difference	(i,j)	Vaule	$J/\psi J/\psi$
Mass/B_T		6482.7	6184.5	298.2	(1,2)	0.377	
Variational Parameters (fm^{-2})	C_{11}	8.9	12.5		(1.3)	0.403	0.318(J/ψ)
	C_{22}	8.9	12.5				
	C_{33}	6.9	-		(2,3)	0.403	
Quark Mass		7672.0	7672.0	0.0	(1,4)	0.403	
Confinement Potential		-1973.6	-2294.4	320.8	(2,4)	0.403	0.318(J/ψ)
Kinetic Energy		752.0	769.9	-10.9	(3,4)	0.377	
CS Interaction		32.3	43.9	-11.6	(1,2)-(3,4):	0.302 fm	
V^C	(1,2)	-14.6			Radius:	0.241 fm	
	(2,3)	5.4					
	(1,4)	5.5			(1,3)	5.4	$-164.2(J/\psi)$
	Subtotal	-7.6	-328.4	320.8	(3,4)	-14.6	
Total Contribution		776.7	478.5	298.2	(2,4)	5.4	$-164.2(J/\psi)$

Total Wave function:

$\Psi_{tot}=|F\rangle|R^s\rangle|[\phi_1\chi_1]\rangle=0.577|F\rangle|R^s\rangle|[\psi_1\zeta_1]\rangle-0.816|F\rangle|R^s\rangle|[\psi_2\zeta_1]\rangle$

The rearrangement strong decay channel: $J/\psi J/\psi$

The radiative decay widths:

$\Gamma_{T_{c^2\bar{c}^2}(6482.7,2^{++})\to T_{c^2\bar{c}^2}(6384.3,0^{++})\Upsilon}=0$ keV

$\Gamma_{T_{c^2\bar{c}^2}(6482.7,2^{++})\to T_{c^2\bar{c}^2}(6451.5,1^{+-})\Upsilon}=70.4$ keV

The magnetic moments: $\mu_{T_{c^2\bar{c}^2}(6451.5,1^{+-})}=\langle\Psi_{tot}^{1^{+-}}|\hat{\mu^z}|\Psi_{tot}^{1^{+-}}\rangle=0.$

The transition magnetic moments:

$\mu_{T_{c^2\bar{c}^2}(6482.7,2^{++})\to T_{c^2\bar{c}^2}(6384.3,0^{++})\gamma}=\langle\Psi_{tot}^{2^{++}}|\hat{\mu^z}|\Psi_{tot}^{0^{++}}\rangle=0$

$\mu_{T_{c^2\bar{c}^2}(6482.7,2^{++})\to T_{c^2\bar{c}^2}(6451.4,1^{+-})\gamma}=\langle\Psi_{tot}^{2^{++}}|\hat{\mu^z}|\Psi_{tot}^{1^{+-}}\rangle=\mu_c-\mu_{\bar{c}}=0.750\mu_N$

Overall	Present Work		CMI Model	
	Contribution	Value	Ref. [110]	Ref. [123]
c-quark: m_c^{eff}	$2m_c$	3836.0		
	$\frac{\mathbf{p}_{x_1}^2}{2m'_1}$	270.4		
	$\frac{m_{\bar{c}}}{m_c+m_{\bar{c}}}\frac{\mathbf{p}_{x_3}^2}{2m'_3}$	105.6	$\frac{1}{2}m_{cc}$	
	$V^C(12)$	-14.6	1585.8	
	$\frac{1}{2}[V^C(13)+V^C(14)+V^C(23)+V^C(24)]$	10.8	$\frac{1}{2}m_{c\bar{c}}$	$2m_c$
	$-D$	-983.0	1534.3	3449.6
	Subtotal	3225.2	3120.0	3449.6
$\bar{c}$-quark: $m_{\bar{c}}^{eff}$	$2m_c$	3836.0		
	$\frac{\mathbf{p}_{x_2}^2}{2m'_2}$	270.4		
	$\frac{m_{\bar{c}}}{m_c+m_{\bar{c}}}\frac{\mathbf{p}_{x_3}^2}{2m'_3}$	105.6	$\frac{1}{2}m_{cc}$	
	$V^C(12)$	-14.6	1585.8	
	$\frac{1}{2}[V^C(13)+V^C(14)+V^C(23)+V^C(24)]$	10.8	$\frac{1}{2}m_{c\bar{c}}$	$2m_c$
	$-D$	-983.0	1534.3	3449.6
Subtotal	3225.2	3120.0	3449.6	
CS Interaction	$\frac{1}{2}V^{SS}(12)$	8.5	$\frac{8}{3}v_{cc}$	$\frac{8}{3}C_{cc}$
			9.5	14.1
	$\frac{1}{2}V^{SS}(34)$	8.5	$\frac{8}{3}v_{\bar{c}\bar{c}}$	$\frac{8}{3}C_{\bar{c}\bar{c}}$
			9.5	14.1
	$\frac{1}{4}(V^{SS}(13)+V^{SS}(14)+V^{SS}(23)+V^{SS}(24)$	15.3	$\frac{16}{3}v_{c\bar{c}}$	$\frac{16}{3}C_{c\bar{c}}$
			28.4	28.2
	Subtotal	32.3	47.4	56.5
Total contribution		6482.7	6287.3	6956.0

$bb\bar{b}\bar{b}$ $J^{PC}=2^{++}$		Value	$\Upsilon\Upsilon$	Difference	Relative Lengths (fm)		
Mass/B_T		19327.9	18938.8	390.1	(i,j)	Value	$\Upsilon\Upsilon$
Variational Parameters (fm^{-2})	C_{11}	30.0	49.4		(1.2)	0.205	
	C_{22}	30.0	49.4		(1,3)	0.220	0.160(Υ)
	C_{33}	23.0	-				
Quark Mass		21372.0	21372.0	0.0	(2,3)	0.220	
Confinement Potential		-2977.3	-3559.5	582.2	(1,4)	0.220	
Kinetic Energy		908.1	1087.3	-179.2	(2,4)	0.220	0.160(Υ)
CS Interaction		25.1	38.0	-12.9	(3,4)	0.205	
V^C	(1,2)	-269.1			(1,2)-(3,4):	0.165 fm	
	(2,3)	-118.3			Radius:	0.132 fm	
	(1,4)	-118.3			(1,3)	-118.3	$-796.7(\Upsilon)$
	Subtotal	-1011.3	-1593.5	582.2	(3,4)	-269.1	
Total Contribution		-78.1	-468.2	390.1	(2,4)	-118.3	$-796.7(\Upsilon)$

Total Wave function:

$\Psi_{tot}=|F\rangle|R^s\rangle|[\phi_1\chi_2]\rangle=0.577|F\rangle|R^s\rangle|[\psi_1\zeta_1]\rangle-0.816|F\rangle|R^s\rangle|[\psi_2\zeta_1]\rangle$

The rearrangement strong decay channel: $B_c^*B_c^*$

The radiative decay widths:

$\Gamma_{T_{b^2\bar{b}^2}(19327.9,2^{++})\to T_{b^2\bar{b}^2}(19240.0,0^{++})\gamma}=0$ keV

$\Gamma_{T_{b^2\bar{b}^2}(19327.9,2^{++})\to T_{b^2\bar{b}^2}(19303.9,1^{+-})\gamma}=1.0$ keV

The magnetic moments: $\mu_{T_{b^2\bar{b}^2}(19303.9,1^{+-})}=\langle\Psi_{tot}^{1^{+-}}|\hat{\mu^z}|\Psi_{tot}^{1^{+-}}\rangle=0$

The transition magnetic moments:

$\mu_{T_{b^2\bar{b}^2}(19327.9,2^{++})\to T_{b^2\bar{b}^2}(19240.0,0^{++})\gamma}=\langle\Psi_{tot}^{2^{++}}|\hat{\mu^z}|\Psi_{tot}^{0^{++}}\rangle=0$

$\mu_{T_{b^2\bar{b}^2}(19327.9,2^{++})\to T_{b^2\bar{b}^2}(19303.9,1^{+-})\gamma}=\langle\Psi_{tot}^{2^{++}}|\hat{\mu^z}|\Psi_{tot}^{1^{+-}}\rangle=\mu_b-\mu_{\bar{b}}=-0.125\mu_N$

Contribution	Value	Ref. [110]	Ref. [123]	
b-quark: m_b^{eff}	$2m_b$	10686.0		
	$\frac{\mathbf{p}_{x_1}^2}{2m'_1}$	328.0		
	$\frac{m_{\bar{b}}}{m_b+m_{\bar{b}}}\frac{\mathbf{p}_{x_3}^2}{2m'_3}$	126.0	$\frac{1}{2}m_{bb}$	
	$V^C(12)$	-269.1	4764.8	
	$\frac{1}{2}[V^C(13)+V^C(14)+V^C(23)+V^C(24)]$	-236.6	$\frac{1}{2}m_{b\bar{b}}$	$2m_b$
	$-D$	-983.0	4722.5	10105.8
	Subtotal	9651.3	9487.3	10105.8
$\bar{b}$-quark: $m_{\bar{b}}^{eff}$	$2m_b$	10686.0		
	$\frac{\mathbf{p}_{x_2}^2}{2m'_2}$	328.0		
	$\frac{m_{\bar{b}}}{m_b+m_{\bar{b}}}\frac{\mathbf{p}_{x_3}^2}{2m'_3}$	126.0	$\frac{1}{2}m_{bb}$	
	$V^C(12)$	-269.1	4764.8	
	$\frac{1}{2}[V^C(13)+V^C(14)+V^C(23)+V^C(24)]$	-236.6	$\frac{1}{2}m_{b\bar{b}}$	$2m_b$
	$-D$	-983.0	4722.5	10105.8
	Subtotal	9651.3	9487.3	10105.8
CS Interaction	$\frac{1}{2}V^{SS}(12)$	6.6	$\frac{8}{3}v_{bb}$	$\frac{8}{3}C_{bb}$
			5.1	7.7
	$\frac{1}{2}V^{SS}(34)$	6.6	$\frac{8}{3}v_{\bar{b}\bar{b}}$	$\frac{8}{3}C_{\bar{b}\bar{b}}$
			5.1	7.7
	$\frac{1}{4}(V^{SS}(13)+V^{SS}(14)+V^{SS}(23)+V^{SS}(24)$	11.9	$\frac{16}{3}v_{b\bar{b}}$	$\frac{16}{3}C_{b\bar{b}}$
			15.3	15.5
	Subtotal	25.1	25.5	30.9
Total contribution		19327.9	19000.1	20243.0

Table 9 The masses, binding energies, variational parameters, the internal contribution, total wave functions, magnetic moments, transition magnetic moments, radiative decay widths, rearrangement strong width ratios, and the relative lengths between quarks for the $J^{PC}=0^{++}$, 1^{+-} $bb\bar{b}\bar{b}$ states and their lowest meson–meson thresholds. The notation is the same as that in Table 7

$bb\bar{b}\bar{b}$	The contribution from each term			
$J^{PC}=0^{++}$		Value	$\eta_b\eta_b$	Difference
Mass/B_T		19240.0	18778.1	461.9
Variational Parameters (fm^{-2})	C_{11}	24.6	57.4	
	C_{22}	24.6	57.4	
	C_{33}	39.5	-	
Quark Mass		21372.0	21372.0	0.0
Confinement Potential		-3101.0	-3724.2	623.2
Kinetic Energy		970.4	1255.9	-285.5
CS Interaction		17.0	-125.5	142.5
V^C	(1,2)	-111.8		
	(2,3)	-339.7		
	(1,4)	-339.7		
	Subtotal	-1135.0	-1758.2	623.2
Total Contribution		-147.6	-627.9	480.3

Relative Lengths (fm)		
(i,j)	Vaule	$\eta_b\eta_b$
(1,2)	0.227	
(1.3)	0.204	$0.148(\eta_b)$
(2,3)	0.204	
(1,4)	0.204	
(2,4)	0.204	$0.148(\eta_b)$
(3,4)	0.227	
(1,2)-(3,4):	0.126 fm	
Radius:	0.130 fm	

V^C		
(1,3)	-339.7	$-879.1(\eta_b)$
(3,4)	-111.8	
(2,4)	-339.7	$-879.1(\eta_b)$

Total Wave function:

$$\Psi_{tot}=0.352|F\rangle|R^s\rangle|[\phi_1\chi_5]\rangle-0.936|F\rangle|R^s\rangle|[\phi_2\chi_6]\rangle=0.558|F\rangle|R^s\rangle|[\psi_1\zeta_5]\rangle +0.560|F\rangle|R^s\rangle|[\psi_1\zeta_6]\rangle+0.021|F\rangle|R^s\rangle|[\psi_2\zeta_5]\rangle+0.612|F\rangle|R^s\rangle|[\psi_2\zeta_6]\rangle$$

The rearrangement strong width ratios:

$$\Gamma_{T_{c^2\bar{c}^2}(19240.0,0^{++})\to\Upsilon\Upsilon}:\Gamma_{T_{c^2\bar{c}^2}(1924.0,0^{++})\to\eta_b\eta_b}=1:1.2$$

The radiative decay widths:

$$\Gamma_{T_{b^2\bar{b}^2}(19327.9,2^{++})\to T_{b^2\bar{b}^2}(19240.0,0^{++})\gamma}=0\,\mathrm{keV}$$

$$\Gamma_{T_{b^2\bar{b}^2}(19303.9,1^{+-})\to T_{b^2\bar{b}^2}(19240.0,0^{++})\gamma}=2.8\,\mathrm{keV}$$

The magnetic moments: $\mu_{T_{b^2\bar{b}^2}(19240.0,0^{++})}=\langle\Psi_{tot}^{0^{++}}|\hat{\mu^z}|\Psi_{tot}^{0^{++}}\rangle=0$

The transition magnetic moments:

$$\mu_{T_{b^2\bar{b}^2}(19327.9,2^{++})\to T_{b^2\bar{b}^2}(19240.0,0^{++})\gamma}=\langle\Psi_{tot}^{2^{++}}|\hat{\mu^z}|\Psi_{tot}^{0^{++}}\rangle=0$$

$$\mu_{T_{b^2\bar{b}^2}(19393.9,1^{+-})\to T_{b^2\bar{b}^2}(19240.0,0^{++})\gamma}=\langle\Psi_{tot}^{1^{+-}}|\hat{\mu^z}|\Psi_{tot}^{0^{++}}\rangle=0.352\times\frac{4}{\sqrt{6}}(\mu_b-\mu_{\bar{b}})=-0.072\mu_N$$

Overall	Present Work		CMI Model	
	Contribution	Value	Ref. [110]	Ref. [123]
b-quark: m_b^{eff}	$2m_b$	10686.0		
	$\frac{\mathbf{p}^2_{x_1}}{2m'_1}$	269.2		
	$\frac{m_{\bar{c}}}{m_b+m_{\bar{b}}}\frac{\mathbf{p}^2_{x_3}}{2m'_3}$	216.0		
	$V^C(12)$	111.8	$-\frac{1}{4}m_{bb}$	
	$\frac{1}{2}[V^C(13)+V^C(14)$ $+V^C(23)+V^C(24)]$	-697.4	-2382.4 $\frac{5}{4}m_{b\bar{b}}$	$2m_b$
	$-D$	-983.0	11806.2	10105.8
	Subtotal	9602.6	9423.8	10105.8
$\bar{b}$-quark: $m_{\bar{b}}^{eff}$	$2m_b$	10686.0		
	$\frac{\mathbf{p}^2_{x_2}}{2m'_2}$	216.0		
	$\frac{m_{\bar{c}}}{m_b+m_{\bar{b}}}\frac{\mathbf{p}^2_{x_3}}{2m'_3}$	216.0		
	$V^C(34)$	111.8	$-\frac{1}{4}m_{bb}$	
	$\frac{1}{2}[V^C(13)+V^C(14)$ $+V^C(23)+V^C(24)]$	-697.4	-2382.4 $\frac{5}{4}m_{b\bar{b}}$	$2m_b$
	$-D$	-983.0	11806.2	10105.8
	Subtotal	9602.6	9423.8	10105.8
CS Interaction	$\frac{3}{4}V^{SS}(12)$	8.5	$4v_{bb}$ 7.7	$4C_{bb}$ 11.6
	$\frac{3}{4}V^{SS}(34)$	8.5	$4v_{\bar{b}\bar{b}}$ 7.7	$4C_{\bar{b}\bar{b}}$ 11.6
	Subtotal	17.0	15.4	23.2
Matrix nondiagonal element		17.8	-27.0	-40.2
Total contribution		19240.0	18836.0	20275.0

$J^{PC}=1^{+-}$		Value	$\Upsilon\eta_b$	Difference
Mass/B_T		19303.9	18857.9	446.0
Variational Parameters (fm^{-2})	C_{11}	30.7	57.4	
	C_{22}	30.7	49.4	
	C_{33}	24.0	-	
Quark Mass		21372.0	21372.0	0.0
Confinement Potential		-3003.4	-3641.9	638.4
Kinetic Energy		934.0	1171.6	-237.6
CS Interaction		1.3	-43.8	45.1
V^C	(1,2)	-274.5		
	(2,3)	-122.1		
	(1,4)	-122.1		
	Subtotal	-1037.4	-1675.9	638.5
Total Contribution		-102.1	-548.1	446.0

Relative Lengths (fm)		
(i,j)	Value	$\Upsilon\eta_b$
(1.2)	0.203	
(1.3)	0.217	$0.148(\eta_b)$
(2,3)	0.217	
(1,4)	0.217	
(2,4)	0.217	$0.160(\Upsilon)$
(3,4)	0.203	
(1,2)-(3,4):	0.162 fm	
Radius:	0.130 fm	

V^C		
(1,3)	-122.1	$-879.1(\eta_b)$
(3,4)	-274.5	
(2,4)	-122.1	$-796.7(\Upsilon)$

Total Wave function: $\Psi_{tot}=|F\rangle|R^s\rangle|[\phi_1\chi_2]\rangle=-0.408|F\rangle|R^s\rangle|[\psi_1\zeta_2]\rangle$ $-0.408|F\rangle|R^s\rangle|[\psi_1\zeta_3]\rangle+0.577|F\rangle|R^s\rangle|[\psi_2\zeta_5]\rangle+0.577|F\rangle|R^s\rangle|[\psi_2\zeta_6]\rangle$

The rearrangement strong decay channel: $J/\psi\eta_c$

The radiative decay widths:

$$\Gamma_{T_{b^2\bar{b}^2}(19327.9,2^{++})\to T_{b^2\bar{b}^2}(19303.9,1^{+-})\gamma}=1.0\,\mathrm{keV}$$

$$\Gamma_{T_{b^2\bar{b}^2}(19303.9,1^{+-})\to T_{b^2\bar{b}^2}(19240.0,0^{++})\gamma}=2.8\,\mathrm{keV}$$

The magnetic moments: $\mu_{T_{b^2\bar{b}^2}(19303.9,1^{+-})}=\langle\Psi_{tot}^{1^{+-}}|\hat{\mu^z}|\Psi_{tot}^{1^{+-}}\rangle=0$

The transition magnetic moments:

$$\mu_{T_{b^2\bar{b}^2}(19327.9,2^{++})\to T_{b^2\bar{b}^2}(19303.9,1^{+-})\gamma}=\langle\Psi_{tot}^{2^{++}}|\hat{\mu^z}|\Psi_{tot}^{1^{+-}}\rangle=-0.125\mu_N$$

$$\mu_{T_{b^2\bar{b}^2}(19393.9,1^{+-})\to T_{b^2\bar{b}^2}(19240.0,0^{++})\gamma}=\langle\Psi_{tot}^{1^{+-}}|\hat{\mu^z}|\Psi_{tot}^{0^{++}}\rangle=-0.072\mu_N$$

	Contribution	Value	Ref. [110]	Ref. [123]
b-quark: m_b^{eff}	$2m_b$	10686.0		
	$\frac{\mathbf{p}^2_{x_1}}{2m'_1}$	335.6		
	$\frac{m_{\bar{b}}}{m_b+m_{\bar{b}}}\frac{\mathbf{p}^2_{x_3}}{2m'_3}$	131.4	$\frac{1}{2}m_{bb}$	
	$V^C(12)$	-274.5	4764.8	
	$\frac{1}{2}[V^C(13)+V^C(14)$ $+V^C(23)+V^C(24)]$	-244.2	$\frac{1}{2}m_{b\bar{b}}$	$2m_b$
	$-D$	-983.0	4722.5	10105.8
	Subtotal	9653.3	9487.3	10105.8
$\bar{b}$-quark: $m_{\bar{b}}^{eff}$	$2m_b$	10686.0		
	$\frac{\mathbf{p}^2_{x_2}}{2m'_2}$	335.6		
	$\frac{m_{\bar{b}}}{m_b+m_{\bar{b}}}\frac{\mathbf{p}^2_{x_3}}{2m'_3}$	131.4	$\frac{1}{2}m_{bb}$	
	$V^C(12)$	-274.5	4764.8	
	$\frac{1}{2}[V^C(13)+V^C(14)$ $+V^C(23)+V^C(24)]$	-244.2	$\frac{1}{2}m_{b\bar{b}}$	$2m_b$
	$-D$	-983.0	4722.5	10105.8
	Subtotal	9653.3	9487.3	10105.8
CS Interaction	$\frac{1}{2}V^{SS}(12)$	6.7	$\frac{8}{3}v_{bb}$ 5.1	$\frac{8}{3}C_{bb}$ 7.7
	$\frac{1}{2}V^{SS}(34)$	6.7	$\frac{8}{3}v_{\bar{b}\bar{b}}$ 5.1	$\frac{8}{3}C_{\bar{b}\bar{b}}$ 7.7
	$-\frac{1}{4}(V^{SS}(13)+V^{SS}(14)$ $+V^{SS}(23)+V^{SS}(24)$	-12.2	$-\frac{16}{3}v_{b\bar{b}}$ -15.3	$-\frac{16}{3}C_{b\bar{b}}$ -15.5
	Subtotal	1.3	-5.1	0.0
Total contribution		19303.9	18696.4	20211.6

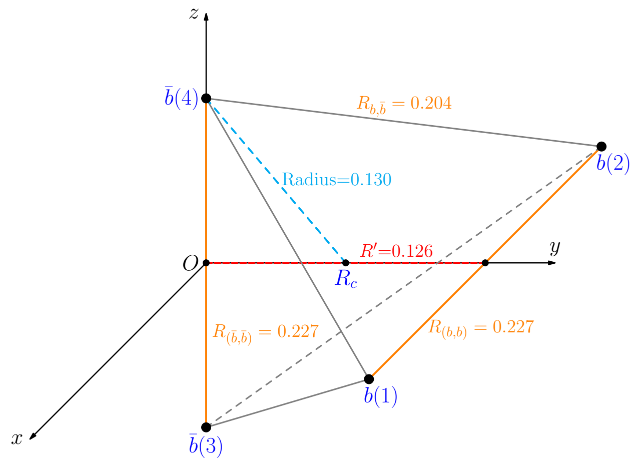

Fig. 1 Relative positions for four valence quarks and R_c in the $J^{PC} = 0^{++}$ $bb\bar{b}\bar{b}$ ground state. Meanwhile, we label the relative distances of $R_{b,b}$, $R_{b,\bar{b}}$, $R_{\bar{b},\bar{b}}$, R', and the radius (units: fm)

hadrons. According to Table 9, we easily find that the relative distances of (1,2), (1,3), (1,4), (2,3), (2,4), and (3,4) quark pairs are all 0.227 or 0.204 fm. Meanwhile, the radius of the state is only 0.130 fm. Thus, in this state, all the distances between the quark pairs are roughly the same order of magnitude. If it is a molecular configuration, the distances between two quarks and two antiquarks should be much greater than the distances in the compact multiquark scheme, and the radius of molecular configuration can reach several femtometers. Therefore, our calculations are consistent with the compact tetraquark expectations.

4.2.2 The internal contribution

Let us now turn our discussion to the internal mass contribution for the $J^{PC} = 0^{++}$ $bb\bar{b}\bar{b}$ ground state.

First, for the kinetic energy, this $bb\bar{b}\bar{b}$ state has 814.0 MeV, which can be understood as the sum of three internal kinetic energies: kinetic energies of two pairs of the $b-\bar{b}$, and the $(b\bar{b})-(b\bar{b})$ pair. Accordingly, the sum of the internal kinetic energies of the $\eta_b\eta_b$ state only comes from the two pairs of the $b-\bar{b}$. Therefore, this $bb\bar{b}\bar{b}$ state has an additional kinetic energy needed to bring the $\eta_b\eta_b$ into a compact configuration. The actual kinetic energies of two pairs of the $b-\bar{b}$ in the $J^{PC} = 0^{++}$ $bb\bar{b}\bar{b}$ ground state are smaller than those in the $\eta_b\eta_b$ state. This is because, as can be seen in Table 9, the distance of $b-\bar{b}$ is larger in the tetraquark state than in the meson: the distance of $b-\bar{b}$ is 0.204 fm in this $bb\bar{b}\bar{b}$ state, while it is 0.148 fm in η_b. Meanwhile, we find that even if we consider the additional kinetic energy between the $(b\bar{b})-(b\bar{b})$ pair, the total kinetic energy in this $bb\bar{b}\bar{b}$ state is still smaller than that in the $\eta_b\eta_b$ state. However, this does not lead the ground $J^{PC} = 0^{++}$ $bb\bar{b}\bar{b}$ state to a stable state because of the confinement potential part.

As for the confinement potential part, the contributions from V^C for the $J^{PC} = 0^{++}$ $bb\bar{b}\bar{b}$ ground state in Table 9 are all attractive. Thus, this state has a large positive binding energy. However, it is still above the meson–meson threshold because the $V^C(b\bar{b})$ in η_b is very attractive. As for the other internal contributions, the quark contents of this state are the same as the corresponding rearrangement decay threshold. Moreover, the mass contribution from the hyperfine potential term is negligible compared to the contributions from other terms.

4.2.3 Comparison with two models of chromomagnetic interaction

Now, we compare the numerical values for the $cc\bar{c}\bar{c}$ and $bb\bar{b}\bar{b}$ systems between the constituent quark model and two CMI models [110,123] in Tables 7, 8, and 9. The comparisons of the values for $cc\bar{c}\bar{c}$ and $bb\bar{b}\bar{b}$ states, which are in the last three columns of Tables 7, 8, and 9, can be summarized in the following important conclusions.

First, we find that there is no stable state below the lowest heavy quarkonium pair thresholds in any of the models. In all three models, we consider two possible color configurations, the color-sextet $|(QQ)^{3_c}(\bar{Q}\bar{Q})^{\bar{3}_c}\rangle$ and the color-triplet $|(QQ)^{6_c}(\bar{Q}\bar{Q})^{\bar{6}_c}\rangle$. According to the extended chromomagnetic model [110], the ground state is always dominated by the color-sextet configuration. This view is consistent with the specific wave function of the ground state in Eq. (22) given by the constituent quark model.

In contrast, the masses obtained from the constituent quark model are systematically larger than those from the extended CMI model [110] according to Tables 7, 8, and 9. Meanwhile, the masses obtained from the CMI model [123] are obviously larger than those of the constituent quark model. Their mass differences are mainly due to the effective quark masses as given in the last three columns of Tables 7, 8, and 9. The effective quark masses are the sum of the quark mass, the relevant kinetic term, and all the relevant interaction terms in the constituent quark model, which indeed seems to approximately reproduce the effective quark mass from two CMI models [110,123]. We compare the subtotal values of the c and $\bar{c}$ quark part in Table 8. The c effective quark mass in the constituent quark model is 3225 MeV, which is about 100 MeV larger than that of the extended CMI model in the $J^{PC} = 0^{++}$ $cc\bar{c}\bar{c}$ state. Correspondingly, we also find that the c effective quark mass in the CMI model [123] is 3450 MeV, and about 200 MeV larger than that of the constituent quark model. The effective quark masses in the extended CMI model depend on the parameters of the traditional hadron. However, the effective quark masses should be different depending on whether they are inside a meson, a baryon, or a tetraquark. The effective quark masses trend to be large when they are inside configurations with larger constituents in the extended CMI model, as can be seen from the comparisons of the last three columns in Tables 7, 8, and 9. Moreover, we note that a similar situation occurs in the $ud\bar{c}\bar{c}$ state in Table X of Ref. [61].

4.3 $cc\bar{b}\bar{b}$ state

Here, we will concentrate on the $cc\bar{b}\bar{b}$ system. Similar to the $cc\bar{c}\bar{c}$ and $bb\bar{b}\bar{b}$ systems, the $cc\bar{b}\bar{b}$ system is satisfied with fully antisymmetry for diquarks and antiquarks. There are two $J^P = 0^+$ states, one $J^P = 1^+$ state, and one $J^P = 2^+$ state in the $cc\bar{b}\bar{b}$ system. We show the masses of the ground states, the variational parameters, the internal mass contributions, the relative lengths between the quarks, their lowest meson–meson thresholds, the specific wave function, the magnetic moments, the transition magnetic moments, the radiative decay widths, and the rearrangement strong width ratios in Tables 11 and 12.

First, we take the $J^P = 0^+$ $cc\bar{b}\bar{b}$ ground state as an example to discuss its properties with the variational method. A similar situation occurs in the other two quantum numbers according to Tables 11 and 12. The mass of the lowest $J^P = 0^+$ $cc\bar{b}\bar{b}$ state is 12,920.0 MeV, and the corresponding binding energy B_T is +344.2 MeV according to Table 11. Thus, the state is obviously higher than the corresponding rearrangement meson–meson thresholds. The wave function is given by

$$|\Psi_{\rm tot}\rangle = -0.966|F\rangle|R^s\rangle|[\phi_1\chi_5]\rangle + 0.259|F\rangle|R^s\rangle|[\phi_2\chi_6]\rangle. \tag{36}$$

Here, we see that the mass contribution of the ground state comes mainly from the $|(Q_1Q_2)^{\bar{3}}_1(\bar{Q}_3\bar{Q}_4)^3_1\rangle_0$ component, and the $|(Q_1Q_2)^6_0(\bar{Q}_3\bar{Q}_4)^{\bar{6}}_0\rangle_0$ component is negligible. Its variational parameters are given as $C_{11} = 23.9$ fm^{-2}, $C_{22} = 10.5$ fm^{-2}, and $C_{33} = 12.3$ fm^{-2}.

The meson–meson configuration is connected to the diquark–antidiquark configuration by a linear transformation. Then, we obtain the total wave function in the meson–meson configuration:

$$\begin{aligned}|\Psi_{\rm tot}\rangle &= -0.589|F\rangle|R^s\rangle|[\psi_1\zeta_5]\rangle + 0.095|F\rangle|R^s\rangle|[\psi_1\zeta_6]\rangle\\ &\quad + 0.608|F\rangle|R^s\rangle|[\psi_2\zeta_5]\rangle + 0.524|F\rangle|R^s\rangle|[\psi_2\zeta_6]\rangle.\end{aligned} \tag{37}$$

According to Eq. (37), we are sure that the overlaps c_i of B_cB_c and $B_c^*B_c^*$ are 0.095 and 0.589, respectively. Then, based on Eq. (21), the rearrangement strong width ratios is

$$\frac{\Gamma_{T_{c^2\bar{b}^2}(12920.0,0^+)\to B_c^*B_c^*}}{\Gamma_{T_{c^2\bar{b}^2}(12920.0,0^+)\to B_cB_c}} = 1{:}50, \tag{38}$$

i.e., B_cB_c is the dominant rearrangement decay channel for the $T_{c^2\bar{b}^2}(12920.0, 0^+)$ state.

As for the magnetic moment of the $J^P = 0^+$ $cc\bar{b}\bar{b}$ ground state, its value is 0, while the magnetic moment of all $J^P = 0^+$ tetraquark states is 0. As for the $J^P = 1^+$ $cc\bar{b}\bar{b}$ state, we construct its flavor ⊗ spin wave functions as

$$\begin{aligned}&|\Psi\rangle^{S=1;S_z=1}_{T_{c^2\bar{b}^2}(12939.9,1^+)}\\ &\quad = |R^s\rangle|\psi\rangle|cc\bar{b}\bar{b}\rangle|\frac{1}{2}(\uparrow\uparrow\uparrow\downarrow + \uparrow\uparrow\downarrow\uparrow - \downarrow\uparrow\uparrow\downarrow - \downarrow\uparrow\downarrow\uparrow\rangle.\end{aligned} \tag{39}$$

So the corresponding transition magnetic momentum is

$$\begin{aligned}&\mu_{T_{c^2\bar{b}^2}(12939.9,1^+)}\\ &= \langle\Psi^{1^+}_{\rm tot}|\hat{\mu}^z|\Psi^{1^+}_{\rm tot}\rangle = \mu_c + \mu_{\bar{b}} = 0.490\mu_N.\end{aligned} \tag{40}$$

We also discuss the transition magnetic moment of the $T_{c^2\bar{b}^2}(12939.9, 1^+) \to T_{c^2\bar{b}^2}(12920.0, 0^+)\gamma$ process. We still construct their flavor ⊗ spin wave functions as

$$\begin{aligned}|\Psi\rangle^{S=1;S_z=0}_{T_{c^2\bar{b}^2}(1^+)} &= |R^s\rangle|\psi\rangle|cc\bar{b}\bar{b}\rangle|\frac{1}{\sqrt{2}}(\uparrow\uparrow\downarrow\downarrow - \downarrow\downarrow\uparrow\uparrow)\rangle,\\ |\Psi\rangle^{S=0;S_z=0}_{T_{c^2\bar{b}^2}(0^+)} &= |R^s\rangle|\psi\rangle|cc\bar{b}\bar{b}\rangle\\ &\quad |0.966\frac{1}{\sqrt{3}}(\uparrow\uparrow\downarrow\downarrow + \downarrow\downarrow\uparrow\uparrow) + \cdots\rangle.\end{aligned} \tag{41}$$

And then the transition magnetic momentum of the $T_{c^2\bar{b}^2}(12939.9, 1^+) \to T_{c^2\bar{b}^2}(12920.0, 0^+)\gamma$ process can be described by the z-component of the magnetic moment operator $\hat{\mu}^z$ sandwiched by the flavor-spin wave functions of the $T_{c^2\bar{b}^2}(12939.9, 1^+)$ and $T_{c^2\bar{b}^2}(12920.0, 0^+)$. Thus the corresponding transition magnetic momentum is

$$\begin{aligned}&\mu_{T_{c^2\bar{b}^2}(12939.9,1^+)\to T_{c^2\bar{b}^2}(12920.0,0^+)\gamma} = \langle\Psi^{1^+}_{\rm tot}|\hat{\mu}^z|\Psi^{0^+}_{\rm tot}\rangle\\ &= 0.966 \times \frac{1}{\sqrt{6}}(4\mu_c - 4\mu_{\bar{b}}) = 0.534\mu_N.\end{aligned} \tag{42}$$

Further, according to Eqs. (19) and (42), we also obtain the radiative decay widths

$$\Gamma_{T_{c^2\bar{b}^2}(12960.9,2^+)\to T_{c^2\bar{b}^2}(12939.9,1^+)\gamma} = 3.6\,\text{keV}. \tag{43}$$

Finally, we turn to the internal contribution for the $cc\bar{b}\bar{b}$ ground state. For the kinetic energy part, the $J^P = 0^+$ $cc\bar{b}\bar{b}$ state receives 835.9 MeV, which is smaller than that of the meson–meson threshold B_cB_c. The potential part of this state is much smaller than that of the lowest meson–meson threshold. Furthermore, we find that all the V^C for this state are attractive. However, compared to the V^C of B_cB_c, these attractive values seem trivial. This is because the length between $c - \bar{b}$ in tetraquarks is longer than that in B_c according to Tables 11 and 12. In summary, we tend to think that these $cc\bar{b}\bar{b}$ states are unstable compact states.

4.4 $cc\bar{c}\bar{b}$ and $bb\bar{b}\bar{c}$ states

Here, we discuss the $cc\bar{c}\bar{b}$ and $bb\bar{b}\bar{c}$ systems. For these two systems, they only need to satisfy the antisymmetry for the diquark. Thus, compared to the above three systems, the $cc\bar{c}\bar{b}$ and $bb\bar{b}\bar{c}$ systems have more allowed states. There are two $J^P = 0^+$ states, three $J^P = 1^+$ states, and one $J^P = 2^+$ state in the $cc\bar{c}\bar{b}$ and $bb\bar{b}\bar{c}$ systems. We calculate the masses of the ground states, the corresponding variational parameters, the various internal contributions, the relative lengths between the quarks, their lowest meson-meson thresholds, specific wave functions, magnetic moments, transition magnetic moments, radiative decay widths, and rearrangement strong width ratios in Tables 13, 14, and 15, respectively.

We now analyze the numerical results of the $J^P = 1^+$ ground $bb\bar{b}\bar{c}$ state obtained from the variational method according to Table 14. Other states would have similar discussions from Tables 13, 14, and 15. The mass of the lowest $J^P = 1^+$ $bb\bar{b}\bar{c}$ state is 16043.2 MeV, and the corresponding binding energy B_T is +303.7 MeV. Thus, the state is obviously above the lowest rearrangement meson–meson decay channel $B_c^*\eta_b$, and it is an unstable tetraquark state. Its variational parameters are given as $C_{11} = 12.4$ fm^{-2}, $C_{22} = 21.0$ fm^{-2}, and $C_{33} = 28.9$ fm^{-2}. The corresponding wave function is given by

$$|\Psi_{\rm tot}\rangle = 0.984|F\rangle|R^s\rangle|[\phi_2\chi_4]\rangle + 0.171|F\rangle|R^s\rangle|[\phi_1\chi_3]\rangle - 0.044|F\rangle|R^s\rangle|[\phi_1\chi_2]\rangle. \quad (44)$$

Here, we note that the mass contribution of the ground state comes mainly from the $|(Q_1Q_2)_0^6(\bar{Q}_3\bar{Q}_4)_1^{\bar{6}}\rangle_1$ component, and the other two components are negligible. Then we transform Eq. (44) into the meson–meson configuration via a linear transformation, and the corresponding wave function is given as

$$|\Psi_{\rm tot}\rangle = 0.494|F\rangle|R^s\rangle|[\psi_1\zeta_2]\rangle - 0.396|F\rangle|R^s\rangle|[\psi_1\zeta_3]\rangle - 0.487|F\rangle|R^s\rangle|[\psi_1\zeta_4]\rangle + 0.111|F\rangle|R^s\rangle|[\psi_2\zeta_2]\rangle - 0.246|F\rangle|R^s\rangle|[\psi_2\zeta_3]\rangle - 0.537|F\rangle|R^s\rangle|[\psi_2\zeta_4]\rangle. \quad (45)$$

Furthermore, we can be sure that its rearrangement strong width ratios are

$$\Gamma_{T_{b^2\bar{b}\bar{c}}(16043.2,1^+)\to B_c^*\Upsilon} : \Gamma_{T_{b^2\bar{b}\bar{c}}(16043.2,1^+)\to B_c\Upsilon} : \Gamma_{T_{b^2\bar{b}\bar{c}}(16043.2,1^+)\to B_c^*\eta_b} = 1{:}1.3{:}1.5. \quad (46)$$

And its radiative decay widths are

$$\Gamma_{T_{b^2\bar{b}\bar{c}}(16149.2,2^+)\to T_{c^2\bar{c}\bar{b}}(16043.2,1^+)\gamma} = 435.0\,\text{keV},$$
$$\Gamma_{T_{c^2\bar{c}\bar{b}}(16043.9,0^+)\to T_{c^2\bar{c}\bar{b}}(16043.2,1^+)\gamma} = 10^{-6}\,\text{keV}.$$

Let us now focus on the internal contributions for this state and the relative lengths between the quarks. For the kinetic energy part, the state obtains 876.1 MeV, which is obviously smaller than that of the lowest meson–meson threshold $B_c\eta_b$. The actual kinetic energy of the $b-\bar{b}$ ($b-\bar{c}$) in the $J^P = 1^+$ $bb\bar{b}\bar{c}$ state is smaller than that in the η_b (B_c^*) meson. The reason for this can be seen in Table 14. The size of this pair is larger in the $J^P = 1^+$ $bb\bar{b}\bar{c}$ state than in the meson: the distance (3,4) is 0.245 fm in this tetraquark, while it is 0.148 fm in η_b.

Here, let us turn our discussion to the potential parts. The potential part of this state is much smaller than that of its lowest meson–meson threshold. Although the V^C between quark and antiquark are attractive, the V^C in the diquark and antiquark are repulsive. However, relative to the η_b and B_c mesons, the V^C in the tetraquark are less attractive. Therefore, they still have relatively large positive binding energy in this state.

4.5 $cb\bar{c}\bar{b}$ state

Finally, we investigate the $cb\bar{c}\bar{b}$ system. Similar to the $cc\bar{c}\bar{c}$ and $bb\bar{b}\bar{b}$ systems, the $cb\bar{c}\bar{b}$ system is a pure neutral system and has a certain C-parity. Thus the corresponding magnetic moment is $0\mu_N$ for all the ground $cb\bar{c}\bar{b}$ states. Moreover, the Pauli principle does not impose any constraints on the wave functions of the $cb\bar{c}\bar{b}$ system. Thus, compared to other tetraquark systems discussed above, the $cb\bar{c}\bar{b}$ system has more allowed states. There are four $J^{PC} = 0^{++}$ states, four $J^{PC} = 1^{+-}$ states, two $J^{PC} = 1^{++}$ states, and two $J^{PC} = 2^{++}$ states in the $cb\bar{c}\bar{b}$ system.

We now analyze the numerical results for the $cb\bar{c}\bar{b}$ system obtained from the variational method. Here, we take the $J^{PC} = 0^{++}$ $cb\bar{c}\bar{b}$ ground state as an example for discussion, and others would have similar discussions. The mass of the lowest $J^{PC} = 0^{++}$ $cb\bar{c}\bar{b}$ state is 12,759.3 MeV, and the corresponding binding energy B_T is +371.8 MeV. Thus, the state obviously has a larger mass than the lowest rearrangement meson–meson decay channel $\eta_b\eta_c$, and it should be an unstable compact tetraquark state. Its variational parameters are given as $C_{11} = 11.9$ fm^{-2}, $C_{22} = 11.9$ fm^{-2}, and $C_{33} = 22.9$ fm^{-2}. Since this state is a pure neutral state, we naturally find that the value of C_{11} is equal to C_{22}, which means that the distance of $(b-b)$ is equal to $(\bar{b}-\bar{b})$. Our results also reflect these properties according to Table 16. The corresponding wave function is given as

$$\Psi_{\rm tot} = 0.961|F\rangle|R^s\rangle|[\phi_2\chi_5]\rangle + 0.114|F\rangle|R^s\rangle|[\phi_2\chi_6]\rangle - 0.069|F\rangle|R^s\rangle|[\phi_1\chi_5]\rangle - 0.241|F\rangle|R^s\rangle|[\phi_1\chi_6]\rangle. \quad (47)$$

Based on Eq. (47), we find that its mass contribution to the ground state comes mainly from the $6 \otimes \bar{6}$ component, the corresponding $3 \otimes \bar{3}$ component being negligible. Then we transform Eq. (47) into $c\bar{c} - b\bar{b}$ and $c\bar{b} - b\bar{c}$ configurations via a linear transformation, and the corresponding two wave functions are given as

$$|\Psi_{\rm tot}\rangle = -0.830|F\rangle|R^s\rangle|[\psi_1\zeta_5]\rangle + 0.211|F\rangle|R^s\rangle|[\psi_1\zeta_6]\rangle - 0.367|F\rangle|R^s\rangle|[\psi_2\zeta_5]\rangle + 0.363|F\rangle|R^s\rangle|[\psi_2\zeta_6]\rangle$$
$$= -0.668|F\rangle|R^s\rangle|[\psi_1'\zeta_5']\rangle + 0.333|F\rangle|R^s\rangle|[\psi_1'\zeta_6']\rangle - 0.398|F\rangle|R^s\rangle|[\psi_2'\zeta_5']\rangle + 0.533|F\rangle|R^s\rangle|[\psi_2'\zeta_6']\rangle. \quad (48)$$

Further, we can ascertain its rearrangement strong width ratios. For the $c\bar{b} - b\bar{c}$ decay mode

$$\Gamma_{T_{cb\bar{c}\bar{b}}(12796.9,1^{+-})\to B_c^*\bar{B}_c^*} : \Gamma_{T_{cb\bar{c}\bar{b}}(12796.9,1^{+-})\to B_c^*\bar{B}_c} : \Gamma_{T_{cb\bar{c}\bar{b}}(12796.9,1^{+-})\to B_c\bar{B}_c^*} = 1:3.9:3.9, \quad (49)$$

where both the $B_c^*\bar{B}_c$ and $B_c\bar{B}_c^*$ channels are the dominant decay modes for the $T_{cb\bar{c}\bar{b}}(12796.9, 1^{+-})$ tetraquark state.

$$\Gamma_{T_{cb\bar{c}\bar{b}}(12796.9,1^{+-})\to \eta_b J/\psi} : \Gamma_{T_{cb\bar{c}\bar{b}}(12796.9,1^{+-})\to \Upsilon\eta_c} = 1:18.4. \quad (50)$$

The dominant decay channel is the $\Upsilon\eta_c$ final states in the $c\bar{c} - b\bar{b}$ decay mode.

We also calculate the transition magnetic moments for this state:

$$\mu_{T_{cb\bar{c}\bar{b}}(12882.4,2^{++})\to T_{cb\bar{c}\bar{b}}(12759.6,0^{++})\gamma} = 0,$$
$$\mu_{T_{cb\bar{c}\bar{b}}(12856.6,1^{++})\to T_{cb\bar{c}\bar{b}}(12759.6,0^{++})\gamma} = 0,$$
$$\mu_{T_{cb\bar{c}\bar{b}}(12796.9,1^{+-})\to T_{cb\bar{c}\bar{b}}(12759.6,0^{++})\gamma} = 0.081, \quad (51)$$

which are in units of μ_N. Furthermore, we can obtain its radiative decay widths as

$$\Gamma_{T_{cb\bar{c}\bar{b}}(12882.4,2^{++})\to T_{cb\bar{c}\bar{b}}(12759.6,0^{++})\gamma} = 0,$$
$$\Gamma_{T_{cb\bar{c}\bar{b}}(12856.6,1^{++})\to T_{cb\bar{c}\bar{b}}(12759.6,0^{++})\gamma} = 0,$$
$$\Gamma_{T_{cb\bar{c}\bar{b}}(12797.3,1^{+-})\to T_{cb\bar{c}\bar{b}}(12759.6,0^{++})\gamma} = 33.1, \quad (52)$$

which are in units of keV.

Let us now turn our discussion to the internal contribution for the $J^{PC} = 1^{+-}$ $cb\bar{c}\bar{b}$ ground state. For the kinetic energy part, the state obtains 858.5 MeV, which is smaller than the 1001.2 MeV of the lowest meson–meson threshold $B_c\eta_b$ according to Table 16. As for the potential part, although the V^C between quark and antiquark are attractive, the V^C in the diquark and antiquark are repulsive. However, relative to the lowest meson–meson threshold $B_c\eta_b$, the total V^C is less attractive than the $B_c\eta_b$, which leads to this state having a relatively larger mass.

We also note that the $V^C(1,3)$, $V^C(2,3)$, $V^C(1,4)$, and $V^C(2,4)$ are absolutely the same, and meanwhile the distances of (1,3), (1,4), (2,3), and (2,4) are also the same. These actually reflect $\langle\Psi_{\rm tot}|(\mathbf{R}_{1,2}\cdot\mathbf{R}_{3,4})|\Psi_{\rm tot}\rangle = \langle\Psi_{\rm tot}|(\mathbf{R}_{1,2}\cdot\mathbf{R}')|\Psi_{\rm tot}\rangle = \langle\Psi_{\rm tot}|(\mathbf{R}_{3,4}\cdot\mathbf{R}')|\Psi_{\rm tot}\rangle = 0$. Obviously, it is unreasonable that the distance of $c\bar{c}$ is exactly the same as that of the $c\bar{b}$ and $b\bar{b}$. According to Sec IV of Ref. [65], it is not sufficient to consider only the single Gaussian form where the spatial part of the wave function is $l_1 = l_2 = l_3 = 0$ in the spatial part of the total wave function is not sufficient. These lead to the $cb\bar{c}\bar{b}$ state, which is far away from the real structures in nature. We have reason enough to believe that the $\langle\Psi_{\rm tot}|(\mathbf{R}_{1,2}\cdot\mathbf{R}_{3,4})|\Psi_{\rm tot}\rangle$ should not be zero. Meanwhile, considering other spatial basis would reduce the corresponding binding energy B_T [65]. But these corrections would be powerless against the higher binding energy B_T of the ground $J^{PC} = 1^{+-}$ $cb\bar{c}\bar{b}$. In conclusion, we tend to think that the $J^{PC} = 1^{+-}$ $cb\bar{c}\bar{b}$ ground state should be an unstable compact state.

5 Comparison with other work

Mass spectra have been studied with different approaches such as different nonrelativistic constituent quark models, different chromomagnetic models, relativistic quark models, nonrelativistic chiral quark model, diquark models, the diffusion Monte Carlo calculation, and the QCD sum rule. In addition, these fully heavy tetraquark systems have been discussed with different color structures such as the $8_{Q\bar{Q}}\otimes 8_{Q\bar{Q}}$ configuration, the diquark–antiquark configuration ($3\otimes\bar{3}$ and the $6\otimes\bar{6}$), and the couplings between the above color configurations. For comparison, we briefly list our results and other theoretical results in Table 10.

Compared to other systems, the most extensive discussion is found for the $cc\bar{c}\bar{c}$ system. Thus, we will concentrate on the $cc\bar{c}\bar{c}$ system, but other systems can be discussed in a similar way. After comparing our results with those of other studies, we can see that most theoretical masses of $cc\bar{c}\bar{c}$ in ground states lie in a wide range of 6.0–6.8 GeV in Table 10. Our results are 6.38, 6.45, and 6.48 GeV for the 0^{++}, 1^{+-}, and 2^{++} $cc\bar{c}\bar{c}$ ground states, respectively. These three ground states are expected to be broad because they can all decay to charmonium pairs $\eta_c\eta_c$, $\eta_c J/\psi$, or $J/\psi J/\psi$ through the quark (antiquark) rearrangements. Therefore, these types of decays are favored both dynamically and kinematically. According to Table 10, we can conclude that the obtained masses of the ground states are obviously smaller than the $X(6900)$ observed by the LHCb Collaboration. The observed $X(6900)$ is less likely to be the ground compact tetraquark state and could be a first or second radial excited $cc\bar{c}\bar{c}$ state.

Although we all use a similar Hamiltonian expression as in the nonrelativistic constituent quark model [111,141–143], the spatial wave function is mostly expanded in the Gaussian basis according to Ref. [144], while we treat the spatial function as a Gaussian function, which is convenient for use in further variational methods to handle calculations in the four-body problem. Our results for the $cc\bar{c}\bar{c}$ system are roughly compatible with other nonrelativistic constituent quark models, although different papers have chosen different potential forms.

Table 10 Comparison of the results of different methods for the $QQ\bar{Q}\bar{Q}$ tetraquark states

Systems		$cc\bar{c}\bar{c}$				$bb\bar{b}\bar{b}$				$cc\bar{b}\bar{b}$			
$J^{P(C)}$		0^{++}		1^{+-}	2^{++}	0^{++}		1^{+-}	2^{++}	0^{+}		1^{+}	2^{+}
The nonrelativistic constituent quark models	Our result	6384	6512	6452	6483	19352	19240	19304	19328	12920	13008	12940	12961
	Ref. [111]	6377	6425	6425	6432	19215	19247	19247	19249	12847	12866	12864	12868
		6371	6483	6450	6479	19243	19305	19311	19325	12886	12946	12924	12940
	Ref. [142]	6487	6518	6500	6524	19332	19338	19329	19341	12947	13039	12960	12972
	Ref. [143]	6500	6411	6453	6475	19200	19235	19216	19225	12880	12981	12890	12902
	Ref. [78]	6477	6695	6528	6573	-	-	-	-	-	-	-	-
	Ref. [141]	6491		6580	6607	19357		19413	19429	12963		13024	13041
Multiquark color flux-tube model	Ref. [141]	6407		6463	6486	19329		19373	19387	12906		12946	12960
The chromo-magnetic model	Ref. [141]	6035		6139	6194	18834		18890	18921	12597		12660	12695
	Ref. [79]	6192		-	-	18826		-	-	-		-	-
	Ref. [123]	6899	7016	6899	6956	20155	20275	20212	20243	13496	13634	13560	13595
		6035	6253	6137	6194	18834	18954	18890	18921	12597	12734	12660	12695
	Ref. [110]	6045	6271	6231	6287	18836	18981	18969	19000	12596	12712	12672	12703
	Ref. [107]	6034	6254	6137	6194	18834	18953	18890	18921	-	-	-	-
The Bethe-Salpeter equations	Ref.[150]	6419		6456	6516	19205		19221	19253	-		-	-
The relativistic quark model	Ref. [100]	6190		6271	6367	19314		19320	19330	12846		12859	12883
	Ref. [94]	6435	6542	6515	6543	19201	19255	19251	19262	-	-	-	-
Monte Carlo method	Ref. [146]	6351		6441	6471	19199		19276	19289	12865		12908	12926
The diquark model	Ref. [149]	5966		6051	6223	18754		18808	18916	-		-	-
	Ref. [147, 151]	6322		6354	6385	19666		19673	19680	12401		12409	12427
The QCD sum rule method	Ref. [145]	6360	6540	6470	6520	18130	18150	18140	18150	-	-	-	-
	Ref. [152, 153]	5990		6050	6090	18840		18840	18850	-		-	-
The nonrelativistic chiral quark model	Ref. [148, 154]	6510		6600	6708	-		-	-	12684		12737	12791
An effective potential model	Ref. [91]	6346	6476	6441	6475	19154	19226	19214	19232	-	-	-	-

Systems	$cb\bar{c}\bar{b}$						$cc\bar{c}\bar{b}$				$bb\bar{b}\bar{c}$			
$J^{P(C)}$	0^{++}		1^{+-}		1^{++}	2^{++}	0^{+}	1^{+}		2^{+}	0^{+}	1^{+}		2^{+}
Our result	12760	12851	12797	12856	12857	128824	9621	96246	9706	9731	16044	16043	16125	16149
	12989	13008	12999	13056	12960	12971	9766	9729			16163	16144		
Ref. [143]	12783	12850	12802	12835	12851	12852	9665	9676	9699	9713	16061	16046	16079	16089
	12966	13035	12949	12964	12938	12964	9732	9718			16100	16089		
Ref. [142]	12835	12864	12852	12864	12870	12864	9740	9746	9749	9768	16158	16157	16164	16176
	12864	13050	13047	13052	13056	13070	9763	9757			16158	16167		
Ref. [141]	12894			12955		13000	9735	9766		9839	16175	16179		16274
	12829			12881		12925	9670	9683		9732	16126	16130		16182
	12354			12436		12548	9705	9705		9732	15713	15729		15806
Ref. [110]	12363	12509	12425	12477	12524	12537	9318	9335	9384	9526	15712	15719	15851	15882
	12682	12747	12720	12744	12703	12755	9506	9499			15862	15854		
Ref. [123]	13396	13634	13478	13592	13510	13590	10144	10174	10231	10273	16832	16840	16884	16917
	13483	13553	13520	13555	13599	13599	10322	10282			16952	16915		
	12354	12592	12436	12550	12468	12548	9313	9343	9400	9442	15713	15729	15773	15806
	12441	12511	12478	12513	12557	12557	9491	9451			15841	15804		
	12578	12620	12496	12583	12611	12690								
	12656	12693	12653	12735	12700	12700								
Ref. [100]	12813	12824	12826	12831	12831	12849	9572	9602	9619	9647	16109	16117	16117	16132
Ref. [146]	12534		12510		12569	12582	9615	9610		9719	16040	16013		16129
Ref. [149]	12359	12471	12424	12488	12485	12566	-	-	-	-	-	-	-	-
Ref. [154]	-		-		-	-	9579		9590	9613	16060		16062	16068

It is also interesting to note that relatively larger results are also given by the QCD sum rules [145], the Monte Carlo method [146], the diquark model [147], and the chiral quark model [148]. However, the results given by the QCD sum rules [145] are about 1 GeV below those of the constituent quark models for the $bb\bar{b}\bar{b}$ system. In contrast, our results are obviously larger than the chromomagnetic models [79,107,110,123] and the diquark models [100,149], where these models usually neglect the kinematic term and explicitly include confining potential contributions or adopt a diquark picture.

6 Summary

The discovery of exotic structures in the di-J/ψ invariant mass spectrum from the LHCb, CMS, and ATLAS collaborations gives us strong confidence to investigate the fully heavy tetraquark system. Thus, we use the variational method to systematically calculate the masses of all possible configurations for fully heavy tetraquarks within the framework of the constituent quark model. Meanwhile, we also give the corresponding internal mass contributions, the relative lengths between (anti)quarks, their lowest meson–meson thresholds, the specific wave function, magnetic moments, transition magnetic moments, the radiative decay widths, rearrangement strong width ratios, and comparisons with the two different CMI models.

To obtain the above results, we need to construct the total wave functions of the tetraquark states, including the flavor part, color part, spin part, and spatial part, which is chosen to be a simple Gaussian form. Here, we first estimate the theoretical values of traditional hadrons, which are used to compare the experimental values to prove the reliability of this model. Before discussing the numerical analysis, we analyze the stability condition using only the color-spin interaction. Then, we obtain the specific numerical values and show them in corresponding tables and the spatial distribution of valence quarks for the $J^{PC}=0^{++}$ $bb\bar{b}\bar{b}$ ground state in Fig. 1.

For the $cc\bar{c}\bar{c}$ and $bb\bar{b}\bar{b}$ systems, there are two pure neutral systems with definite C-parity. There are only two $J^{PC}=0^{++}$ states, one $J^{PC}=1^{+-}$ state, and one $J^{PC}=2^{++}$ state, due to the Pauli principle. We also find that these states with different quantum numbers are all above the lowest thresholds, and have larger masses. Since these states are pure neutral particles, the corresponding magnetic moments are all 0 for the ground $cc\bar{c}\bar{c}$ and $bb\bar{b}\bar{b}$ states. Meanwhile, of course, the variational parameters C_{11} and C_{22} are the same, so the distances of the diquark and antidiquark are also the same. Moreover, the distances between quark and antiquark are all the same according to the symmetry analysis of Eqs. (31–32). Furthermore, three Jacobi coordinates are orthogonal to each other according to Eqs. (33–35). Based on this, we take the $J^{PC}=0^{++}$ $bb\bar{b}\bar{b}$ ground state as an example to show the spatial distribution of four valence quarks. As for the internal contribution, although the kinetic energy part is smaller than that of the $\eta_b\eta_b$ state, the V^C in η_b is much more attractive relative to the $J^{PC}=0^{++}$ $bb\bar{b}\bar{b}$ ground state, which is the main reason that this state has a larger mass than the meson–meson threshold. Similar situations occur in other systems.

Similar to the $cc\bar{c}\bar{c}$ and $bb\bar{b}\bar{b}$ systems, the $cc\bar{b}\bar{b}$ system has the same number of allowed ground states. According to the specific function, their mass contribution comes mainly from the $\bar{3}\otimes 3$ component within the diquark–antiquark configuration. Furthermore, we obtain the relevant values of the magnetic moments, the transition magnetic moments, and the radiative decay widths. We also obtain the rearrangement strong width ratios within the meson–meson configuration.

As for the $cc\bar{c}\bar{b}$ and $bb\bar{b}\bar{c}$ systems, there are more allowed states due to fewer symmetry restrictions. Considering only the hyperfine potential, we can expect to have a compact stable state for the $J^P=1^+$ $bb\bar{b}\bar{c}$ configuration. However, since the V^C of the tetraquark are less attractive than the corresponding mesons, this state still has a mass larger than the meson–meson threshold.

In the $cb\bar{c}\bar{b}$ system, these states are also pure neutral particles, and we naturally obtain that their variational parameters C_{11} and C_{22} are the same. There is no constraint from the Pauli principle, so there are four $J^{PC}=0^{++}$ states, four $J^{PC}=1^{+-}$ states, two $J^{PC}=1^{++}$ states, and two $J^{PC}=2^{++}$ states. All of the $cb\bar{c}\bar{b}$ states have larger masses relative to the lowest thresholds. Moreover, they all have two different rearrangement strong decay modes: $c\bar{c}-b\bar{b}$ and $c\bar{b}-b\bar{c}$.

Then we compare our results with other theoretical work. Our results are roughly compatible with other nonrelativistic constituent quark models, although different papers have chosen different potential forms. Meanwhile, it is also interesting to find that similar mass ranges are given by the QCD sum rules, the Monte Carlo method, and the chiral quark model. This shows that our results are quite reasonable.

In summary, our theoretical calculations show that the masses of the $cc\bar{c}\bar{c}$ ground states are around 6.45 GeV, which is obviously lower than 6.9 GeV. Thus, the experimentally observed $X(6900)$ state does not seem to be a ground $cc\bar{c}\bar{c}$ tetraquark state, but could be a radially or orbitally excited state. We also find that these lowest states all have a large positive binding energy B_T. In other words, all these states are found to have masses greater than the corresponding two meson decay thresholds via the quark rearrangement. Hence, we conclude that there is no compact bound fully heavy tetraquark ground state which is stable against the strong decay into two mesons within the constituent quark model. Finally, we hope that more relevant experimental analyses will be able to focus on this system in the near future.

Acknowledgements This work is supported by the China National Funds for Distinguished Young Scientists under Grant No. 11825503, National Key Research and Development Program of China under Contract No. 2020YFA0406400, the 111 Project under Grant No. B20063, the National Natural Science Foundation of China under Grant No. 12247101, and the project for top-notch innovative talents of Gansu province. Z.W.L. is grateful for the support from the National Natural Science Foundation of China under Grants No. 12175091 and 11965016, and CAS Interdisciplinary Innovation Team.

Data Availability Statement This manuscript has no associated data or the data will not be deposited. [Authors' comment: This is a theoretical study and no experimental data.]

Appendix

In this appendix, we show the masses, binding energies, variational parameters, internal contribution, total wave functions, magnetic moments, transition magnetic moments, radiative decay widths, rearrangement strong width ratios, and the relative lengths between the quarks for the $cc\bar{b}\bar{b}$, $cc\bar{c}\bar{b}$, $bb\bar{b}\bar{c}$, and $cb\bar{c}\bar{b}$ states with different $J^{P(C)}$ quantum numbers and their lowest meson–meson thresholds (Tables 11, 12, 13, 14, 15, 16, 17).

Table 11 The masses, binding energies, variational parameters, the internal contribution, total wave functions, magnetic moments, transition magnetic moments, radiative decay widths, rearrangement strong width ratios, and the relative lengths between quarks for the $J^P = 0^+$, 1^+ $cc\bar{b}\bar{b}$ states and their lowest meson–meson thresholds. The notation is the same as that of Table 7

$J^P = 0^+$

$cc\bar{b}\bar{b}$, $J^P = 0^+$		Value	B_cB_c	Difference
Mass/B_T		12920.0	12575.8	344.2
Variational Parameters (fm^{-2})	C_{11}	23.9	22.9	
	C_{22}	10.5	22.9	
	C_{33}	12.3	-	
Quark Mass		14522.0	14522.0	0.0
Confinement Potential		-2420.1	-2795.5	375.4
Kinetic Energy		835.9	947.3	-111.4
CS Interaction		-7.0	-98.0	91.0
V^C	(1,2)	-46.9		
	(2,3)	-47.5		
	(1,4)	-47.5		
	Subtotal	-454.0	-829.5	375.3
Total Contribution		-374.9	19.8	355.1

Relative Lengths (fm) (i,j)	Value	B_cB_c
(1,2)	0.348	
(1.3)	0.308	$0.235(B_c)$
(2,3)	0.308	
(1,4)	0.308	
(2,4)	0.308	$0.235(B_c)$
(3,4)	0.230	
(1,2)-(3,4):	0.226 fm	
Radius:	0.151 fm	
(1,3)	-47.5	$-414.8(B_c)$
(3,4)	-217.1	
(2,4)	-47.5	$-414.8(B_c)$

Total Wave function:

$$\Psi_{tot} = 0.259|F\rangle|R^s\rangle|[\phi_2\chi_6]\rangle - 0.966|F\rangle|R^s\rangle|[\phi_1\chi_5]\rangle = -0.589|F\rangle|R^s\rangle|[\psi_1\zeta_5]\rangle$$
$$+0.095|F\rangle|R^s\rangle|[\psi_1\zeta_6]\rangle + 0.608|F\rangle|R^s\rangle|[\psi_2\zeta_5]\rangle + 0.524|F\rangle|R^s\rangle|[\psi_2\zeta_6]\rangle$$

The rearrangement strong width ratios :

$$\Gamma_{T_{c^2\bar{b}^2}(12920.0,0^{++})\to B_c^*B_c^*} : \Gamma_{T_{c^2\bar{b}^2}(12920.0.0,0^{++})\to B_cB_c} = 1:50$$

The radiative decay widths :

$$\Gamma_{T_{c^2\bar{b}^2}(12960.9,2^+)\to T_{c^2\bar{b}^2}(12920.0,0^+)\gamma} = 0\,\mathrm{keV}\ ;$$
$$\Gamma_{T_{c^2\bar{b}^2}(12939.9,1^+)\to T_{c^2\bar{b}^2}(12920.0,0^+)\gamma} = 3.8\,\mathrm{keV}$$

The magnetic moments : $\mu_{T_{c^2\bar{b}^2}(12920.0,0^+)} = \langle\Psi_{tot}^{0^+}|\hat{\mu^z}|\Psi_{tot}^{0^+}\rangle = 0$

The transition magnetic moments:

$$\mu_{T_{c^2\bar{b}^2}(12960.9,2^+)\to T_{c^2\bar{b}^2}(19240.0,0^+)\gamma} = \langle\Psi_{tot}^{2^+}|\hat{\mu^z}|\Psi_{tot}^{0^+}\rangle = 0$$
$$\mu_{T_{c^2\bar{b}^2}(12939.9,1^+)\to T_{c^2\bar{b}^2}(12920.0,0^+)\gamma} = \langle\Psi_{tot}^{1^+}|\hat{\mu^z}|\Psi_{tot}^{0^+}\rangle = 0.966\times\frac{4}{\sqrt{6}}(\mu_c-\mu_{\bar{b}}) = 0.534\mu_N$$

Overall	Present Work: Contribution	Present Work: Value	CMI Model: Ref. [110]	CMI Model: Ref. [123]
c-quark: m_c^{eff}	$2m_c$	3836.0		
	$\frac{\mathbf{p}_{x_1}^2}{2m_1'}$	319.0		
	$\frac{m_{\bar{b}}}{m_c+m_{\bar{b}}}\frac{\mathbf{p}_{x_3}^2}{2m_3'}$	188.0		
	$V^C(12)$	-46.9	$\frac{1}{2}m_{cc}$	
	$\frac{1}{2}[V^C(13)+V^C(14)$ $+V^C(23)+V^C(24)]$	-95.0	1585.8 $\frac{m_c}{m_{\bar{b}}+m_c}m_{c\bar{b}}$	$2m_c$
	$-D$	-983.0	1578.7	3449.6
	Subtotal	3218.1	3164.5	3449.6
$\bar{b}$-quark: $m_{\bar{b}}^{eff}$	$2m_b$	10686.0		
	$\frac{\mathbf{p}_{x_2}^2}{2m_2'}$	216.4		
	$\frac{m_c}{m_c+m_{\bar{b}}}\frac{\mathbf{p}_{x_3}^2}{2m_3'}$	67.5		
	$V^C(34)$	-217.1	$\frac{1}{2}m_{bb}$	
	$\frac{1}{2}[V^C(13)+V^C(14)$ $+V^C(23)+V^C(24)]$	-95.0	4764.8 $\frac{m_{\bar{b}}}{m_{\bar{b}}+m_c}m_{c\bar{b}}$	$2m_b$
	$-D$	-983.0	4743.6	10105.8
	Subtotal	9674.8	9508.4	10105.8
CS Interaction	$\frac{1}{2}V^{SS}(12)$	9.6	$\frac{8}{3}v_{cc}+\frac{8}{3}v_{bb}$	$\frac{8}{3}C_{cc}+\frac{8}{3}C_{bb}$
	$\frac{1}{2}V^{SS}(34)$	5.5	9.5+5.1	14.1+7.7
	$-\frac{1}{2}(V^{SS}(13)+V^{SS}(14)$ $V^{SS}(23)+V^{SS}(24))$	-22.1	$-\frac{32}{3}v_{c\bar{b}}$ -31.5	$-\frac{32}{3}C_{c\bar{b}}$ -35.2
	Subtotal	-7.0	-16.9	-13.3
Matrix nondiagonal element		-10.7	-59.7	46.1
Total contribution		12920.0	12596.3	13496.0

$J^P = 1^+$

$J^P = 1^+$		Value	$B_c^*B_c$	Difference
Mass/B_T		12939.9	12638.4	301.5
Variational Parameters (fm^{-2})	C_{11}	24.8	20.2	
	C_{22}	10.3	22.9	
	C_{33}	11.1	-	
Quark Mass		14522.0	14522.0	0.0
Confinement Potential		-2400.7	-2741.1	340.4
Kinetic Energy		814.0	891.5	-77.5
CS Interaction		4.6	-34.0	38.6
V^C	(1,2)	-43.5		
	(2,3)	-41.6		
	(1,4)	-41.6		
	Subtotal	-454.0	-829.5	375.3
Total Contribution		383.9	82.4	301.5

Relative Lengths (fm) (i,j)	Value	$B_c^*B_c$
(1,2)	0.351	
(1,3)	0.317	$0.250(B_c^*)$
(2,3)	0.317	
(1,4)	0.317	
(2,4)	0.317	$0.235(B_c)$
(3,4)	0.226	
(1,2)-(3,4):	0.238 fm	
Radius:	0.157 fm	
(1,3)	-41.6	$-360.4(B_c^*)$
(3,4)	-225.5	
(2,4)	-41.6	$-414.8(B_c)$

Total Wave function: $\Psi_{tot} = |F\rangle|R^s\rangle|[\phi_1\chi_2]\rangle =$

$$-0.419|F\rangle|R^s\rangle|[\psi_1\zeta_2]\rangle - 0.393|F\rangle|R^s\rangle|[\psi_1\zeta_3]\rangle - 0.066|F\rangle|R^s\rangle|[\psi_1\zeta_4]\rangle$$
$$+0.587|F\rangle|R^s\rangle|[\psi_2\zeta_2]\rangle + 0.557|F\rangle|R^s\rangle|[\psi_2\zeta_3]\rangle + 0.105|F\rangle|R^s\rangle|[\psi_2\zeta_4]\rangle$$

The rearrangement strong decay channel: B^*B_c

The radiative decay widths: $\Gamma_{T_{c^2\bar{b}^2}(12960.9,2^+)\to T_{c^2\bar{b}^2}(12939.9.9,1^+)\gamma} = 3.6\,\mathrm{keV}$

$\Gamma_{T_{c^2\bar{b}^2}(12939.9,1^+)\to T_{c^2\bar{b}^2}(12920.0,0^+)\gamma} = 3.8\,\mathrm{keV}$

The magnetic moments:

$$\mu_{T_{c^2\bar{b}^2}(12939.9,1^+)} = \langle\Psi_{tot}^{1^+}|\hat{\mu^z}|\Psi_{tot}^{1^+}\rangle = \mu_c+\mu_{\bar{b}} = 0.490\mu_N$$

Overall	Contribution	Value	Ref. [110]	Ref. [123]
c-quark: m_c^{eff}	$2m_c$	3836.0		
		$\frac{\mathbf{p}_{x_1}^2}{2m_1'}$	312.7	
	$\frac{m_{\bar{b}}}{m_c+m_{\bar{b}}}\frac{\mathbf{p}_{x_3}^2}{2m_3'}$	169.1	$\frac{1}{2}m_{cc}$	
	$V^C(12)$	-43.5	1585.8	
	$\frac{1}{2}[V^C(13)+V^C(14)$ $+V^C(23)+V^C(24)]$	-83.2	$\frac{m_c}{m_{\bar{b}}+m_c}m_{c\bar{b}}$	$2m_c$
	$-D$	-983.0	1587.7	3449.6
	Subtotal	3208.1	3164.5	3449.6
$\bar{b}$-quark: $m_{\bar{b}}^{eff}$	$2m_b$	10686.0		
	$\frac{\mathbf{p}_{x_2}^2}{2m_2'}$	271.5		
	$\frac{m_c}{m_c+m_{\bar{b}}}\frac{\mathbf{p}_{x_3}^2}{2m_3'}$	60.7	$\frac{1}{2}m_{bb}$	
	$V^C(34)$	-225.5	4764.8	
	$\frac{1}{2}[V^C(13)+V^C(14)$ $+V^C(23)+V^C(24)]$	-83.2	$\frac{m_{\bar{b}}}{m_{\bar{b}}+m_c}m_{c\bar{b}}$	$2m_b$
	$-D$	-983.0	4743.6	10105.8
	Subtotal	9726.5	9508.4	10105.8
CS Interaction	$\frac{1}{2}V^{SS}(12)$	5.7	$\frac{8}{3}v_{cc}+\frac{8}{3}v_{\bar{b}\bar{b}}$	$\frac{8}{3}C_{cc}+\frac{8}{3}C_{\bar{b}\bar{b}}$
	$\frac{1}{2}V^{SS}(34)$	4.6	9.5+5.1	14.1+7.7
	$-\frac{1}{4}(V^{SS}(13)+V^{SS}(14)$ $+V^{SS}(23)+V^{SS}(24)$	-10.6	$-\frac{16}{3}v_{\bar{c}\bar{b}}$ -15.7	$-\frac{16}{3}C_{\bar{c}\bar{b}}$ -17.6
	Subtotal	4.6	-1.2	4.3
Total contribution		12939.9	12671.6	13560.0

The transition magnetic moments: $\mu_{T_{b^2\bar{b}^2}(12960.9,2^+)\to T_{b^2\bar{b}^2}(12939.9,1^+)\gamma} = \langle\Psi_{tot}^{2^+}|\hat{\mu^z}|\Psi_{tot}^{1^+}\rangle = \mu_c-\mu_{\bar{b}} = 0.342\mu_N$

$$\mu_{T_{c^2\bar{b}^2}(12939.9,1^+)\to T_{c^2\bar{b}^2}(12920.0,0^+)\gamma} = \langle\Psi_{tot}^{1^+}|\hat{\mu^z}|\Psi_{tot}^{0^+}\rangle = 0.966\times\frac{4}{\sqrt{6}}(\mu_c-\mu_{\bar{b}}) = 0.534\mu_N$$

Table 12 The masses, binding energies, variational parameters, the internal contribution, total wave functions, magnetic moments, transition magnetic moments, radiative decay widths, rearrangement strong width ratios, and the relative lengths between quarks for the $J^P = 2^+$ $cc\bar{b}\bar{b}$ state and its lowest meson–meson threshold. The notation is the same as that in Table 7

$cc\bar{b}\bar{b}$	The contribution from each term				Relative Lengths (fm)		
$J^P = 2^+$		Value	$B_c^* B_c^*$	Difference	(i,j)	Value	$B_c^* B_c^*$
Mass/B_T		12960.9	12700.9	260.0	(1,2)	0.355	
Variational Parameters (fm^{-2})	C_{11}	24.5	20.2		(1.3)	0.322	$0.250(B_c^*)$
	C_{22}	10.1	20.2		(2,3)	0.322	
	C_{33}	10.7	-				
Quark Mass		14522.0	14522.0	0.0	(1,4)	0.322	
Confinement Potential		-2382.1	-2686.8	304.7	(2,4)	0.322	$0.250(B_c^*)$
Kinetic Energy		795.6	835.7	-40.1	(3,4)	0.227	
CS Interaction		25.3	30.0	-4.7	(1,2)-(3,4):		0.243 fm
V^C	(1,2)	-38.9			Radius:		0.160 fm
	(2,3)	-38.7					
	(1,4)	-38.7			(1,3)	-38.7	$-360.4(B_c^*)$
	Subtotal	-416.0	-720.8	304.8	(3,4)	-222.4	
Total Contribution		404.9	144.9	260.0	(2,4)	-38.7	$-360.4(B_c^*)$

Overall	Present Work		CMI Model	
	Contribution	Value	Ref. [110]	Ref. [123]
c-quark: m_c^{eff}	$2m_c$	3836.0		
	$\frac{\mathbf{p}_{x_1}^2}{2m_1'}$	306.2		
	$\frac{m_{\bar{b}}}{m_c+m_{\bar{b}}}\frac{\mathbf{p}_{x_3}^2}{2m_3'}$	163.1	$\frac{1}{2}m_{cc}$	
	$V^C(12)$	-38.9	1585.8	
	$\frac{1}{2}[V^C(13)+V^C(14)+V^C(23)+V^C(24)]$	-77.4	$\frac{m_c}{m_{\bar{b}}+m_c}m_{c\bar{b}}$	$2m_c$
	$-D$	-983.0	1587.7	3449.6
	Subtotal	3206.0	3164.5	3449.6
$\bar{b}$-quark: $m_{\bar{b}}^{eff}$	$2m_b$	10686.0		
	$\frac{\mathbf{p}_{x_2}^2}{2m_2'}$	268.8		
	$\frac{m_c}{m_c+m_{\bar{b}}}\frac{\mathbf{p}_{x_3}^2}{2m_3'}$	58.5	$\frac{1}{2}m_{bb}$	
	$V^C(34)$	-222.4	4764.8	
	$\frac{1}{2}[V^C(13)+V^C(14)+V^C(23)+V^C(24)]$	-77.4	$\frac{m_{\bar{b}}}{m_{\bar{b}}+m_c}m_{c\bar{b}}$	$2m_b$
	$-D$	-983.0	4743.6	10105.8
	Subtotal	9730.5	9508.4	10105.8
CS Interaction	$\frac{1}{2}V^{SS}(12)$	9.3	$\frac{8}{3}v_{cc}$	$\frac{8}{3}C_{cc}$
			9.5	14.1
	$\frac{1}{2}V^{SS}(34)$	4.6	$\frac{8}{3}v_{\bar{b}\bar{b}}$	$\frac{8}{3}C_{\bar{b}\bar{b}}$
			5.1	7.7
	$\frac{1}{4}[V^{SS}(13)+V^{SS}(14)+V^{SS}(23)+V^{SS}(24)]$	10.3	$\frac{16}{3}v_{c\bar{b}}$	$\frac{16}{3}C_{c\bar{b}}$
			15.7	17.6
	Subtotal	25.3	30.3	39.5
Total contribution		12960.9	12703.1	13595.0

Total Wave function:

$\Psi_{tot} = |F\rangle|R^s\rangle|[\phi_1\chi_2]\rangle = 0.577|F\rangle|R^s\rangle|[\psi_1\zeta_1]\rangle - 0.816|F\rangle|R^s\rangle|[\psi_2\zeta_1]\rangle$

The rearrangement strong decay channel: $B_c^* B_c^*$

The radiative decay widths: $\Gamma_{T_{c^2\bar{b}^2}(12960.9,2^+)\to T_{c^2\bar{b}^2}(12920.0,0^+)\gamma} = 0\,\text{keV}$

$\Gamma_{T_{c^2\bar{b}^2}(12960.9,2^+)\to T_{c^2\bar{b}^2}(12939.9.9,1^+)\gamma} = 3.6\,\text{keV}$

The magnetic moments:

$\mu_{T_{c^2\bar{b}^2}(12969.9,2^+)} = \langle\Psi_{tot}^{2^+}|\hat{\mu^z}|\Psi_{tot}^{2^+}\rangle = 2\mu_c + 2\mu_{\bar{b}} = 0.982\mu_N$

The transition magnetic moments :

$\mu_{T_{c^2\bar{b}^2}(12960.9,2^+)\to T_{c^2\bar{b}^2}(19240.0,0^+)\gamma} = \langle\Psi_{tot}^{2^+}|\hat{\mu^z}|\Psi_{tot}^{0^+}\rangle = 0$;

$\mu_{T_{b^2\bar{b}^2}(12960.9,2^+)\to T_{b^2\bar{b}^2}(12939.9,1^+)\gamma} = \langle\Psi_{tot}^{2^+}|\hat{\mu^z}|\Psi_{tot}^{1^+}\rangle = \mu_c - \mu_{\bar{b}} = 0.342\mu_N$

Table 13 The masses, binding energy, variational parameters, the internal contribution, total wave functions, magnetic moments, transition magnetic moments, radiative decay widths, rearrangement strong width ratios, and the relative lengths between quarks for the $J^P = 0^+$, 1^+ $cc\bar{c}\bar{b}$ states and their lowest meson–meson thresholds. The notation is the same as that in Table 7

$cc\bar{c}\bar{b}$		The contribution from each term			Relative Lengths (fm)		
$J^P=0^+$		Value	$B_c\eta_c$	Difference	(i,j)	Value	$B_c\eta_c$
Mass/B_T		9620.5	9286.4	332.1	(1,2)	0.418	
Variational Parameters (fm^{-2})	C_{11}	11.4	22.9		(1.3)	0.325	0.290(η_c)
	C_{22}	7.2	15.0		(2,3)	0.325	
	C_{33}	15.2	-				
Quark Mass		11097.0	11097.0	0.0	(1,4)	0.336	
Confinement Potential		-2280.0	-2618.0	338.0	(2,4)	0.336	0.235(B_c)
Kinetic Energy		810.3	931.2	-120.9	(3,4)	0.333	
CS Interaction		18.2	-123.8	142.0	(1,2)-(3,4):	0.204 fm	
V^C	(1,2)	-12.6			(1,3)	-91.9	-237.2(η_c)
	(1,4)	-74.8			(2,3)	-91.9	
	Subtotal	-314.0	-652.0	338.0	(2,4)	-74.8	−414.8(B_c)
Total Contribution		514.4	155.4	359.0	(3,4)	32.0	

Overall	Present Work Contribution	Value	CMI Model Ref. [110]	Ref. [123]
c-quark: m_c^{eff}	$2m_c$	3836.0	$-\frac{1}{4}m_{cc}$	
	$\frac{\mathbf{p}^2_{x_1}}{2m'_1}+\frac{m_c+m_{\bar{b}}}{3m_c+m_{\bar{b}}}\frac{\mathbf{p}^2_{x_3}}{2m'_3}$	451.6	-792.9	
	$V^C(12)$	-12.6	$\frac{5m_c}{4(m_c+m_{\bar{c}})}m_{c\bar{c}}$	
	$\frac{1}{2}[V^C(13)+V^C(23)]$	-91.8	1917.8	
	$\frac{1}{2}[V^C(14)+V^C(24)]$	-74.8	$\frac{5m_c}{4(m_c+m_{\bar{b}})}m_{c\bar{b}}$	$2m_c$
	$-D$	-983.0	1973.7	3449.6
	Subtotal	3125.4	3098.6	3449.6
$\bar{c}$-quark: $m_{\bar{c}}^{eff}$	$m_{\bar{c}}$	1918.0	$\frac{-m_{\bar{c}}}{4(m_{\bar{b}}+m_{\bar{c}})}m_{\bar{c}\bar{b}}$	
	$\frac{m_{\bar{b}}}{m_{\bar{c}}+m_{\bar{b}}}\frac{\mathbf{p}^2_{x_2}}{2m'_2}+\frac{m_c}{3m_c+m_{\bar{b}}}\frac{\mathbf{p}^2_{x_3}}{2m'_3}$	235.0	-400.5	
	$\frac{1}{2}V^C(34)$	16.0		
	$\frac{1}{2}[V^C(13)+V^C(23)]$	-91.9	$\frac{5m_c}{4(m_c+m_{\bar{b}})}m_{c\bar{b}}$	$m_{\bar{c}}$
	$-\frac{1}{2}D$	-491.5	1917.8	1724.8
	Subtotal	1585.6	1517.3	1724.8
$\bar{b}$-quark: $m_{\bar{b}}^{eff}$	$m_{\bar{b}}$	5343.0	$\frac{-m_{\bar{b}}}{4(m_{\bar{b}}+m_{\bar{c}})}m_{\bar{c}\bar{b}}$	
	$\frac{m_{\bar{c}}}{m_{\bar{c}}+m_{\bar{b}}}\frac{\mathbf{p}^2_{x_2}}{2m'_2}+\frac{m_c}{3m_c+m_{\bar{b}}}\frac{\mathbf{p}^2_{x_3}}{2m'_3}$	123.6	-1203.5	
	$\frac{1}{2}V^C(34)$	16.0		
	$\frac{1}{2}[V^C(14)+V^C(24)]$	-74.8	$\frac{5m_{\bar{b}}}{4(m_c+m_{\bar{b}})}m_{c\bar{b}}$	$m_{\bar{b}}$
	$-\frac{1}{2}D$	-491.5	5929.5	5052.9
	Subtotal	4916.3	4726.0	5052.9
CS Interaction	$\frac{3}{4}V^{SS}(12)$	10.8	$4v_{cc}$ 14.3	$4C_{cc}$ 21.2
	$\frac{3}{4}V^{SS}(34)$	7.3	$4v_{\bar{c}\bar{b}}$ 7.9	$4C_{\bar{c}\bar{b}}$ 13.2
	Subtotal	18.2	22.1	34.4
Matrix nondiagonal element		-25.0	-46.2	-117.7
Total contribution		9620.5	9317.5	10144.0

Total Wave function:

$\Psi_{tot}=0.401|F\rangle|R^s\rangle|[\phi_1\chi_5]\rangle-0.916|F\rangle|R^s\rangle|[\phi_2\chi_6]\rangle=-0.574|F\rangle|R^s\rangle|[\psi_1\zeta_5]\rangle$
$-0.532|F\rangle|R^s\rangle|[\psi_1\zeta_6]\rangle+0.019|F\rangle|R^s\rangle|[\psi_2\zeta_5]\rangle-0.622|F\rangle|R^s\rangle|[\psi_2\zeta_6]\rangle$

The rearrangement strong decay channel:

$\Gamma_{T_{c2\bar{b}2}(9620.5,0^+)\to B_c^* J/\psi}:\Gamma_{T_{c2\bar{b}2}(9620.5,0^+)\to B_c\eta_c}=1:1.2$

The radiative decay widths: $\Gamma_{T_{c2\bar{c}\bar{b}}(9730.5,2^+)\to T_{c2\bar{c}\bar{b}}(9620.5,0^+)\gamma}=0\text{keV}$
$\Gamma_{T_{c2\bar{c}\bar{b}}(9624.6,1^+)\to T_{c2\bar{c}\bar{b}}(9620.5,0^+)\gamma}=0.007\text{keV}$

The magnetic moments: $\mu_{T_{c2\bar{c}\bar{b}}(9620.5,0^+)}=\langle\Psi^{0^+}_{tot}|\hat{\mu^z}|\Psi^{0^+}_{tot}\rangle=0$

The transition magnetic moments:

$\mu_{T_{c2\bar{c}\bar{b}}(9730.5,2^+)\to T_{c2\bar{c}\bar{b}}(9620.5,0^+)\gamma}=\langle\Psi^{2^+}_{tot}|\hat{\mu^z}|\Psi^{0^+}_{tot}\rangle=0$

$\mu_{T_{c2\bar{c}\bar{b}}(9624.6,1^+)\to T_{c2\bar{c}\bar{b}}(9620.5,0^+)\gamma}=\langle\Psi^{1^+}_{tot}|\hat{\mu^z}|\Psi^{0^+}_{tot}\rangle=-0.096\mu_N$

$J^P=1^+$		Value	$B_c^*\eta_c$	Difference	Relative Lengths (fm)		
Mass/B_T		9624.6	9349.0	275.6	(i,j)	Value	$B_c^*\eta_c$
Variational Parameters (fm^{-2})	C_{11}	11.1	20.2		(1.2)	0.429	
	C_{22}	6.9	15.0		(1,3)	0.328	0.290(η_c)
	C_{33}	15.3	-				
Quark Mass		11097.0	11097.0	0.0	(2,3)	0.328	
Confinement Potential		-2266.2	-2563.6	297.4	(1,4)	0.340	
Kinetic Energy		795.2	875.4	-80.2	(2,4)	0.340	0.250(B_c^*)
CS Interaction		8.0	-59.9	67.9	(3,4)	0.338	
V^C	(1,2)	-17.4			(1,2)-(3,4):	0.204 fm	
	(2,3)	-87.0					
	(1,4)	-68.9			(2,4)	-68.9	−360.4(B_c^*)
	Subtotal	-300.2	-597.6	297.4	(3,4)	29.0	
Total Contribution		503.0	218.0	285.0	(1,3)	-87.0	−237.2(η_c)

Overall	Contribution	Value	Ref. [110]	Ref. [123]
c-quark: m_c^{eff}	$2m_c$	3836.0	$-\frac{1}{4}m_{cc}$	
	$\frac{\mathbf{p}^2_{x_1}}{2m'_1}+\frac{m_c+m_{\bar{b}}}{3m_c+m_{\bar{b}}}\frac{\mathbf{p}^2_{x_3}}{2m'_3}$	442.8	-792.9	
	$V^C(12)$	-17.4	$\frac{5m_c}{4(m_c+m_{\bar{c}})}m_{c\bar{c}}$	
	$\frac{1}{2}[V^C(13)+V^C(23)]$	-87.0	1917.8	
	$\frac{1}{2}[V^C(14)+V^C(24)]$	-68.9	$\frac{5m_c}{4(m_c+m_{\bar{b}})}m_{c\bar{b}}$	$2m_c$
	$-D$	-983.0	1973.7	3449.6
	Subtotal	3122.5	3098.6	3449.6
$\bar{c}$-quark: $m_{\bar{c}}^{eff}$	$m_{\bar{c}}$	1918.0	$\frac{-m_{\bar{c}}}{4(m_{\bar{b}}+m_{\bar{c}})}m_{\bar{c}\bar{b}}$	
	$\frac{m_{\bar{b}}}{m_{\bar{c}}+m_{\bar{b}}}\frac{\mathbf{p}^2_{x_2}}{2m'_2}+\frac{m_c}{3m_c+m_{\bar{b}}}\frac{\mathbf{p}^2_{x_3}}{2m'_3}$	230.3	-400.5	
	$\frac{1}{2}V^C(34)$	14.5		
	$\frac{1}{2}[V^C(13)+V^C(23)]$	-87.0	$\frac{5m_c}{4(m_c+m_{\bar{b}})}m_{c\bar{b}}$	$m_{\bar{c}}$
	$-\frac{1}{2}D$	-491.5	1917.8	1724.8
	Subtotal	1584.3	1517.3	1724.8
$\bar{b}$-quark: $m_{\bar{b}}^{eff}$	$m_{\bar{b}}$	5343.0	$\frac{-m_{\bar{b}}}{4(m_{\bar{b}}+m_{\bar{c}})}m_{\bar{c}\bar{b}}$	
	$\frac{m_{\bar{c}}}{m_{\bar{c}}+m_{\bar{b}}}\frac{\mathbf{p}^2_{x_2}}{2m'_2}+\frac{m_c}{3m_c+m_{\bar{b}}}\frac{\mathbf{p}^2_{x_3}}{2m'_3}$	122.1		-1203.5
	$\frac{1}{2}V^C(34)$	14.5		
	$\frac{1}{2}[V^C(14)+V^C(24)]$	-68.9	$\frac{5m_{\bar{b}}}{4(m_c+m_{\bar{b}})}m_{c\bar{b}}$	$m_{\bar{b}}$
	$-\frac{1}{2}D$	-491.5	5929.5	5052.9
	Subtotal	4919.2	4726.0	5052.9
CS Interaction	$-\frac{1}{4}V^{SS}(12)$	-2.3	$-\frac{4}{3}v_{\bar{c}\bar{b}}$ -2.6	$-\frac{4}{3}C_{\bar{c}\bar{b}}$ -4.4
	$\frac{3}{4}V^{SS}(34)$	10.4	$4v_{cc}$ 14.2	$4C_{cc}$ 21.2
	Subtotal	8.0	11.6	16.8
Matrix nondiagonal element		-9.3	-18.4	-100.0
Total contribution		9624.6	9335.1	10144

Total Wave function:

$\Psi_{tot}=0.220|F\rangle|R^s\rangle|[\phi_1\chi_3]\rangle+0.968|F\rangle|R^s\rangle|[\phi_2\chi_4]\rangle+0.118|F\rangle|R^s\rangle|[\phi_1\chi_2]\rangle$
$=0.494|F\rangle|R^s\rangle|[\psi_1\zeta_2]\rangle-0.396|F\rangle|R^s\rangle|[\psi_1\zeta_3]\rangle-0.487|F\rangle|R^s\rangle|[\psi_1\zeta_4]\rangle$
$+0.111|F\rangle|R^s\rangle|[\psi_2\zeta_2]\rangle-0.246|F\rangle|R^s\rangle|[\psi_2\zeta_3]\rangle-0.537|F\rangle|R^s\rangle|[\psi_2\zeta_4]\rangle$

The rearrangement strong decay channel: $\Gamma_{T_{c2\bar{c}\bar{b}}(9624.6,1^+)\to B_c^* J/\psi}:$
$\Gamma_{T_{c2\bar{c}\bar{b}}(9624.6,1^+)\to B_c J/\psi}:\Gamma_{T_{c2\bar{c}\bar{b}}(9624.6,1^+)\to B_c^*\eta_c}=1:0.8:1.2$

The radiative decay widths: $\Gamma_{T_{c2\bar{c}\bar{b}}(9730.5,2^+)\to T_{c2\bar{c}\bar{b}}(9624.6,1^+)\gamma}=145.0\text{keV}$
$\Gamma_{T_{c2\bar{c}\bar{b}}(9624.6,1^+)\to T_{c2\bar{c}\bar{b}}(9620.5,0^+)\gamma}=0.007\text{keV}$

The magnetic moments: $\mu_{T_{c2\bar{c}\bar{b}}(9624.6,1^+)}=\langle\Psi^{1^+}_{tot}|\hat{\mu^z}|\Psi^{1^+}_{tot}\rangle=-0.233\mu_N$

The transition magnetic moments:

$\mu_{T_{c2\bar{c}\bar{b}}(9624.6,1^+)\to T_{c2\bar{c}\bar{b}}(9620.5,0^+)\gamma}=\langle\Psi^{1^+}_{tot}|\hat{\mu^z}|\Psi^{0^+}_{tot}\rangle=-0.096\mu_N$ $\mu_{T_{c2\bar{c}\bar{b}}(9730.5,2^+)\to T_{c2\bar{c}\bar{b}}(9624.6,1^+)\gamma}=\langle\Psi^{2^+}_{tot}|\hat{\mu^z}|\Psi^{1^+}_{tot}\rangle=-0.294\mu_N$

Table 14 The masses, binding energy, variational parameters, the internal contribution, total wave functions, magnetic moments, transition magnetic moments, radiative decay widths, rearrangement strong width ratios, and the relative lengths between quarks for the $J^P = 0^+$, 1^+ $bb\bar{b}\bar{c}$ states and their lowest meson–meson thresholds. The notation is the same as that in Table 7

$bb\bar{b}\bar{c}$	The contribution from each term				Relative Lengths (fm)		
$J^P = 0^+$		Value	$B_c\eta_b$	Difference	(i,j)	Vaule	$B_c\eta_b$
Mass/B_T		16043.9	15676.9	367.0	(1,2)	0.242	
Variational Parameters (fm^{-2})	C_{11}	12.5	22.9		(1.3)	0.239	0.148(η_b)
	C_{22}	21.7	58.8		(2,3)	0.239	
	C_{33}	28.7	-				
Quark Mass		17947.0	17947.0	0.0	(1,4)	0.249	
Confinement Potential		-2786.7	-3259.9	473.2	(2,4)	0.249	0.235(B_c)
Kinetic Energy		883.3	1101.6	-218.3	(3,4)	0.318	
CS Interaction		15.5	-111.8	127.3	(1,2)-(3,4):	0.148 fm	
V^C	(1,2)	97.7			(1,3)	-251.3	-879.1(η_b)
	(1,4)	-225.8			(2,3)	-251.3	
	Subtotal	-820.7	-1293.9	473.2	(2,4)	-228.3	$-414.8(B_c)$
Total Contribution		78.1	-304.1	382.2	(3,4)	40.8	

Total Wave function:

$$\Psi_{tot} = 0.308|F\rangle|R^s\rangle|[\phi_1\chi_5]\rangle - 0.951|F\rangle|R^s\rangle|[\phi_2\chi_6]\rangle = -0.543|F\rangle|R^s\rangle|[\psi_1\zeta_5]\rangle$$
$$-0.584|F\rangle|R^s\rangle|[\psi_1\zeta_6]\rangle - 0.056|F\rangle|R^s\rangle|[\psi_2\zeta_5]\rangle - 0.602|F\rangle|R^s\rangle|[\psi_2\zeta_6]\rangle.$$

The rearrangement strong decay channel:

$\Gamma_{T_{b^2\bar{b}\bar{c}}(16043.9,0^+)\to B_c^*\Upsilon} : \Gamma_{T_{b^2\bar{b}\bar{c}}(16043.9,0^+)\to B_c\eta_b} = 1 : 1.4.$

The radiative decay widths: $\Gamma_{T_{b^2\bar{b}\bar{c}}(16149.2,2^+)\to T_{b^2\bar{b}\bar{c}}(16043.9,0^+)\gamma} = 0\,\text{keV}$

$\Gamma_{T_{c^2\bar{c}\bar{b}}(16043.9,0^+)\to T_{c^2\bar{c}\bar{b}}(16043.2,1^+)\gamma} = 10^{-6}\,\text{keV}$

The magnetic moments: $\mu_{T_{b^2\bar{b}\bar{c}}(16043.9,0^+)} = \langle\Psi_{tot}^{0^+}|\hat{\mu^z}|\Psi_{tot}^{0^+}\rangle = 0$

The transition magnetic moments:

$\mu_{T_{b^2\bar{b}\bar{c}}(16149.2,2^+)\to T_{b^2\bar{b}\bar{c}}(16043.9,0^+)\gamma} = \langle\Psi_{tot}^{2^+}|\hat{\mu^z}|\Psi_{tot}^{0^+}\rangle = 0$

$\mu_{T_{b^2\bar{b}\bar{c}}(16043.9,0^+)\to T_{b^2\bar{b}\bar{c}}(16043.2,1^+)\gamma} = \langle\Psi_{tot}^{0^+}|\hat{\mu^z}|\Psi_{tot}^{1^+}\rangle = 0.096\mu_N$

Overall	Present Work		CMI Model	
	Contribution	Value	Ref. [110]	Ref. [123]
b-quark: m_b^{eff}	$2m_b$	10686.0	$-\frac{1}{4}m_{bb}$	
	$\frac{\mathbf{p}_{x_1}^2}{2m_1'} + \frac{m_c+m_{\bar{b}}}{3m_c+m_{\bar{b}}}\frac{\mathbf{p}_{x_3}^2}{2m_3'}$	393.8	-2382.4	
	$V^C(12)$	97.7	$\frac{5m_b}{4(m_b+m_{\bar{b}})}m_{b\bar{b}}$	
	$\frac{1}{2}[V^C(13)+V^C(23)]$	-251.3	5903.1	
	$\frac{1}{2}[V^C(14)+V^C(24)]$	-228.3	$\frac{5m_b}{4(m_b+m_{\bar{c}})}m_{b\bar{c}}$	$2m_b$
	$-D$	-983.0	5929.5	10105.8
	Subtotal	9714.9	9450.2	10105.8
$\bar{b}$-quark: $m_{\bar{b}}^{eff}$	$m_{\bar{b}}$	5343.0	$\frac{-m_{\bar{b}}}{4(m_{\bar{c}}+m_{\bar{b}})}m_{\bar{c}\bar{b}}$	
	$\frac{m_{\bar{c}}}{m_{\bar{b}}+m_{\bar{c}}}\frac{\mathbf{p}_{x_2}^2}{2m_2'} + \frac{m_b}{3m_b+m_{\bar{c}}}\frac{\mathbf{p}_{x_3}^2}{2m_3'}$	183.8	-1203.5	
	$\frac{1}{2}V^C(34)$	20.4		
	$\frac{1}{2}[V^C(13)+V^C(23)]$	-251.3	$\frac{5m_b}{4(m_b+m_{\bar{c}})}m_{b\bar{b}}$	$m_{\bar{b}}$
	$-\frac{1}{2}D$	-491.5	5903.1	5052.9
	Subtotal	4804.4	4699.6	5052.9
$\bar{c}$-quark: $m_{\bar{c}}^{eff}$	$m_{\bar{c}}$	1918.0	$\frac{-m_{\bar{c}}}{4(m_{\bar{c}}+m_{\bar{b}})}m_{\bar{b}\bar{c}}$	
	$\frac{m_{\bar{b}}}{m_{\bar{b}}+m_{\bar{c}}}\frac{\mathbf{p}_{x_2}^2}{2m_2'} + \frac{m_b}{3m_b+m_{\bar{c}}}\frac{\mathbf{p}_{x_3}^2}{2m_3'}$	305.7		-400.5
	$\frac{1}{2}V^C(34)$	20.4		
	$\frac{1}{2}[V^C(14)+V^C(24)]$	-228.3	$\frac{5m_{\bar{c}}}{4(m_b+m_{\bar{c}})}m_{b\bar{c}}$	$m_{\bar{c}}$
	$-\frac{1}{2}D$	-491.5	1973.8.8	1724.8
	Subtotal	1524.3	1573.3	1724.8
CS Interaction	$\frac{3}{4}V^{SS}(12)$	7.9	$4v_{bb}$ 7.7	$4C_{bb}$ 11.6
	$\frac{3}{4}V^{SS}(34)$	7.7	$4v_{\bar{c}\bar{b}}$ 7.9	$4C_{\bar{c}\bar{b}}$ 13.2
	Subtotal	15.5	15.5	24.8
Matrix nondiagonal element		-15.2	-26.7	43.7
Total contribution		16043.9	15711.9	16932.0

$J^P = 1^+$		Value	$B_c^*\eta_b$	Difference	Relative Lengths (fm)		
					(i,j)	Value	$B_c^*\eta_b$
Mass/B_T		16043.2	15739.5	303.7	(1.2)	0.245	
Variational Parameters (fm^{-2})	C_{11}	12.4	20.2		(1,3)	0.240	0.148(η_b)
	C_{22}	21.0	57.4		(2,3)	0.240	
	C_{33}	28.9	-				
Quark Mass		17947.0	17947.0	0.0	(1,4)	0.250	
Confinement Potential		-2779.8	-3205.5	425.7			
Kinetic Energy		876.1	961.5	-123.3	(2,4)	0.250	0.250(B_c^*)
CS Interaction		4.8	-47.8	52.6	(3,4)	0.320	
V^C	(1,2)	94.5			(1,2)-(3,4):	0.148 fm	
	(2,3)	-248.2					
	(1,4)	-225.8			(2,4)	-225.8	$-360.4(B_c^*)$
	Subtotal	-813.7	-1239.5	425.7	(3,4)	39.7	
Total Contribution		67.1	-241.5	308.6	(1,3)	-248.2	$-879.1(\eta_b)$

Total Wave function:

$$\Psi_{tot} = 0.171|F\rangle|R^s\rangle|[\phi_1\chi_3]\rangle + 0.984|F\rangle|R^s\rangle|[\phi_2\chi_4]\rangle + 0.044|F\rangle|R^s\rangle|[\phi_1\chi_2]\rangle$$
$$= 0.431|F\rangle|R^s\rangle|[\psi_1\zeta_2]\rangle - 0.467|F\rangle|R^s\rangle|[\psi_1\zeta_3]\rangle - 0.500|F\rangle|R^s\rangle|[\psi_1\zeta_4]\rangle$$
$$+0.240|F\rangle|R^s\rangle|[\psi_2\zeta_2]\rangle - 0.188|F\rangle|R^s\rangle|[\psi_2\zeta_3]\rangle - 0.502|F\rangle|R^s\rangle|[\psi_2\zeta_4]\rangle$$

The rearrangement strong decay channel: $\Gamma_{T_{b^2\bar{b}\bar{c}}(16043.2,1^+)\to B_c^*\Upsilon} :$

$\Gamma_{T_{b^2\bar{b}\bar{c}}(16043.2,1^+)\to B_c\Upsilon} : \Gamma_{T_{b^2\bar{b}\bar{c}}(16043.2,1^+)\to B_c^*\eta_b} = 1 : 1.3 : 1.5$

The radiative decay widths: $\Gamma_{T_{b^2\bar{b}\bar{c}}(16149.2,2^+)\to T_{c^2\bar{c}\bar{b}}(16043.2,1^+)\gamma} = 435.0\text{keV}$

$\Gamma_{T_{c^2\bar{c}\bar{b}}(16043.9,0^+)\to T_{c^2\bar{c}\bar{b}}(16043.2,1^+)\gamma} = 10^{-6}\text{keV}$

The magnetic moments: $\mu_{T_{b^2\bar{b}\bar{c}}(19043.2,1^+)} = \langle\Psi_{tot}^{1^+}|\hat{\mu^z}|\Psi_{tot}^{1^+}\rangle = -0.346\mu_N$

The transition magnetic moments:

$\mu_{T_{b^2\bar{b}\bar{c}}(16043.9,0^+)\to T_{b^2\bar{b}\bar{c}}(16043.2,1^+)\gamma} = \langle\Psi_{tot}^{0^+}|\hat{\mu^z}|\Psi_{tot}^{1^+}\rangle = 0.201\mu_N$ $\mu_{T_{b^2\bar{b}\bar{c}}(16149.2,2^+)\to T_{b^2\bar{b}\bar{c}}(16043.2,1^+)\gamma} = \langle\Psi_{tot}^{2^+}|\hat{\mu^z}|\Psi_{tot}^{1^+}\rangle = 0.329\mu_N$

Overall	Contribution	Value	Ref. [110]	Ref. [123]
b-quark: m_b^{eff}	$2m_b$	10686.0	$-\frac{1}{4}m_{bb}$	
	$\frac{\mathbf{p}_{x_1}^2}{2m_1'} + \frac{m_{\bar{b}}+m_{\bar{c}}}{3m_b+m_{\bar{c}}}\frac{\mathbf{p}_{x_3}^2}{2m_3'}$	387.9	-2382.4	
	$V^C(12)$	94.5	$\frac{5m_b}{4(m_b+m_{\bar{b}})}m_{b\bar{b}}$	
	$\frac{1}{2}[V^C(13)+V^C(23)]$	-248.2	5903.1	
	$\frac{1}{2}[V^C(14)+V^C(24)]$	-225.8	$\frac{5m_b}{4(m_b+m_{\bar{c}})}m_{b\bar{c}}$	$2m_b$
	$-D$	-983.0	5929.5	10105.8
	Subtotal	9711.4	9450.2	10105.8
$\bar{b}$-quark: $m_{\bar{b}}^{eff}$	$m_{\bar{b}}$	5342.0	$\frac{-m_{\bar{b}}}{4(m_{\bar{c}}+m_{\bar{b}})}m_{\bar{b}\bar{c}}$	
	$\frac{m_{\bar{c}}}{m_{\bar{b}}+m_{\bar{c}}}\frac{\mathbf{p}_{x_2}^2}{2m_2'} + \frac{m_b}{3m_b+m_{\bar{c}}}\frac{\mathbf{p}_{x_3}^2}{2m_3'}$	183.8	-1203.5	
	$\frac{1}{2}V^C(34)$	19.9		
	$\frac{1}{2}[V^C(13)+V^C(23)]$	-248.2	$\frac{5m_b}{4(m_b+m_{\bar{c}})}m_{b\bar{c}}$	$m_{\bar{b}}$
	$-\frac{1}{2}D$	-491.5	5903.1	5052.9
	Subtotal	4807.0	4699.6	5052.9
$\bar{c}$-quark: $m_{\bar{c}}^{eff}$	$m_{\bar{c}}$	1918.0	$\frac{-m_{\bar{c}}}{4(m_{\bar{c}}+m_{\bar{b}})}m_{\bar{b}\bar{c}}$	
	$\frac{m_{\bar{b}}}{m_{\bar{b}}+m_{\bar{c}}}\frac{\mathbf{p}_{x_2}^2}{2m_2'} + \frac{m_b}{3m_b+m_{\bar{c}}}\frac{\mathbf{p}_{x_3}^2}{2m_3'}$	304.4	-400.5	
	$\frac{1}{2}V^C(34)$	19.9		
	$\frac{1}{2}[V^C(14)+V^C(24)]$	-225.8	$\frac{5m_{\bar{c}}}{4(m_b+m_{\bar{c}})}m_{b\bar{c}}$	$m_{\bar{c}}$
	$-\frac{1}{2}D$	-491.5	1973.8	1724.8
	Subtotal	1525.0	1573.3	1724.8
CS Interaction	$-\frac{1}{4}V^{SS}(12)$	-2.6	$-\frac{4}{3}v_{\bar{b}\bar{c}}$ -2.6	$-\frac{4}{3}C_{\bar{b}\bar{c}}$ -4.4
	$\frac{3}{4}V^{SS}(34)$	7.5	$4v_{bb}$ 7.7	$4C_{bb}$ 11.6
	Subtotal	4.8	5.0	7.2
Matrix nondiagonal element		-5.0	-8.6	24.3
Total contribution		16048.1	15719.1	16915.0

Table 15 The masses, binding energy, variational parameters, the internal contribution, total wave functions, magnetic moments, transition magnetic moments, radiative decay widths, rearrangement strong width ratios, and the relative lengths between quarks for the $J^P = 2^+$ $cc\bar{c}\bar{b}$ and $bb\bar{b}\bar{c}$ states and their lowest meson–meson thresholds. The notation is the same as that in Table 7

$cc\bar{c}\bar{b}$	The contribution from each term				Relative Lengths (fm)		
$J^P = 2^+$		Value	$B_c^* J/\psi$	Difference	(i,j)	Vaule	$B_c J/\psi$
Mass/B_T		9730.5	9442.7	287.8	(1,2)	0.378	
Variational Parameters (fm^{-2})	C_{11}	13.7	20.2		(1.3)	0.350	0.318(J/ψ)
	C_{22}	8.9	12.5				
	C_{33}	9.1	-		(2,3)	0.350	
Quark Mass		11097.0	11097.0	0.0	(1,4)	0.359	
Confinement Potential		-2158.4	-2490.6	332.2	(2,4)	0.359	0.250(B_c^*)
Kinetic Energy		763.9	799.3	-35.4	(3,4)	0.304	
CS Interaction		28.0	36.9	-8.9	(1,2)-(3,4):	0.264 fm	
V^C	(1,2)	-14.3			(1,3)	-21.9	-164.2(J/ψ)
	(1,4)	-17.3			(2,3)	-21.9	
	Subtotal	-192.4	-524.6	332.2	(2,4)	-17.3	$-360.4(B_c^*)$
Total Contribution		599.5	311.7	287.8	(3,4)	-99.6	

Total Wave function:

$\Psi_{tot} = |F\rangle|R^s\rangle|[\phi_1\chi_1]\rangle = 0.577|F\rangle|R^s\rangle|[\psi_1\zeta_1]\rangle - 0.816|F\rangle|R^s\rangle|[\psi_2\zeta_1]\rangle$

The rearrangement strong decay channel: $B_c^* J/\psi$.

The radiative decay widths:

$\Gamma_{T_{c^2\bar{c}\bar{b}}(9730.5,2^+)\to T_{c^2\bar{c}\bar{b}}(9620.5,0^+)\gamma} = 0\,\text{keV}$

$\Gamma_{T_{c^2\bar{c}\bar{b}}(9730.5,2^+)\to T_{c^2\bar{c}\bar{b}}(9624.6,1^+)\gamma} = 145.0\,\text{keV}$

The magnetic moments:

$\mu_{T_{c^2\bar{c}\bar{b}}(9730.5,2^+)} = \langle\Psi^{2+}_{tot}|\hat{\mu^z}|\Psi^{2+}_{tot}\rangle = 2\mu_c + \mu_{\bar{c}} + \mu_{\bar{b}} = 0.464\mu_N$

The transition magnetic moments:

$\mu_{T_{c^2\bar{c}\bar{b}}(9730.5,2^+)\to T_{c^2\bar{c}\bar{b}}(9620.5,0^+)\gamma} = \langle\Psi^{2+}_{tot}|\hat{\mu^z}|\Psi^{0+}_{tot}\rangle = 0$

$\mu_{T_{c^2\bar{c}\bar{b}}(9730.5,2^+)\to T_{c^2\bar{c}\bar{b}}(9624.6,1^+)\gamma} = \langle\Psi^{2+}_{tot}|\hat{\mu^z}|\Psi^{1+}_{tot}\rangle = -0.294\mu_N$

Overall	Present Work		CMI Model	
	Contribution	Value	Ref. [110]	Ref. [123]
c-quark	$2m_c$	3836.0	$\frac{1}{2}m_{cc}$ 1585.8	
	$\frac{\mathbf{p}^2_{x_1}}{2m'_1} + \frac{m_c+m_{\bar{b}}}{3m_c+m_{\bar{b}}}\frac{\mathbf{p}^2_{x_3}}{2m'_3}$	408.0	$\frac{m_c}{4(m_c+m_{\bar{c}})}m_{c\bar{c}}$ 767.1	
	$V^C(12)$	-14.3		
	$\frac{1}{2}[V^C(13)+V^C(23)]$	-21.9	$\frac{m_c}{4(m_c+m_{\bar{b}})}m_{c\bar{b}}$ 789.3	$2m_c$ 3449.6
	$\frac{1}{2}[V^C(14)+V^C(24)]$	-17.3		
	$-D$	-983.0		
	Subtotal	3207.5	3142.2	3449.6
$\bar{c}$-quark	$m_{\bar{c}}$	1918.0	$\frac{m_{\bar{c}}}{4(m_{\bar{c}}+m_c)}m_{c\bar{c}}$ 767.1	
	$\frac{m_{\bar{b}}}{m_{\bar{c}}+m_{\bar{b}}}\frac{\mathbf{p}^2_{x_2}}{2m'_2} + \frac{m_c}{3m_c+m_{\bar{b}}}\frac{\mathbf{p}^2_{x_3}}{2m'_3}$	244.7		
	$\frac{1}{2}V^C(34)$	-49.8		
	$\frac{1}{2}[V^C(13)+V^C(23)]$	-21.9	$\frac{m_{\bar{c}}}{4(m_{\bar{c}}+m_{\bar{b}})}m_{\bar{c}\bar{b}}$ 801.1	$m_{\bar{c}}$ 1724.8
	$-\frac{1}{2}D$	-491.5		
	Subtotal	1599.5	1568.2	1724.8
$\bar{b}$-quark	$m_{\bar{b}}$	5343.0	$\frac{m_{\bar{b}}}{4(m_{\bar{b}}+m_{\bar{c}})}m_{\bar{c}\bar{b}}$	2407.0
	$\frac{m_{\bar{c}}}{m_{\bar{c}}+m_{\bar{b}}}\frac{\mathbf{p}^2_{x_2}}{2m'_2} + \frac{m_c}{3m_c+m_{\bar{b}}}\frac{\mathbf{p}^2_{x_3}}{2m'_3}$	111.2		
	$\frac{1}{2}V^C(34)$	-49.8		
	$\frac{1}{2}[V^C(14)+V^C(24)]$	-17.4	$\frac{m_{\bar{b}}}{4(m_c+m_{\bar{b}})}m_{c\bar{b}}$ 2371.8	$m_{\bar{b}}$ 5052.9
	$-\frac{1}{2}D$	-491.5		
	Subtotal	4895.5	4778.8	5052.9
CS Interaction	$\frac{1}{2}V^{SS}(12)$	5.6	$\frac{8}{3}v_{cc}+\frac{8}{3}v_{\bar{c}\bar{b}}$ 9.5+5.2	$\frac{8}{3}C_{cc}+\frac{8}{3}C_{\bar{c}\bar{b}}$ 14.1+8.8
	$\frac{1}{2}V^{SS}(34)$	8.5		
	$\frac{1}{4}(V^{SS}(13)+V^{SS}(23))$	9.5	$\frac{8}{3}v_{c\bar{c}}+\frac{8}{3}v_{c\bar{b}}$ 14.2+7.9	$\frac{8}{3}C_{c\bar{c}}+\frac{8}{3}C_{c\bar{b}}$ 14.1+8.8
	$\frac{1}{4}(V^{SS}(14)+V^{SS}(24))$	4.3		
	Subtotal	28.0	36.8	45.9
Total contribution		9730.5	9526.0	10273.2

$bb\bar{b}\bar{c}$ $J^P = 2^+$		Value	$B_c^*\Upsilon$	Difference	Relative Lengths (fm)		
					(i,j)	Value	$B_c^*\Upsilon$
Mass/B_T		16149.2	15819.4	329.8	(1.2)	0.210	
Variational Parameters (fm^{-2})	C_{11}	14.4	20.2		(1,3)	0.256	0.160(Υ)
	C_{22}	28.6	49.7				
	C_{33}	16.9	-		(2,3)	0.256	
Quark Mass		17947.0	17497.0	0.0	(1,4)	0.266	
Confinement Potential		-2659.7	-3123.1	463.4	(2,4)	0.266	0.250(B_c^*)
Kinetic Energy		838.2	961.5	-123.3	(3,4)	0.296	
CS Interaction		23.8	34.0	-10.2	(1,2)-(3,4):	0.194 fm	
V^C	(1,2)	-257.5					
	(2,3)	-85.5					
	(1,4)	-77.6			(2,4)	-77.6	$-360.4(B_c^*)$
	Subtotal	-693.7	-1157.1	463.4	(3,4)	-110.1	
Total Contribution		168.2	-161.6	329.8	(1,3)	-85.5	$-796.7(\Upsilon)$

Total Wave function:

$\Psi_{tot} = |F\rangle|R^s\rangle|[\phi_1\chi_1]\rangle = 0.577|F\rangle|R^s\rangle|[\psi_1\zeta_1]\rangle - 0.816|F\rangle|R^s\rangle|[\psi_2\zeta_1]\rangle$

The rearrangement strong decay channel: $B_c^*\Upsilon$.

The radiative decay widths: $\Gamma_{T_{b^2\bar{b}\bar{c}}(16149.2,2^+)\to T_{b^2\bar{b}\bar{c}}(16043.9,0^+)\gamma} = 0\,\text{keV}$

$\Gamma_{T_{b^2\bar{b}\bar{c}}(16149.2,2^+)\to T_{c^2\bar{c}\bar{b}}(16043.2,1^+)\gamma} = 435.0\,\text{keV}$

The magnetic moments:

$\mu_{T_{c^2\bar{c}\bar{b}}(16149.2,2^+)} = \langle\Psi^{2+}_{tot}|\hat{\mu^z}|\Psi^{2+}_{tot}\rangle = 2\mu_b + \mu_{\bar{b}} + \mu_{\bar{c}} = -0.472\mu_N$

The transition magnetic moments:

$\mu_{T_{b^2\bar{b}\bar{c}}(16149.2,2^+)\to T_{b^2\bar{b}\bar{c}}(16043.2,1^+)\gamma} = \langle\Psi^{2+}_{tot}|\hat{\mu^z}|\Psi^{1+}_{tot}\rangle = 0.329\mu_N$

$\mu_{T_{b^2\bar{b}\bar{c}}(16149.2,2^+)\to T_{b^2\bar{b}\bar{c}}(16043.9,0^+)\gamma} = \langle\Psi^{2+}_{tot}|\hat{\mu^z}|\Psi^{0+}_{tot}\rangle = 0$

Overall	Contribution	Value	Ref. [110]	Ref. [123]
b-quark	$2m_c$	10686.0	$\frac{1}{2}m_{bb}$ 4764.8	
	$\frac{\mathbf{p}^2_{x_1}}{2m'_1} + \frac{m_b+m_{\bar{c}}}{3m_b+m_{\bar{c}}}\frac{\mathbf{p}^2_{x_3}}{2m'_3}$	404.4	$\frac{m_b}{4(m_b+m_{\bar{b}})}m_{b\bar{b}}$ 2361.2	
	$V^C(12)$	-257.5		
	$\frac{1}{2}[V^C(13)+V^C(23)]$	-85.5	$\frac{m_b}{4(m_b+m_{\bar{c}})}m_{b\bar{c}}$ 2371.8	$2m_b$ 10105.8
	$\frac{1}{2}[V^C(14)+V^C(24)]$	-77.6		
	$-D$	-983.0		
	Subtotal	9527.1	9497.8	10105.8
$\bar{b}$-quark	$m_{\bar{b}}$	5343.0	$\frac{m_{\bar{b}}}{4(m_{\bar{b}}+m_b)}m_{b\bar{b}}$ 2382.4	
	$\frac{m_{\bar{c}}}{m_{\bar{c}}+m_{\bar{b}}}\frac{\mathbf{p}^2_{x_2}}{2m'_2} + \frac{m_b}{3m_b+m_{\bar{c}}}\frac{\mathbf{p}^2_{x_3}}{2m'_3}$	146.6		
	$\frac{1}{2}V^C(34)$	-55.1		
	$\frac{1}{2}[V^C(13)+V^C(23)]$	-85.5	$\frac{m_{\bar{b}}}{4(m_{\bar{b}}+m_{\bar{c}})}m_{\bar{b}\bar{c}}$ 2360.6	$m_{\bar{b}}$ 5052.9
	$-\frac{1}{2}D$	-491.5		
	Subtotal	4857.5	4743.0	5052.9
$\bar{c}$-quark	$m_{\bar{c}}$	1918.0	$\frac{m_{\bar{c}}}{4(m_{\bar{b}}+m_{\bar{c}})}m_{\bar{b}\bar{c}}$	801.3
	$\frac{m_{\bar{b}}}{m_{\bar{c}}+m_{\bar{b}}}\frac{\mathbf{p}^2_{x_2}}{2m'_2} + \frac{m_b}{3m_b+m_{\bar{c}}}\frac{\mathbf{p}^2_{x_3}}{2m'_3}$	287.2		
	$\frac{1}{2}V^C(34)$	-55.1		
	$\frac{1}{2}[V^C(14)+V^C(24)]$	-77.6	$\frac{m_{\bar{c}}}{4(m_b+m_{\bar{c}})}m_{b\bar{c}}$ 789.3	$m_{\bar{c}}$ 1724.8
	$-\frac{1}{2}D$	-491.5		
	Subtotal	1581.2	1590.6	1724.8
CS Interaction	$\frac{1}{2}V^{SS}(12)$	5.9	$\frac{8}{3}v_{bb}+\frac{8}{3}v_{\bar{c}\bar{b}}$ 5.1+5.2	$\frac{8}{3}C_{bb}+\frac{8}{3}C_{\bar{c}\bar{b}}$ 7.7+8.8
	$\frac{1}{2}V^{SS}(34)$	6.4		
	$\frac{1}{4}(V^{SS}(13)+V^{SS}(23))$	4.6	$\frac{8}{3}v_{b\bar{b}}+\frac{8}{3}v_{b\bar{c}}$ 7.7+7.9	$\frac{8}{3}C_{b\bar{b}}+\frac{8}{3}C_{b\bar{c}}$ 7.7+8.8
	$\frac{1}{4}(V^{SS}(14)+V^{SS}(24))$	6.9		
	Subtotal	23.8	25.9	33.1
Total contribution		16149.2	15882.3	16917.0

Table 16 The masses, binding energies, variational parameters, the internal contribution, total wave functions, magnetic moments, transition magnetic moments, radiative decay widths, rearrangement strong width ratios, and the relative lengths between quarks for the $J^{PC} = 0^{++}$, 2^{++} $cb\bar{c}\bar{b}$ states and their lowest meson–meson thresholds. The notation is the same as that in Table 7

$cb\bar{c}\bar{b}$	The contribution from each term			
$J^{PC}=0^{++}$		Value	$\eta_b\eta_c$	Difference
Mass/B_T		12759.6	12387.5	372.1
Variational Parameters (fm^{-2})	C_{11}	12.7	15.0	
	C_{22}	12.7	57.4	
	C_{33}	23.6	-	
Quark Mass		14522.0	14522.0	0.0
Confinement Potential		-2571.3	-3082.3	511.0
Kinetic Energy		905.8	1085.5	-179.7
CS Interaction		-81.1	-137.6	56.6
V^C	(1,2)	42.6		
	(1,4)	-172.6		
	Subtotal	-605.3	-1116.3	511.0
Total Contribution		219.3	-168.5	387.8

Relative Lengths (fm)		
(i,j)	Value	$\eta_b\eta_c$
(1,2)	0.315	
(1,3)	0.277	0.290(η_c)
(2,3)	0.277	
(1,4)	0.277	
(2,4)	0.277	0.148(η_b)
(3,4)	0.315	
(1,2)-(3,4):	0.164 fm	
(1,3)	-172.6	-237.2(η_c)
(2,3)	-172.6	
(2,4)	-172.6	$-879.1(\eta_b)$
(3,4)	42.6	

Overall	Present Work		CMI Model	
	Contribution	Value	Ref. [110]	Ref. [123]
c-quark: m_c^{eff}	m_c	1918.0	$\frac{-m_c}{4(m_c+m_b)}m_{cb}$	
	$\frac{m_b}{m_c+m_b}\frac{\mathbf{p}^2_{x_1}}{2m'_1}$	193.7	-400.5	
	$\frac{m_b}{2m_c+2m_b}\frac{\mathbf{p}^2_{x_3}}{2m'_3}$	139.6	$\frac{5m_c}{8(m_c+m_{\bar{b}})}m_{c\bar{b}}$	
	$\frac{1}{2}V^C(12)$	21.3	986.7	
	$\frac{1}{2}[V^C(13)+V^C(14)]$	-172.6	$\frac{5m_c}{8(m_c+m_{\bar{c}})}m_{c\bar{c}}$	m_c
	$-1/2D$	-491.5	958.9	1724.8
	Subtotal	1608.5	1545.1	1724.8
b-quark: m_b^{eff}	$m_{\bar{b}}$	5343.0	$\frac{-m_b}{4(m_c+m_b)}m_{cb}$	
	$\frac{m_c}{m_c+m_b}\frac{\mathbf{p}^2_{x_1}}{2m'_1}$	69.5	-1203.8	
	$\frac{m_c}{2m_c+2m_b}\frac{\mathbf{p}^2_{x_3}}{2m'_3}$	50.1	$\frac{5m_b}{8(m_c+m_{\bar{b}})}m_{c\bar{b}}$	
	$\frac{1}{2}V^C(12)$	21.3	2965.5	
	$\frac{1}{2}[V^C(23)+V^C(24)]$	-172.6	$\frac{5m_b}{8(m_b+m_{\bar{b}})}m_{b\bar{b}}$	m_b
	$-1/2D$	-491.5	2951.6	5052.9
	Subtotal	4819.8	4713.3	5052.9
CS Interaction	$-\frac{1}{4}(V^{SS}(12)+V^{SS}(34))$	-5.3	$-\frac{8}{3}v_{cb}-\frac{20}{3}v_{\bar{c}\bar{c}}$	$-\frac{8}{3}C_{cb}-\frac{20}{3}C_{\bar{c}\bar{c}}$
	$-\frac{5}{4}V^{SS}(13)$	-33.3	-5.1-35.5	-8.8-35.3
	$-\frac{5}{4}V^{SS}(24)$	-10.1	$-\frac{20}{3}v_{b\bar{b}}-\frac{40}{3}v_{b\bar{c}}$	$-\frac{20}{3}C_{b\bar{b}}-\frac{40}{3}C_{b\bar{c}}$
	$-\frac{5}{4}(V^{SS}(14)+V^{SS}(23))$	-32.5	-19.2-39.3	-19.3-44.3
	Subtotal	-81.1	-99.2	-107.5
Matrix nondiagonal element		-15.8	-80.7	-51.9
Total contribution		12759.6	12336.1	13396.0

Total Wave function:

$$\Psi_{tot}=0.961|F\rangle|R^s\rangle|[\phi_2\chi_5]\rangle+0.114|F\rangle|R^s\rangle|[\phi_2\chi_6]\rangle-0.069|F\rangle|R^s\rangle|[\phi_1\chi_5]\rangle$$
$$-0.241|F\rangle|R^s\rangle|[\phi_1\chi_6]\rangle=0.211|F\rangle|R^s\rangle|[\psi_1\zeta_6]\rangle-0.830|F\rangle|R^s\rangle|[\psi_1\zeta_5]\rangle$$
$$-0.367|F\rangle|R^s\rangle|[\psi_2\zeta_5]\rangle+0.363|F\rangle|R^s\rangle|[\psi_2\zeta_6]\rangle=0.333|F\rangle|R^s\rangle|[\psi'_1\zeta'_6]\rangle$$
$$-0.668|F\rangle|R^s\rangle|[\psi'_1\zeta'_5]\rangle-0.398|F\rangle|R^s\rangle|[\psi'_2\zeta'_5]\rangle+0.533|F\rangle|R^s\rangle|[\psi'_2\zeta'_6]\rangle$$

The rearrangement strong decay channel:

$\Gamma_{T_{cb\bar{c}\bar{b}}(12759.6,0^{++})\to\eta_c\eta_b}:\Gamma_{T_{cb\bar{c}\bar{b}}(12759.6,0^{++})\to J/\psi\Upsilon}=21:1$

$\Gamma_{T_{cb\bar{c}\bar{b}}(12759.6,0^{++})\to B_cB_c}:\Gamma_{T_{cb\bar{c}\bar{b}}(12759.6,0^{++})\to B_c^*B_c^*}=7.6:1$

The radiative decay widths:

$\Gamma_{T_{cb\bar{c}\bar{b}}(12797.3,1^{+-})\to T_{cb\bar{c}\bar{b}}(12759.6,0^{++})\gamma}=33.1\,\text{keV}$

$\Gamma_{T_{cb\bar{c}\bar{b}}(12856.6,1^{++})\to T_{cb\bar{c}\bar{b}}(12759.6,0^{++})\gamma}=0$

$\Gamma_{T_{cb\bar{c}\bar{b}}(12882.4,2^{++})\to T_{cb\bar{c}\bar{b}}(12759.6,0^{++})\gamma}=0$

The magnetic moments: $T_{cb\bar{c}\bar{b}}(12759.6,0^{++})=<\Psi^{0^{++}}_{tot}|\hat{\mu^z}|\Psi^{0^{++}}_{tot}>=0$

The transition magnetic moments: $\mu_{T_{cb\bar{c}\bar{b}}(12882.4,2^{++})\to T_{cb\bar{c}\bar{b}}(12759.6,0^{++})\gamma}=<\Psi^{2^{++}}_{tot}|\hat{\mu^z}|\Psi^{0^{++}}_{tot}>=0$

$\mu_{T_{cb\bar{c}\bar{b}}(12856.6,1^{++})\to T_{cb\bar{c}\bar{b}}(12759.6,0^{++})\gamma}=<\Psi^{1^{++}}_{tot}|\hat{\mu^z}|\Psi^{0^{++}}_{tot}>=0$

$\mu_{T_{cb\bar{c}\bar{b}}(12796.9,1^{+-})\to T_{cb\bar{c}\bar{b}}(12759.6,0^{++})\gamma}=<\Psi^{1^{+-}}_{tot}|\hat{\mu^z}|\Psi^{0^{++}}_{tot}>=0.226\times2\sqrt{\frac{1}{6}}(\mu_c-\mu_b)=0.081\mu_N$

$J^{PC}=2^{++}$		Value	$\Upsilon J/\psi$	Difference
Mass/B_T		12882.4	12561.1	321.3
Variational Parameters (fm^{-2})	C_{11}	11.0	12.5	
	C_{22}	11.0	49.7	
	C_{33}	21.0	-	
Quark Mass		14522.0	14522.0	0.0
Confinement Potential		-2460.7	-2926.9	466.2
Kinetic Energy		791.7	925.1	-133.4
CS Interaction		29.5	41.0	-11.5
V^C	(1,2)	28.0		
	(2,3)	-137.7		
	(1,4)	-137.7		
	Subtotal	-494.7	-960.9	466.2
Total Contribution		326.5	5.1	321.4

Relative Lengths (fm)		
(i,j)	Value	$\Upsilon J/\psi$
(1.3)	0.340	
(1,3)	0.296	0.318(J/ψ)
(2,3)	0.296	
(1,4)	0.296	
(2,4)	0.296	0.160(Υ)
(3,4)	0.340	
(1,2)-(3,4):	0.174 fm	
(2,4)	-137.7	$-796.7(\Upsilon)$
(3,4)	28.0	
(1,3)	-137.7	$-164.2(J/\psi)$

	Contribution	Value	Ref. [110]	Ref. [123]
c-quark: m_c^{eff}	m_c	1918.0	$\frac{-m_c}{4(m_c+m_b)}m_{cb}$	
	$\frac{m_b}{m_c+m_b}\frac{\mathbf{p}^2_{x_1}}{2m'_1}$	167.1	-400.5	
	$\frac{m_b}{2m_c+2m_b}\frac{\mathbf{p}^2_{x_3}}{2m'_3}$	124.2	$\frac{5m_c}{8(m_c+m_{\bar{b}})}m_{c\bar{b}}$	
	$\frac{1}{2}V^C(12)$	14.0	986.7	
	$\frac{1}{2}[V^C(13)+V^C(14)]$	-137.7	$\frac{5m_c}{8(m_c+m_{\bar{c}})}m_{c\bar{c}}$	m_c
	$-1/2D$	-491.5	958.9	1724.8
	Subtotal	1594.1	1545.1	1724.8
b-quark: m_b^{eff}	$m_{\bar{b}}$	5343.0	$\frac{-m_b}{4(m_c+m_b)}m_{cb}$	
	$\frac{m_c}{m_c+m_b}\frac{\mathbf{p}^2_{x_1}}{2m'_1}$	60.0	-1203.8	
	$\frac{m_c}{2m_c+2m_b}\frac{\mathbf{p}^2_{x_3}}{2m'_3}$	44.6	$\frac{5m_b}{8(m_c+m_{\bar{b}})}m_{c\bar{b}}$	
	$\frac{1}{2}V^C(12)$	14.0	2965.5	
	$\frac{1}{2}[V^C(23)+V^C(24)]$	-137.7	$\frac{5m_b}{8(m_b+m_{\bar{b}})}m_{b\bar{b}}$	m_b
	$-1/2D$	-491.5	2951.6	5052.9
	Subtotal	4832.4	4713.3	5052.9
CS Interaction	$-\frac{1}{4}(V^{SS}(12)+V^{SS}(34))$	-4.7	$-\frac{8}{3}v_{cb}+\frac{10}{3}v_{\bar{c}\bar{c}}$	$-\frac{8}{3}C_{cb}+\frac{10}{3}C_{\bar{c}\bar{c}}$
	$\frac{5}{8}V^{SS}(13)$	15.2	-5.1+17.7	-8.8+17.7
	$\frac{5}{8}V^{SS}(24)$	4.5	$\frac{10}{3}v_{b\bar{b}}+\frac{20}{3}v_{b\bar{c}}$	$\frac{10}{3}C_{b\bar{b}}+\frac{20}{3}C_{b\bar{c}}$
	$\frac{5}{8}(V^{SS}(14)+V^{SS}(23))$	14.7	9.6+19.7	9.6+22.0
	Subtotal	29.5	41.7	40.5
Matrix nondiagonal element		0.1	-29.1	3.2
Total contribution		12882.4	12529.4	13599.0

Total Wave function:

$$\Psi_{tot}=0.999|F\rangle|R^s\rangle|[\phi_2\chi_1]\rangle-0.027|F\rangle|R^s\rangle|[\phi_1\chi_1]\rangle=-0.801|F\rangle|R^s\rangle|[\psi_1\zeta_1]\rangle$$
$$-0.599|F\rangle|R^s\rangle|[\psi_2\zeta_1]\rangle=-0.832|F\rangle|R^s\rangle|[\psi'_1\zeta'_1]\rangle+0.555|F\rangle|R^s\rangle|[\psi'_2\zeta'_1]\rangle$$

The rearrangement strong decay channel: $\Upsilon J/\psi$ and $B_c^*B_c^*$

The magnetic moments: $T_{cb\bar{c}\bar{b}}(12882.4,2^{++})=\langle\Psi^{2^{++}}_{tot}|\hat{\mu^z}|\Psi^{2^{++}}_{tot}\rangle=0$

The radiative decay widths:

$\Gamma_{T_{cb\bar{c}\bar{b}}(12882.4,2^{++})\to T_{cb\bar{c}\bar{b}}(12797.3,1^{+-})\gamma}=4.9\text{ keV}$

$\Gamma_{T_{cb\bar{c}\bar{b}}(12882.4,2^{++})\to T_{cb\bar{c}\bar{b}}(12759.6,0^{++})\gamma}=0$ $\Gamma_{T_{cb\bar{c}\bar{b}}(12882.4,2^{++})\to T_{cb\bar{c}\bar{b}}(12856.6,1^{++})\gamma}=0$

The transition magnetic moments: $\mu_{T_{cb\bar{c}\bar{b}}(12882.4,2^{++})\to T_{cb\bar{c}\bar{b}}(12759.6,1^{+-})\gamma}=\langle\Psi^{2^{++}}_{tot}|\hat{\mu^z}|\Psi^{1^{+-}}_{tot}\rangle=0.774\times(\mu_c+\mu_b)+0.226\times(\mu_c-\mu_b)=0.345\mu_N$

$\mu_{T_{cb\bar{c}\bar{b}}(12882.4,2^{++})\to T_{cb\bar{c}\bar{b}}(12856.6,1^{++})\gamma}=\langle\Psi^{2^{++}}_{tot}|\hat{\mu^z}|\Psi^{1^{++}}_{tot}\rangle=0$ $\mu_{T_{cb\bar{c}\bar{b}}(12882.4,2^{++})\to T_{cb\bar{c}\bar{b}}(12759.3,0^{++})\gamma}=\langle\Psi^{2^{++}}_{tot}|\hat{\mu^z}|\Psi^{0^{++}}_{tot}\rangle=0$

Table 17 The masses, binding energies, variational parameters, the internal contribution, total wave functions, magnetic moments, transition magnetic moments, radiative decay widths, rearrangement strong width ratios, and the relative lengths between quarks for the $J^{PC} = 1^{+-}$, 1^{++} $cb\bar{c}\bar{b}$ states and their lowest meson–meson thresholds. The notation is the same as that in Table 7

$cb\bar{c}\bar{b}$ $J^{PC}=1^{+-}$		The contribution from each term: Value	$\Upsilon\eta_c$	Difference
Mass/B_T		12796.9	12467.4	329.5
Variational Parameters (fm^{-2})	C_{11}	11.9	15.0	
	C_{22}	11.9	49.7	
	C_{33}	22.9	-	
Quark Mass		14522.0	14522.0	0.0
Confinement Potential		-2527.1	-3000.0	472.9
Kinetic Energy		858.5	1001.2	-142.7
CS Interaction		-41.4	-55.8	14.4
V^C	(1,2)	35.6		
	(1,4)	-158.1		
	Subtotal	-561.1	-1034.0	472.9
Total Contribution		256.0	-88.6	344.6

Relative Length (fm) (i,j)	Value	$\Upsilon\eta_c$
(1,2)	0.331	
(1.3)	0.289	$0.290(\eta_c)$
(2,3)	0.289	
(1,4)	0.289	
(2,4)	0.289	$0.160(\Upsilon)$
(3,4)	0.331	
(1,2)-(3,4):	0.168 fm	
(1,3)	-158.1	$-237.2(\eta_c)$
(2,3)	-158.1	
(2,4)	-158.1	$-796.7(\Upsilon)$
(3,4)	35.6	

Overall	Present Work: Contribution	Value	CMI Model: Ref. [110]	Ref. [123]
c-quark: m_c^{eff}	m_c	1918.0	$\frac{-m_c}{4(m_c+m_b)}m_{cb}$	
	$\frac{m_b}{m_c+m_b}\frac{\mathbf{p}_{x_1}^2}{2m_1'}$	180.6	-400.5	
	$\frac{m_b}{2m_c+2m_b}\frac{\mathbf{p}_{x_3}^2}{2m_3'}$	135.3	$\frac{5m_c}{8(m_c+m_{\bar{b}})}m_{c\bar{b}}$	
	$\frac{1}{2}V^C(12)$	17.8	986.7	
	$\frac{1}{2}[V^C(13)+V^C(14)]$	-158.1	$\frac{5m_c}{8(m_c+m_{\bar{c}})}m_{c\bar{c}}$	m_c
	$-1/2D$	-491.5	958.9	1724.8
	Subtotal	1602.1	1545.1	1724.8
b-quark: m_b^{eff}	$m_{\bar{b}}$	5343.0	$\frac{-m_b}{4(m_c+m_b)}m_{cb}$	
	$\frac{m_c}{m_c+m_b}\frac{\mathbf{p}_{x_1}^2}{2m_1'}$	64.8	-1203.8	
	$\frac{m_c}{2m_c+2m_b}\frac{\mathbf{p}_{x_3}^2}{2m_3'}$	48.6	$\frac{5m_b}{8(m_c+m_{\bar{b}})}m_{c\bar{b}}$	
	$\frac{1}{2}V^C(12)$	17.8	2965.5	
	$\frac{1}{2}[V^C(23)+V^C(24)]$	-158.1	$\frac{5m_b}{8(m_b+m_{\bar{b}})}m_{b\bar{b}}$	m_b
	$-1/2D$	-491.5	2951.6	5052.9
	Subtotal	4824.7	4713.3	5052.9
CS Interaction	$-\frac{1}{4}[V^{SS}(12)+V^{SS}(34)]$	-5.0	$-\frac{8}{3}v_{cb}-\frac{10}{3}v_{\bar{c}\bar{c}}$	$-\frac{8}{3}C_{cb}-\frac{10}{3}C_{\bar{c}\bar{c}}$
	$-\frac{5}{8}V^{SS}(13)$	-16.0	-5.2-17.7	-8.8-17.7
	$-\frac{5}{8}V^{SS}(24)$	-4.8	$-\frac{10}{3}v_{b\bar{b}}-\frac{20}{3}v_{b\bar{c}}$	$-\frac{10}{3}C_{b\bar{b}}-\frac{20}{3}C_{b\bar{c}}$
	$-\frac{5}{8}[V^{SS}(14)+V^{SS}(23)]$	-15.6	-9.6-19.7	-9.7-22.0
	Subtotal	-41.4	-52.2	-58.1
Matrix nondiagonal element		-15.3	-54.7	-19.6
Total contribution		12796.9	12409.9	13478.0

Total Wave function:

$$\Psi_{tot} = 0.877|F\rangle|R^s\rangle|[\phi_1\chi_2]\rangle - 0.064|F\rangle|R^s\rangle|[\phi_2\chi_2]\rangle + 0.320|F\rangle|R^s\rangle|[\phi_1\chi_3]\rangle$$
$$+0.320|F\rangle|R^s\rangle|[\phi_1\chi_4]\rangle + 0.105|F\rangle|R^s\rangle|[\phi_2\chi_3]\rangle + 0.105|F\rangle|R^s\rangle|[\phi_2\chi_4]\rangle$$
$$= 0.211|F\rangle|R^s\rangle|[\psi_1\zeta_2]\rangle + 0.854|F\rangle|R^s\rangle|[\psi_1\zeta_3]\rangle + 0.223|F\rangle|R^s\rangle|[\psi_2\zeta_2]\rangle$$
$$+0.420|F\rangle|R^s\rangle|[\psi_2\zeta_3]\rangle$$
$$= -0.481|F\rangle|R^s\rangle|[\psi_1'\zeta_2']\rangle - 0.481|F\rangle|R^s\rangle|[\psi_1'\zeta_3']\rangle + 0.283|F\rangle|R^s\rangle|[\psi_1'\zeta_4']\rangle$$
$$-0.395|F\rangle|R^s\rangle|[\psi_2'\zeta_2']\rangle - 0.395|F\rangle|R^s\rangle|[\psi_2'\zeta_3']\rangle + 0.382|F\rangle|R^s\rangle|[\psi_2'\zeta_4']\rangle$$

The rearrangement strong decay channel:

$\Gamma_{T_{cb\bar{c}\bar{b}}(12796.9,1^{+-})\to\eta_b J/\psi} : \Gamma_{T_{cb\bar{c}\bar{b}}(12796.9,1^{+-})\to\Upsilon\eta_c} = 1:18.4$ $\quad\Gamma_{T_{cb\bar{c}\bar{b}}(12796.9,1^{+-})\to B_c^*\bar{B}_c^*} : \Gamma_{T_{cb\bar{c}\bar{b}}(12796.9,1^{+-})\to B_c^*\bar{B}_c} : \Gamma_{T_{cb\bar{c}\bar{b}}(12796.9,1^{+-})\to B_c\bar{B}_c^*} = 1:3.9:3.9$

The radiative decay widths:

$\Gamma_{T_{cb\bar{c}\bar{b}}(12797.3,1^{+-})\to T_{cb\bar{c}\bar{b}}(12759.6,0^{++})\gamma} = 33.1$ keV

$\Gamma_{T_{cb\bar{c}\bar{b}}(12856.6,1^{++})\to T_{cb\bar{c}\bar{b}}(12796.9,1^{+-})\gamma} = 0.1$ keV

$\Gamma_{T_{cb\bar{c}\bar{b}}(12882.4,2^{++})\to T_{cb\bar{c}\bar{b}}(12796.9,1^{+-})\gamma} = 4.9$ keV

The magnetic moments: $T_{cb\bar{c}\bar{b}}(12796.9,1^{+-}) = \langle\Psi_{tot}^{1^{+-}}|\hat{\mu^z}|\Psi_{tot}^{1^{+-}}\rangle = 0$

The transition magnetic moments: $\mu_{T_{cb\bar{c}\bar{b}}(12882.4,2^{++})\to T_{cb\bar{c}\bar{b}}(12759.6,1^{+-})\gamma} = 0.345\mu_N$

$\mu_{T_{cb\bar{c}\bar{b}}(12856.6,1^{++})\to T_{cb\bar{c}\bar{b}}(12796.9,1^{+-})\gamma} = \langle\Psi_{tot}^{1^{++}}|\hat{\mu^z}|\Psi_{tot}^{1^{+-}}\rangle = 0.113(\mu_c+\mu_b) = 0.036\mu_N$

$\mu_{T_{cb\bar{c}\bar{b}}(12796.9,1^{+-})\to T_{cb\bar{c}\bar{b}}(12759.6,0^{++})\gamma} = \langle\Psi_{tot}^{1^{+-}}|\hat{\mu^z}|\Psi_{tot}^{0^{++}}\rangle = 0.226\times 2\sqrt{\frac{1}{6}}(\mu_c-\mu_b) = 0.081\mu_N$

$J^{PC}=1^{++}$		Value	$\Upsilon J/\psi$	Difference
Mass/B_T		12856.6	12561.1	295.5
Variational Parameters (fm^{-2})	C_{11}	11.4	12.5	
	C_{22}	11.4	49.7	
	C_{33}	21.5	-	
Quark Mass		14522.0	14522.0	0.0
Confinement Potential		-2488.0	-2926.9	438.9
Kinetic Energy		818.6	925.1	-106.5
CS Interaction		10.0	41.0	-31.0
V^C	(1,2)	32.0		
	(2,3)	-146.5		
	(1,4)	-146.5		
	Subtotal	-522.0	-960.9	438.9
Total Contribution		306.6	5.1	301.5

Relative Lengths (fm) (i,j)	Value	$\Upsilon J/\psi$
(1.2)	0.333	
(1,3)	0.291	$0.318(J/\psi)$
(2,3)	0.291	
(1,4)	0.291	
(2,4)	0.291	$0.160(\Upsilon)$
(3,4)	0.333	
(1,2)-(3,4):	0.172 fm	
(2,4)	-146.5	$-796.7(\Upsilon)$
(3,4)	32.0	
(1,3)	-146.5	$-164.2(J/\psi)$

	Contribution	Value	Ref. [110]	Ref. [123]
c-quark: m_c^{eff}	m_c	1918.0	$\frac{-m_c}{4(m_c+m_b)}m_{cb}$	
	$\frac{m_b}{m_c+m_b}\frac{\mathbf{p}_{x_1}^2}{2m_1'}$	174.0	-400.5	
	$\frac{m_b}{2m_c+2m_b}\frac{\mathbf{p}_{x_3}^2}{2m_3'}$	127.2	$\frac{5m_c}{8(m_c+m_{\bar{b}})}m_{c\bar{b}}$	
	$\frac{1}{2}V^C(12)$	16.0	986.7	
	$\frac{1}{2}[V^C(13)+V^C(14)]$	-146.5	$\frac{5m_c}{8(m_c+m_{\bar{c}})}m_{c\bar{c}}$	m_c
	$-1/2D$	-491.5	958.9	1724.8
	Subtotal	1597.2	1545.1	1724.8
b-quark: m_b^{eff}	$m_{\bar{b}}$	5343.0	$\frac{-m_b}{4(m_c+m_b)}m_{cb}$	
	$\frac{m_c}{m_c+m_b}\frac{\mathbf{p}_{x_1}^2}{2m_1'}$	62.5	-1203.8	
	$\frac{m_c}{2m_c+2m_b}\frac{\mathbf{p}_{x_3}^2}{2m_3'}$	45.7	$\frac{5m_b}{8(m_c+m_{\bar{b}})}m_{c\bar{b}}$	
	$\frac{1}{2}V^C(12)$	16.0	2965.5	
	$\frac{1}{2}[V^C(23)+V^C(24)]$	-146.5	$\frac{5m_b}{8(m_b+m_{\bar{b}})}m_{b\bar{b}}$	m_b
	$-1/2D$	-491.5	2951.6	5052.9
	Subtotal	4829.2	4713.3	5052.9
CS Interaction	$\frac{1}{4}[V^{SS}(12)+V^{SS}(34)]$	4.9	$\frac{8}{3}v_{cb}+\frac{10}{3}v_{\bar{c}\bar{c}}$	$\frac{8}{3}C_{cb}+\frac{10}{3}C_{\bar{c}\bar{c}}$
	$\frac{5}{8}V^{SS}(13)$	15.5	5.2+17.7	8.8+17.7
	$\frac{5}{8}V^{SS}(24)$	4.6	$\frac{10}{3}v_{b\bar{b}}-\frac{20}{3}v_{b\bar{c}}$	$\frac{10}{3}C_{b\bar{b}}-\frac{20}{3}C_{b\bar{c}}$
	$-\frac{5}{8}[V^{SS}(14)+V^{SS}(23)]$	-15.0	9.6-19.7	9.7-22.0
	Subtotal	10.0	12.9	14.1
Matrix nondiagonal element		-6.3	-6.1	-59.5
Total contribution		12856.6	12523.6	13510.0

Total Wave function:

$$\Psi_{tot} = 0.693|F\rangle|R^s\rangle|[\phi_2\chi_3]\rangle - 0.693|F\rangle|R^s\rangle|[\phi_2\chi_4]\rangle + 0.139|F\rangle|R^s\rangle|[\phi_1\chi_3]\rangle$$
$$-0.139|F\rangle|R^s\rangle|[\phi_1\chi_4]\rangle = 0.686|F\rangle|R^s\rangle|[\psi_1\zeta_4]\rangle + 0.727|F\rangle|R^s\rangle|[\psi_2\zeta_4]\rangle$$
$$= -0.480|F\rangle|R^s\rangle|[\psi_1'\zeta_2']\rangle - 0.480|F\rangle|R^s\rangle|[\psi_1'\zeta_3']\rangle - 0.395|F\rangle|R^s\rangle|[\psi_2'\zeta_2']\rangle$$
$$-0.395|F\rangle|R^s\rangle|[\psi_2'\zeta_3']\rangle$$

The magnetic moments: $T_{cb\bar{c}\bar{b}}(12856.6,1^{++}) = \langle\Psi_{tot}^{1^{++}}|\hat{\mu^z}|\Psi_{tot}^{1^{++}}\rangle = 0$

The radiative decay widths:

$\Gamma_{T_{cb\bar{c}\bar{b}}(12856.6,1^{++})\to T_{cb\bar{c}\bar{b}}(12759.6,0^{++})\gamma} = 0$ keV

$\Gamma_{T_{cb\bar{c}\bar{b}}(12856.6,1^{++})\to T_{cb\bar{c}\bar{b}}(12796.9,1^{+-})\gamma} = 0.1$ keV

$\Gamma_{T_{cb\bar{c}\bar{b}}(12882.4,2^{++})\to T_{cb\bar{c}\bar{b}}(12856.6,1^{++})\gamma} = 0$ keV

The transition magnetic moments: $\mu_{T_{cb\bar{c}\bar{b}}(12882.4,2^{++})\to T_{cb\bar{c}\bar{b}}(12856.6,1^{++})\gamma} = \langle\Psi_{tot}^{2^{++}}|\hat{\mu^z}|\Psi_{tot}^{1^{++}}\rangle = 0$

$\mu_{T_{cb\bar{c}\bar{b}}(12856.6,1^{++})\to T_{cb\bar{c}\bar{b}}(12759.6,0^{++})\gamma} = \langle\Psi_{tot}^{1^{++}}|\hat{\mu^z}|\Psi_{tot}^{0^{++}}\rangle = 0$

$\mu_{T_{cb\bar{c}\bar{b}}(12856.6,1^{++})\to T_{cb\bar{c}\bar{b}}(12796.9,1^{+-})\gamma} = \langle\Psi_{tot}^{1^{++}}|\hat{\mu^z}|\Psi_{tot}^{1^{+-}}\rangle = 0.113(\mu_c+\mu_b) = 0.036\mu_N$

The radiative decay widths: $J/\psi\Upsilon$ $\quad\Gamma_{T_{cb\bar{c}\bar{b}}(12856.6,1^{++})\to B_c^*\bar{B}_c} : \Gamma_{T_{cb\bar{c}\bar{b}}(12856.6,1^{++})\to B_c\bar{B}_c^*} = 1:1$

References

1. M. Gell-Mann, A schematic model of baryons and mesons. Phys. Lett. **8**, 214–215 (1964)
2. G. Zweig, An SU(3) model for strong interaction symmetry and its breaking. Version 1, CERN-TH-401
3. G. Zweig, An SU(3) model for strong interaction symmetry and its breaking. Version 2, CERN-TH-412
4. S.K. Choi et al. (Belle Collaboration), Observation of a narrow charmonium-like state in exclusive $B^{+-} \to K^{+-}\pi^+\pi^- J/\psi$ decays. Phys. Rev. Lett. **91**, 262001 (2003)
5. D. Acosta et al. (CDF Collaboration), Observation of the narrow state $X(3872) \to J/\psi\pi^+\pi^-$ in $\bar{p}p$ collisions at $\sqrt{s} = 1.96$ TeV. Phys. Rev. Lett. **93**, 072001 (2004)
6. V.M. Abazov et al. (D0 Collaboration), Observation and properties of the $X(3872)$ decaying to $J/\psi\pi^+\pi^-$ in $p\bar{p}$ collisions at $\sqrt{s} = 1.96$ TeV. Phys. Rev. Lett. **93**, 162002 (2004)
7. E.S. Swanson, The new heavy mesons: a status report. Phys. Rep. **429**, 243 (2006)
8. S.L. Zhu, New hadron states. Int. J. Mod. Phys. E **17**, 283 (2008)
9. M.B. Voloshin, Charmonium. Prog. Part. Nucl. Phys. **61**, 455 (2008)
10. N. Drenska, R. Faccini, F. Piccinini, A. Polosa, F. Renga, C. Sabelli, New hadronic spectroscopy. Riv. Nuovo Cim. **33**, 633 (2010)
11. A. Esposito, A.L. Guerrieri, F. Piccinini, A. Pilloni, A.D. Polosa, Four-quark hadrons: an updated review. Int. J. Mod. Phys. A **30**, 1530002 (2015)
12. H.X. Chen, W. Chen, X. Liu, S.L. Zhu, The hidden-charm pentaquark and tetraquark states. Phys. Rep. **639**, 1 (2016)
13. R. Chen, X. Liu, S.L. Zhu, Hidden-charm molecular pentaquarks and their charm-strange partners. Nucl. Phys. A **954**, 406 (2016)
14. A. Hosaka, T. Iijima, K. Miyabayashi, Y. Sakai, S. Yasui, Exotic hadrons with heavy flavors XY Z and related states. PTEP **2016**(6), 062C01 (2016)
15. J.M. Richard, Exotic hadrons: review and perspectives. Few Body Syst. **57**(12), 1185 (2016)
16. R.F. Lebed, R.E. Mitchell, E.S. Swanson, Heavy-quark QCD exotica. Prog. Part. Nucl. Phys. **93**, 143–194 (2017)
17. A. Esposito, A. Pilloni, A.D. Polosa, Multiquark resonances. Phys. Rep. **668**, 1–97 (2017)
18. A. Ali, J.S. Lange, S. Stone, Exotics: heavy pentaquarks and tetraquarks. Prog. Part. Nucl. Phys. **97**, 123–198 (2017)
19. N. Brambilla, S. Eidelman, C. Hanhart, A. Nefediev, C.P. Shen, C.E. Thomas, A. Vairo, C.Z. Yuan, The XYZ states: experimental and theoretical status and perspectives. Phys. Rep. **873**, 1–154 (2020)
20. Y.R. Liu, H.X. Chen, W. Chen, X. Liu, S.L. Zhu, Pentaquark and tetraquark states. Prog. Part. Nucl. Phys. **107**, 237–320 (2019)
21. H.X. Chen, W. Chen, X. Liu, Y.R. Liu, S.L. Zhu, An updated review of the new hadron states. Rep. Prog. Phys. **86**(2), 026201 (2023)
22. R. Aaij et al. (LHCb Collaboration), Observation of $J/\psi p$ resonances consistent with pentaquark states in $\Lambda_b^0 \to J/\psi K^- p$ decays. Phys. Rev. Lett. **115**, 072001 (2015)
23. R. Aaij et al., Model-independent evidence for $J/\psi p$ contributions to $\Lambda_b^0 \to J/\psi p K^-$ decays. Phys. Rev. Lett. **117**(8), 082002 (2016). (**[LHCb Collaboration]**)
24. R. Aaij et al., Observation of a narrow pentaquark state, $P_c(4312)^+$, and of two-peak structure of the $P_c(4450)^+$. Phys. Rev. Lett. **122**(22), 222001 (2019). (**[LHCb Collaboration]**)
25. B. Aubert et al. (BaBar Collaboration), Observation of a narrow meson decaying to $D_s^+\pi^0$ at a mass of 2.32 GeV/c^2. Phys. Rev. Lett. **90**, 242001 (2003)
26. S. Godfrey, N. Isgur, Mesons in a relativized quark model with chromodynamics. Phys. Rev. D **32**, 189 (1985)
27. T. Barnes, F.E. Close, H.J. Lipkin, Implications of a DK molecule at 2.32-GeV. Phys. Rev. D **68**, 054006 (2003)
28. H.Y. Cheng, W.S. Hou, B decays as spectroscope for charmed four quark states. Phys. Lett. B **566**, 193–200 (2003)
29. A.P. Szczepaniak, Description of the D*(s)(2320) resonance as the D pi atom. Phys. Lett. B **567**, 23–26 (2003)
30. D. Besson et al. (CLEO Collaboration), Observation of a narrow resonance of mass 2.46 GeV/c^2 decaying to $D_s^{*+}\pi^0$ and confirmation of the $D_{sJ}^*(2317)$ state. Phys. Rev. D **68**, 032002 (2003)
31. V. Dmitrasinovic, D_s^{*+} (2317) and D_s^{*+} (2460): tetraquarks bound by the t Hooft instanton-induced interaction? Phys. Rev. D **70**, 096011 (2004)
32. Y.Q. Chen, X.Q. Li, A comprehensive four-quark interpretation of D(s)(2317), D(s)(2457) and D(s)(2632). Phys. Rev. Lett. **93**, 232001 (2004)
33. Y.R. Liu, S.L. Zhu, Y.B. Dai, C. Liu, D+(sJ)(2632): an excellent candidate of tetraquarks. Phys. Rev. D **70**, 094009 (2004)
34. A. Faessler, T. Gutsche, V.E. Lyubovitskij, Y.L. Ma, D* K molecular structure of the D(s1)(2460) meson. Phys. Rev. D **76**, 114008 (2007)
35. D. Ebert, R.N. Faustov, V.O. Galkin, Masses of tetraquarks with open charm and bottom. Phys. Lett. B **696**, 241–245 (2011)
36. C.J. Xiao, D.Y. Chen, Y.L. Ma, Radiative and pionic transitions from the $D_{s1}(2460)$ to the $D_{s0}^*(2317)$. Phys. Rev. D **93**(9), 094011 (2016)
37. S.Y. Kong, J.T. Zhu, D. Song, J. He, Heavy-strange meson molecules and possible candidates Ds0*(2317) Ds1(2460) and X0(2900). Phys. Rev. D **104**(9), 094012 (2021)
38. H.L. Fu, H.W. Grießhammer, F.K. Guo, C. Hanhart, U.G. Meißner, Update on strong and radiative decays of the $D_{s0}^*(2317)$ and $D_{s1}(2460)$ and their bottom cousins. Eur. Phys. J. A **58**(4), 70 (2022)
39. R. Aaij et al. (LHCb), A model-independent study of resonant structure in $B^+ \to D^+D^-K^+$ decays. Phys. Rev. Lett. **125**, 242001 (2020)
40. R. Aaij et al. (LHCb), Amplitude analysis of the $B^+ \to D^+D^-K^+$ decay. Phys. Rev. D **102**, 112003 (2020)
41. X.H. Liu, M.J. Yan, H.W. Ke, G. Li, J.J. Xie, Triangle singularity as the origin of $X_0(2900)$ and $X_1(2900)$ observed in $B^+ \to D^+D^-K^+$. Eur. Phys. J. C **80**(12), 1178 (2020)
42. M. Karliner, J.L. Rosner, First exotic hadron with open heavy flavor: $cs\bar{u}\bar{d}$ tetraquark. Phys. Rev. D **102**(9), 094016 (2020)
43. Z.G. Wang, Analysis of the $X_0(2900)$ as the scalar tetraquark state via the QCD sum rules. Int. J. Mod. Phys. A **35**(30), 2050187 (2020)
44. Y. Huang, J.X. Lu, J.J. Xie, L.S. Geng, Strong decays of $\bar{D}^*K^*$ molecules and the newly observed $X_{0,1}$ states. Eur. Phys. J. C **80**(10), 973 (2020)
45. T.J. Burns, E.S. Swanson, Kinematical cusp and resonance interpretations of the $X(2900)$. Phys. Lett. B **813**, 136057 (2021)
46. M.W. Hu, X.Y. Lao, P. Ling, Q. Wang, $X_0(2900)$ and its heavy quark spin partners in molecular picture. Chin. Phys. C **45**(2), 021003 (2021)
47. G.J. Wang, L. Meng, L.Y. Xiao, M. Oka, S.L. Zhu, Mass spectrum and strong decays of tetraquark $\bar{c}\bar{s}qq$ states. Eur. Phys. J. C **81**(2), 188 (2021)
48. Y. Xue, X. Jin, H. Huang, J. Ping, Tetraquarks with open charm flavor. Phys. Rev. D **103**(5), 054010 (2021)
49. S.S. Agaev, K. Azizi, H. Sundu, Vector resonance $X_1(2900)$ and its structure. Nucl. Phys. A **1011**, 122202 (2021)
50. U. Özdem, K. Azizi, Magnetic moment of the $X_1(2900)$ state in the diquark–antidiquark picture. arXiv:2202.11466 [hep-ph]

51. A. Del Fabbro, D. Janc, M. Rosina, D. Treleani, Production and detection of doubly charmed tetraquarks. Phys. Rev. D **71**, 014008 (2005)
52. D. Ebert, R.N. Faustov, V.O. Galkin, W. Lucha, Masses of tetraquarks with two heavy quarks in the relativistic quark model. Phys. Rev. D **76**, 114015 (2007)
53. T. Hyodo, Y.R. Liu, M. Oka, K. Sudoh, S. Yasui, Production of doubly charmed tetraquarks with exotic color configurations in electron–positron collisions. Phys. Lett. B **721**, 56–60 (2013)
54. Y. Ikeda, B. Charron, S. Aoki, T. Doi, T. Hatsuda, T. Inoue, N. Ishii, K. Murano, H. Nemura, K. Sasaki, Charmed tetraquarks T_{cc} and T_{cs} from dynamical lattice QCD simulations. Phys. Lett. B **729**, 85–90 (2014)
55. A. Esposito, M. Papinutto, A. Pilloni, A.D. Polosa, N. Tantalo, Doubly charmed tetraquarks in B_c and Ξ_{bc} decays. Phys. Rev. D **88**(5), 054029 (2013)
56. R. Aaij et al. (LHCb Collaboration), Observation of the doubly charmed baryon Ξ_{cc}^{++}. Phys. Rev. Lett. **119**(11), 112001 (2017)
57. S.Q. Luo, K. Chen, X. Liu, Y.R. Liu, S.L. Zhu, Exotic tetraquark states with the $qq\bar{Q}\bar{Q}$ configuration. Eur. Phys. J. C **77**(10), 709 (2017)
58. M. Karliner, J.L. Rosner, Discovery of doubly-charmed Ξ_{cc} baryon implies a stable $(bb\bar{u}\bar{d})$ tetraquark. Phys. Rev. Lett. **119**(20), 202001 (2017)
59. E.J. Eichten, C. Quigg, Heavy-quark symmetry implies stable heavy tetraquark mesons $Q_i Q_j \bar{q}_k \bar{q}_l$. Phys. Rev. Lett. **119**(20), 202002 (2017)
60. A. Ali, Q. Qin, W. Wang, Discovery potential of stable and near-threshold doubly heavy tetraquarks at the LHC. Phys. Lett. B **785**, 605–609 (2018)
61. W. Park, S. Noh, S.H. Lee, Masses of the doubly heavy tetraquarks in a constituent quark model. Acta Phys. Pol. B **50**, 1151–1157 (2019)
62. T. Guo, J. Li, J. Zhao, L. He, Mass spectra of doubly heavy tetraquarks in an improved chromomagnetic interaction model. Phys. Rev. D **105**(1), 014021 (2022)
63. Q.F. Lü, D.Y. Chen, Y.B. Dong, Masses of doubly heavy tetraquarks $T_{QQ'}$ in a relativized quark model. Phys. Rev. D **102**(3), 034012 (2020)
64. W. Park, S.H. Lee, Color spin wave functions of heavy tetraquark states. Nucl. Phys. A **925**, 161–184 (2014)
65. S. Noh, W. Park, S.H. Lee, The doubly-heavy tetraquarks $(qq'\bar{Q}\bar{Q}')$ in a constituent quark model with a complete set of harmonic oscillator bases. Phys. Rev. D **103**, 114009 (2021)
66. C. Deng, H. Chen, J. Ping, Systematical investigation on the stability of doubly heavy tetraquark states. Eur. Phys. J. A **56**(1), 9 (2020)
67. R. Aaij et al. (LHCb), Observation of an exotic narrow doubly charmed tetraquark. arXiv:2109.01038
68. Q.F. Lü, D.Y. Chen, Y.B. Dong, E. Santopinto, Triply-heavy tetraquarks in an extended relativized quark model. Phys. Rev. D **104**(5), 054026 (2021)
69. K. Chen, X. Liu, J. Wu, Y.R. Liu, S.L. Zhu, Triply heavy tetraquark states with the $QQ\bar{Q}\bar{q}$ configuration. Eur. Phys. J. A **53**(1), 5 (2017)
70. Y. Xing, Weak decays of triply heavy tetraquarks $b\bar{c}b\bar{q}$. Eur. Phys. J. C **80**(1), 57 (2020)
71. J.F. Jiang, W. Chen, S.L. Zhu, Triply heavy $QQ\bar{Q}\bar{q}$ tetraquark states. Phys. Rev. D **96**(9), 094022 (2017)
72. X.Z. Weng, W.Z. Deng, S.L. Zhu, Triply heavy tetraquark states. Phys. Rev. D **105**(3), 034026 (2022)
73. K.T. Chao, The (cc) - $(\bar{c}\bar{c})$ (diquark–anti-diquark) states in e^+e^- annihilation. Z. Phys. C **7**, 317 (1981)
74. J.P. Ader, J.M. Richard, P. Taxil, Do narrow heavy multi-quark states exist? Phys. Rev. D **25**, 2370 (1982)
75. A.M. Badalian, B.L. Ioffe, A.V. Smilga, Four quark states in the heavy quark system. Nucl. Phys. B **281**, 85 (1987)
76. L. Heller, J.A. Tjon, On bound states of heavy $Q^2\bar{Q}^2$ systems. Phys. Rev. D **32**, 755 (1985)
77. S. Zouzou, B. Silvestre-Brac, C. Gignoux, J.M. Richard, Four quark bound states. Z. Phys. C **30**, 457 (1986)
78. R.J. Lloyd, J.P. Vary, All charm tetraquarks. Phys. Rev. D **70**, 014009 (2004)
79. M. Karliner, S. Nussinov, J.L. Rosner, $QQ\bar{Q}\bar{Q}$ states: masses, production, and decays. Phys. Rev. D **95**(3), 034011 (2017)
80. M.N. Anwar, J. Ferretti, F.K. Guo, E. Santopinto, B.S. Zou, Spectroscopy and decays of the fully-heavy tetraquarks. Eur. Phys. J. C **78**(8), 647 (2018)
81. Y. Bai, S. Lu, J. Osborne, Beauty-full tetraquarks. Phys. Lett. B **798**, 134930 (2019)
82. V.R. Debastiani, F.S. Navarra, Spectroscopy of the all-charm tetraquark. PoS Hadron **2017**, 238 (2018)
83. W. Chen, H.X. Chen, X. Liu, T.G. Steele, S.L. Zhu, Hunting for exotic doubly hidden-charm/bottom tetraquark states. Phys. Lett. B **773**, 247–251 (2017)
84. V. Khachatryan et al. (CMS), Observation of $\Upsilon(1S)$ pair production in proton–proton collisions at $\sqrt{s} = 8$ TeV. JHEP **05**, 013 (2017)
85. A.M. Sirunyan et al. (CMS), Measurement of the $\Upsilon(1S)$ pair production cross section and search for resonances decaying to $\Upsilon(1S)\mu^+\mu^-$ in proton–proton collisions at $\sqrt{s} = 13$ TeV. Phys. Lett. B **808**, 135578 (2020)
86. R. Aaij et al. (LHCb), Search for beautiful tetraquarks in the $\Upsilon(1S)\mu^+\mu^-$ invariant-mass spectrum. JHEP **10**, 086 (2018)
87. R. Aaij et al. (LHCb), Observation of structure in the J/ψ -pair mass spectrum. Sci. Bull. **65**(23), 1983–1993 (2020)
88. A. Hayrapetyan et al. (CMS), Observation of new structure in the J/ψJ/ψ mass spectrum in proton–proton collisions at $\sqrt{s} =$ 13 TeV. arXiv:2306.07164 [hep-ex]
89. J. Zhang et al. (CMS), Recent CMS results on exotic resonances. PoS **ICHEP2022**, 775. arXiv:2212.00504 [hep-ex]
90. Y. Xu (ATLAS), ATLAS results on exotic hadronic resonances. Acta Phys. Pol. Supp. **16**(3), 21 (2023). arXiv:2209.12173 [hep-ex]
91. J. Zhao, S. Shi, P. Zhuang, Fully-heavy tetraquarks in a strongly interacting medium. Phys. Rev. D **102**(11), 114001 (2020)
92. H.X. Chen, W. Chen, X. Liu, S.L. Zhu, Strong decays of fully-charm tetraquarks into di-charmonia. Sci. Bull. **65**, 1994–2000 (2020)
93. M.S. Liu, F.X. Liu, X.H. Zhong, Q. Zhao, Full-heavy tetraquark states and their evidences in the LHCb di-J/ψ spectrum. arXiv:2006.11952 [hep-ph]
94. Q.F. Lü, D.Y. Chen, Y.B. Dong, Masses of fully heavy tetraquarks $QQ\bar{Q}\bar{Q}$ in an extended relativized quark model. Eur. Phys. J. C **80**(9), 871 (2020)
95. Z. Zhao, K. Xu, A. Kaewsnod, X. Liu, A. Limphirat, Y. Yan, Study of charmoniumlike and fully-charm tetraquark spectroscopy. Phys. Rev. D **103**(11), 116027 (2021)
96. M.A. Bedolla, J. Ferretti, C.D. Roberts, E. Santopinto, Spectrum of fully-heavy tetraquarks from a diquark+antidiquark perspective. Eur. Phys. J. C **80**(11), 1004 (2020)
97. F.X. Liu, M.S. Liu, X.H. Zhong, Q. Zhao, Higher mass spectra of the fully-charmed and fully-bottom tetraquarks. Phys. Rev. D **104**(11), 116029 (2021)
98. H.W. Ke, X. Han, X.H. Liu, Y.L. Shi, Tetraquark state $X(6900)$ and the interaction between diquark and antidiquark. Eur. Phys. J. C **81**(5), 427 (2021)
99. M. Karliner, J.L. Rosner, Interpretation of structure in the di-J/ψ spectrum. Phys. Rev. D **102**(11), 114039 (2020)

100. R.N. Faustov, V.O. Galkin, E.M. Savchenko, Masses of the $QQ\bar{Q}\bar{Q}$ tetraquarks in the relativistic diquark–antidiquark picture. Phys. Rev. D **102**, 114030 (2020)
101. B.D. Wan, C.F. Qiao, Gluonic tetracharm configuration of $X(6900)$. Phys. Lett. B **817**, 136339 (2021)
102. C. Gong, M.C. Du, Q. Zhao, X.H. Zhong, B. Zhou, Nature of X(6900) and its production mechanism at LHCb. Phys. Lett. B **824**, 136794 (2022)
103. J.W. Zhu, X.D. Guo, R.Y. Zhang, W.G. Ma, X.Q. Li, A possible interpretation for $X(6900)$ observed in four-muon final state by LHCb—a light Higgs-like boson? arXiv:2011.07799 [hep-ph]
104. J.Z. Wang, D.Y. Chen, X. Liu, T. Matsuki, Producing fully charm structures in the J/ψ-pair invariant mass spectrum. Phys. Rev. D **103**(7), 071503 (2021)
105. J.Z. Wang, X. Liu, Improved understanding of the peaking phenomenon existing in the new di-J/ψ invariant mass spectrum from the CMS Collaboration. Phys. Rev. D **106**(5), 054015 (2022)
106. N. Santowsky, C.S. Fischer, Four-quark states with charm quarks in a two-body Bethe–Salpeter approach. Eur. Phys. J. C **82**(4), 313 (2022)
107. Z. Zhuang, Y. Zhang, Y. Ma, Q. Wang, Lineshape of the compact fully heavy tetraquark. Phys. Rev. D **105**(5), 054026 (2022)
108. E. Lötstedt, L. Wang, R. Yoshida, Y. Zhang, K. Yamanouchi, Error-mitigated quantum computing of Heisenberg spin chain dynamics. Phys. Scr. **98**(3), 035111 (2023)
109. V.R. Debastiani, F.S. Navarra, A non-relativistic model for the $[cc][\bar{c}\bar{c}]$ tetraquark. Chin. Phys. C **43**(1), 013105 (2019)
110. X.Z. Weng, X.L. Chen, W.Z. Deng, S.L. Zhu, Systematics of fully heavy tetraquarks. Phys. Rev. D **103**(3), 034001 (2021)
111. G.J. Wang, L. Meng, S.L. Zhu, Spectrum of the fully-heavy tetraquark state $QQ\bar{Q}'\bar{Q}'$. Phys. Rev. D **100**(9), 096013 (2019)
112. C. Hughes, E. Eichten, C.T.H. Davies, Searching for beauty-fully bound tetraquarks using lattice nonrelativistic QCD. Phys. Rev. D **97**(5), 054505 (2018)
113. J.M. Richard, A. Valcarce, J. Vijande, Few-body quark dynamics for doubly heavy baryons and tetraquarks. Phys. Rev. C **97**(3), 035211 (2018)
114. X. Jin, Y. Xue, H. Huang, J. Ping, Full-heavy tetraquarks in constituent quark models. Eur. Phys. J. C **80**(11), 1083 (2020)
115. H.T. An, S.Q. Luo, Z.W. Liu, X. Liu, Fully heavy pentaquark states in constituent quark model. Phys. Rev. D **105**(7), 7 (2022)
116. W. Park, A. Park, S. H. Lee, Dibaryons in a constituent quark model. Phys. Rev. D **92**(1), 014037 (2015)
117. W. Park, A. Park, S.H. Lee, Dibaryons with two strange quarks and total spin zero in a constituent quark model. Phys. Rev. D **93**(7), 074007 (2016)
118. A. Park, W. Park, S.H. Lee, Dibaryons with two strange quarks and one heavy flavor in a constituent quark model. Phys. Rev. D **94**(5), 054027 (2016)
119. W. Park, A. Park, S. Cho, S.H. Lee, $P_c(4380)$ in a constituent quark model. Phys. Rev. D **95**(5), 054027 (2017)
120. W. Park, S. Cho, S.H. Lee, Where is the stable pentaquark? Phys. Rev. D **99**(9), 094023 (2019)
121. H.Y. Zhou, F.L. Wang, Z.W. Liu, X. Liu, Probing the electromagnetic properties of the Σc(*)D(*)-type doubly charmed molecular pentaquarks. Phys. Rev. D **106**(3), 034034 (2022)
122. S. Kumar, R. Dhir, R.C. Verma, Magnetic moments of charm baryons using effective mass and screened charge of quarks. J. Phys. G **31**(2), 141–147 (2005)
123. J. Wu, Y.R. Liu, K. Chen, X. Liu, S.L. Zhu, Heavy-flavored tetraquark states with the $QQ\bar{Q}\bar{Q}$ configuration. Phys. Rev. D **97**(9), 094015 (2018)
124. W.X. Zhang, H. Xu, D. Jia, Masses and magnetic moments of hadrons with one and two open heavy quarks: heavy baryons and tetraquarks. Phys. Rev. D **104**(11), 114011 (2021)
125. G.J. Wang, R. Chen, L. Ma, X. Liu, S.L. Zhu, Magnetic moments of the hidden-charm pentaquark states. Phys. Rev. D **94**(9), 094018 (2016)
126. F.L. Wang, H.Y. Zhou, Z.W. Liu, X. Liu, What can we learn from the electromagnetic properties of hidden-charm molecular pentaquarks with single strangeness? Phys. Rev. D **106**(5), 054020 (2022)
127. F.L. Wang, H.Y. Zhou, Z.W. Liu, X. Liu, Exploring the electromagnetic properties of the $\Xi_c^{(\prime,*)}\bar{D}_s^*$ and $\Omega_c^{(*)}\bar{D}_s^*$ molecular states. arXiv:2210.02809 [hep-ph]
128. Z.P. Li, The threshold pion photoproduction of nucleons in the chiral quark model. Phys. Rev. D **50**, 5639–5646 (1994)
129. W.J. Deng, H. Liu, L.C. Gui, X.H. Zhong, Spectrum and electromagnetic transitions of bottomonium. Phys. Rev. D **95**(7), 074002 (2017)
130. W.J. Deng, H. Liu, L.C. Gui, X.H. Zhong, Charmonium spectrum and their electromagnetic transitions with higher multipole contributions. Phys. Rev. D **95**(3), 034026 (2017)
131. L.Y. Xiao, K.L. Wang, Q.F. Lu, X.H. Zhong, S.L. Zhu, Strong and radiative decays of the doubly charmed baryons. Phys. Rev. D **96**(9), 094005 (2017)
132. Q.F. Lü, K.L. Wang, L.Y. Xiao, X.H. Zhong, Mass spectra and radiative transitions of doubly heavy baryons in a relativized quark model. Phys. Rev. D **96**(11), 114006 (2017)
133. K.L. Wang, Y.X. Yao, X.H. Zhong, Q. Zhao, Strong and radiative decays of the low-lying S- and P-wave singly heavy baryons. Phys. Rev. D **96**(11), 116016 (2017)
134. Y.X. Yao, K.L. Wang, X.H. Zhong, Strong and radiative decays of the low-lying D-wave singly heavy baryons. Phys. Rev. D **98**(7), 076015 (2018)
135. Z.P. Li, H.X. Ye, M.H. Lu, An unified approach to pseudoscalar meson photoproductions off nucleons in the quark model. Phys. Rev. C **56**, 1099–1113 (1997)
136. S.J. Brodsky, J.R. Primack, The electromagnetic interactions of composite systems. Ann. Phys. **52**, 315–365 (1969)
137. Q. Zhao, J.S. Al-Khalili, Z.P. Li, R.L. Workman, Pion photoproduction on the nucleon in the quark model. Phys. Rev. C **65**, 065204 (2002)
138. H.T. An, K. Chen, X. Liu, Manifestly exotic pentaquarks with a single heavy quark. Phys. Rev. D **105**(3), 034018 (2022)
139. T. Guo, J. Li, J. Zhao, L. He, Mass spectra and decays of open-heavy tetraquark states. Phys. Rev. D **105**(5), 054018 (2022)
140. X.Z. Weng, W.Z. Deng, S.L. Zhu, Doubly heavy tetraquarks in an extended chromomagnetic model. Chin. Phys. C **46**(1), 013102 (2022)
141. C. Deng, H. Chen, J. Ping, Towards the understanding of fully-heavy tetraquark states from various models. Phys. Rev. D **103**(1), 014001 (2021)
142. M.S. Liu, Q.F. Lü, X.H. Zhong, Q. Zhao, All-heavy tetraquarks. Phys. Rev. D **100**(1), 016006 (2019)
143. J. Zhang, J.B. Wang, G. Li, C.S. An, C.R. Deng, J.J. Xie, Spectrum of the S-wave fully-heavy tetraquark states. arXiv:2209.13856 [hep-ph]
144. E. Hiyama, Y. Kino, M. Kamimura, Gaussian expansion method for few-body systems. Prog. Part. Nucl. Phys. **51**, 223–307 (2003)
145. Q.N. Wang, Z.Y. Yang, W. Chen, Exotic fully-heavy $Q\bar{Q}Q\bar{Q}$ tetraquark states in $\mathbf{8}_{[Q\bar{Q}]}\otimes 8_{[Q\bar{Q}]}$ color configuration. Phys. Rev. D **104**(11), 114037 (2021)
146. M.C. Gordillo, F. De Soto, J. Segovia, Diffusion Monte Carlo calculations of fully-heavy multiquark bound states. Phys. Rev. D **102**(11), 114007 (2020)
147. H. Mutuk, Nonrelativistic treatment of fully-heavy tetraquarks as diquark–antidiquark states. Eur. Phys. J. C **81**(4), 367 (2021)
148. X. Chen, Fully-heavy tetraquarks: $bb\bar{c}\bar{c}$ and $bc\bar{b}\bar{c}$. Phys. Rev. D **100**(9), 094009 (2019)

149. A.V. Berezhnoy, A.V. Luchinsky, A.A. Novoselov, Tetraquarks composed of 4 heavy quarks. Phys. Rev. D **86**, 034004 (2012)
150. Q. Li, C.H. Chang, G.L. Wang, T. Wang, Mass spectra and wave functions of $T_{QQ\bar{Q}\bar{Q}}$ tetraquarks. Phys. Rev. D **104**(1), 014018 (2021)
151. H. Mutuk, Spectrum of $cc\bar{b}\bar{b}$, $bc\bar{c}\bar{c}$, and $bc\bar{b}\bar{b}$ tetraquark states in the dynamical diquark model. Phys. Lett. B **834**, 137404 (2022)
152. Z.G. Wang, Analysis of the $QQ\bar{Q}\bar{Q}$ tetraquark states with QCD sum rules. Eur. Phys. J. C **77**(7), 432 (2017)
153. Z.G. Wang, Z.Y. Di, Analysis of the vector and axialvector $QQ\bar{Q}\bar{Q}$ tetraquark states with QCD sum rules. Acta Phys. Pol. B **50**, 1335 (2019)
154. X. Chen, Fully-charm tetraquarks: $cc\bar{c}\bar{c}$. arXiv:2001.06755 [hep-ph]